

**Development of perfluoro-oxa-alkylene units-containing
compounds: Application to preparation of silica
nanocomposites with these fluorinated compounds**

Doctoral Course

Graduate School of Science and Technology

Hirosaki University

Doctor Thesis

March 2016

Eisaku Sumino

Contents

General Introduction	1
1. Synthesis of a novel polymeric perfluoro-oxa-allane diacyl peroxide. A convenient tool for the introduction of the perfluoro-oxa-alkylene unit	15
1.1. Introduction	16
1.2. Experimental	18
1.2.1. Measurements	18
1.2.2. Materials	18
1.2.3. General procedure for the synthesis of acrylic acid oligomers containing the perfluoro-oxa-alkylene unit	19
1.2.4. Antiviral assays	20

1.3.	Results and discussion	21
1.4.	Conclusions	31
2.	Synthesis and properties of 2-Acryloxyethyltrimethylammonium chloride and 2-(methacryloxy)ethanesulfonic acid oligomers containing perfluoro-oxaalkylene groups	35
2.1.	Introduction	36
2.2.	Experimental	37
2.2.1.	Measurements	37
2.2.2.	Materials	37
2.2.3.	Synthesis of cationic and anionic oligomers containing perfluoro-oxaalkylene groups	38
2.2.4.	Anti-HIV and antibacterial activity of fluorinated	41

oligomers

2.3.	Results and discussion	41
2.4.	Conclusion	48
3.	Preparation and properties of fluorinated carboxylic acid/silica nanocomposite-encapsulated low molecular weight compounds	51
3.1.	Introduction	52
3.2.	Experimental	53
3.2.1.	Measurements	54
3.2.2.	Materials	54
3.2.3.	Preparation of perfluoro-2-methyl-3-oxahexanoic acid/silica gel nanocomposites	55

3.2.4.	Preparation of perfluoro-2-methyl-3-oxahexanoic acid/silica gel nanocomposite-encapsulated bisphenol A	56
3.2.5.	Preparation of modified glass treated with perfluoro-2-methyl-3-oxahexanoic acid/silica nanocomposites by dipping method	57
3.3.	Results and discussion	58
3.4.	Conclusion	83
4.	Facile Creation of Superoleophobic and Superhydrophilic Surface by Using Perfluoropolyether Dicarboxylic Acid/Silica Nanocomposites	91
4.1.	Introduction	92
4.2.	Experimental	94
4.2.1.	Measurements	94

4.2.2.	Materials	95
4.2.3.	Preparation of perfluoropolyether dicarboxylic acid (PFPE-DACD)/silica nanocomposites	95
4.2.4	Preparation of perfluoropolyether dicarboxylic acid (PFPE-DACD)/silica nanocomposites - encapsulated bisphenol A	96
4.2.5.	Preparation of modified glass treated with perfluoropolyether dicarboxylic acid acid/silica nanocomposites by dipping method	97
4.3.	Results and discussion	98
4.4.	Conclusion	114
	Conclusions	121
	Publications	125

General Introduction

1. Organofluorine compounds: Development of novel fluoroalkylene units (-R_F)-containing compounds

Organofluorine compounds are essential in a variety of fields because of their unique properties not observed in the corresponding non-fluorinated ones: e.g., low surface activities, physiological activity, chemical resistances, and low refractivity.^{1~3)} In fact, it is well known that Favipiravir (6-fluoro-3-hydroxy-2-pyrazinecarboxamide) is a useful antiviral drug for Ebola virus.²⁾

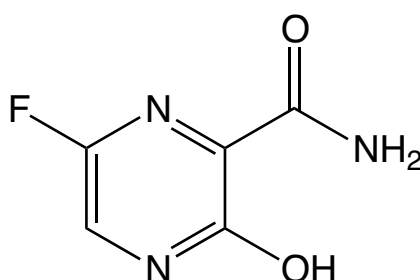
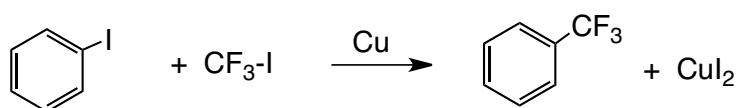


Fig. 1 Structure of Favipiravir

However, except for some naturally occurring mono fluorinated compounds such as fluoroacetate, 4-fluorothreonine, (2*R*, 3*R*)-fluorocitrate, and α -fluoro-oleic acid, all of the fluorine compounds in the world should be essentially man-made.⁴⁾ In general, there have been some difficulties to apply the usual preparative methods, which have been systematized in the field of conventional synthetic chemistry, into the synthesis of organofluorine compounds, especially organic compounds containing fluoroalkyl groups, due to the strong

electronegativity of fluorine.⁵⁾ Therefore, fluoroalkyl groups are in general introduced into organic molecules through the ester bonding. These fluoroalkylated compounds are likely to undergo hydrolysis of the ester groups due to the strong electronegativity of fluorine. From the viewpoint of synthesis and application of fluorinated compounds possessing the unique properties imparted by fluoroalkyl groups for a long time, it is very important to develop new preparative methods of fluoroalkylated compounds, in which fluoroalkyl groups should be directly introduced into organic molecules through the carbon–carbon bond formation.⁵⁾ For the direct fluoroalkylation into organic molecules, for example, the introduction of fluoroalkyl groups into aromatic compounds by the use of the cross-coupling reactions have been already reported (Scheme 1); however, the development of the direct introduction of fluoroalkyl groups has been limited.^{6 ~ 10)}



Scheme 1 Direct trifluoromethylation of aromatic compounds

In these fluoroalkylations, there have been hitherto no reports for the direct introduction of fluoroalkylene units ($-\text{R}_\text{F}-$) into the organic molecules, especially into the polymeric main chain, although such fluoroalkylene units-containing polymeric compounds $[-\text{R}_\text{F}-(\text{M})_n-]$: $\text{M} =$

radical polymerizable monomers] will have high potential for the development of novel AB block-type fluorinated functional copolymers. Because, a considerable interest has been devoted in recent years to block copolymers containing fluoroalkyl groups owing to exhibiting the low surface energy and the self-assembled polymeric aggregates resembling micelle in aqueous and organic media, which cannot be achieved in the corresponding randomly fluoroalkylated copolymers.^{11 ~ 16)}

2. Development of fluorinated polymeric nanocomposites

Fluorinated polymers have a wide variety of unique properties such as heat resistance, chemical resistance, weatherability, electrical characteristics, non-tackiness and slipperiness, which cannot be achieved by the corresponding non-fluorinated ones.^{17 ~ 18)} Therefore, fluorinated polymers have been widely used in numerous fields such as automobiles, aircrafts, semiconductors, information and communication equipment, and household goods. In these fluorinated polymers, poly(tetrafluoroethylene), poly(vinylidene fluoride), and perfluoropolyether are traditional fluorinated functional polymers, because of exhibiting numerous unique properties such as excellent chemical and thermal stability, low surface energy, and low refractive index and dielectric constant, which cannot be achieved by the corresponding nonfluorinated ones.^{19 ~ 21)} Therefore, from the developmental viewpoints of

novel high-performance materials, hybridizations of these fluorinated polymers with metal alkoxides such as silica gel are in particular interest, and in fact, some studies on the hybridization of fluorinated polymers with alkoxysilanes have been hitherto reported (see Fig. 2).^{22 ~ 27)} By incorporating unique characteristics imparted by these fluorinated polymers into the composite matrices, the mechanical strength of the obtained composites should be improved and their cost will be lowered. In fact, a variety of nanocomposites have been developed with targets such as water/oil-repellent materials, solid catalyst, gas permeable membranes, high dielectric constant materials, and low dielectric constant/high-strength materials.^{22 ~ 27)} In this way, the development of fluorinated polymers/inorganic nanocomposites should be actively attempted with the goal of higher functionality in fluorinated polymers.

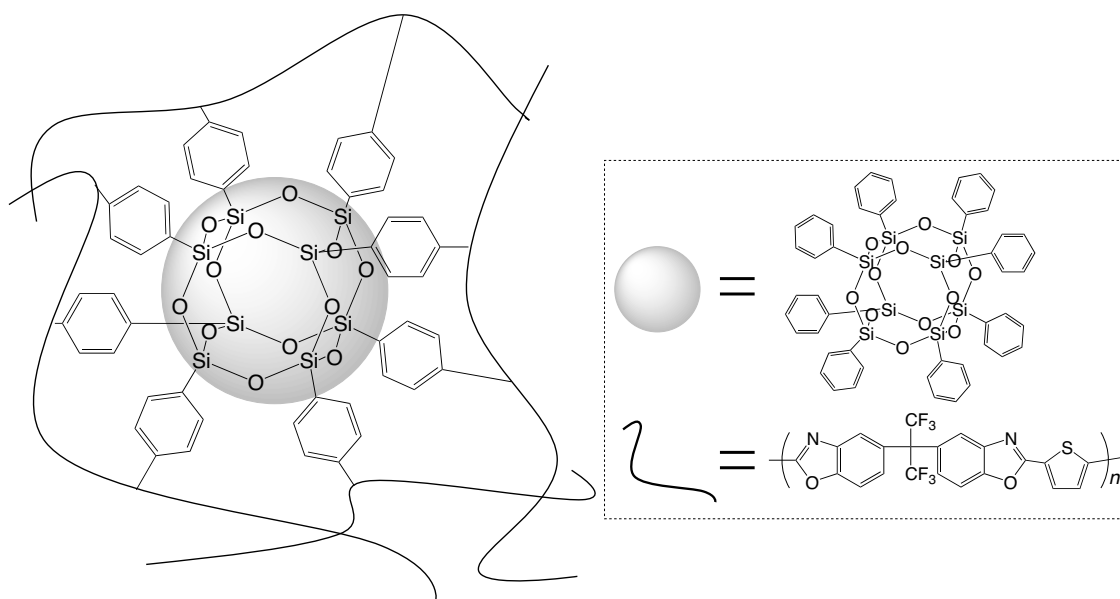
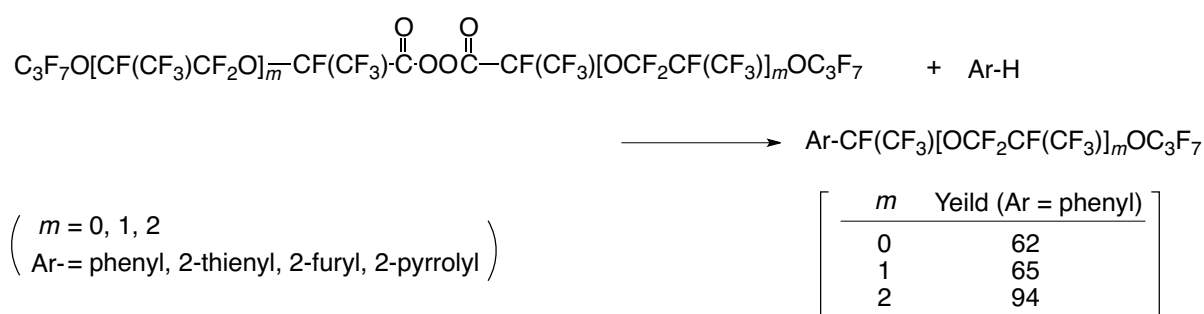


Fig. 2 Fluorinated poly-(2,5-thienylbenzobisoxazole)/polyhedral oligomeric silsesquioxane nanocomposites

3. Development of fluoroalkylene units (-R_F-) – containing compounds/silica nanocomposites

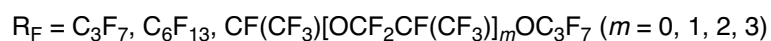
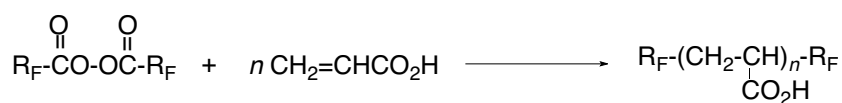
It is well known that perfluoro-oxa-alkanoyl peroxide (R_FCO₂O₂CR_F: R_F = perfluoro-oxa-alkyl group) is a useful tool for the direct introduction of perfluoro-oxa-alkyl groups into aromatic compounds such as benzene, thiophene, and furan through the single-electron transfer reaction from aromatic compounds to the peroxide (see Scheme 2).^{28~}

32)



Scheme 2 Direct perfluoro-oxa-alkylation into aromatic compounds with perfluoro-oxa-alkanoyl peroxides

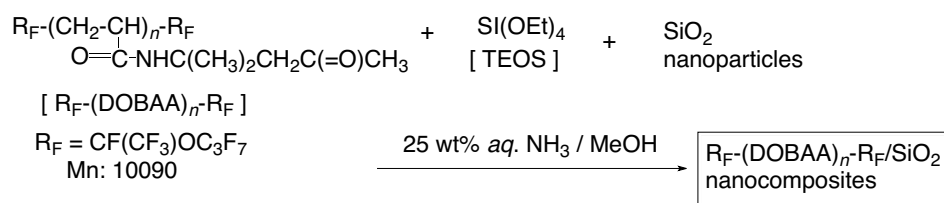
Fluoroalkanoyl peroxides can be also applicable to the preparation of two fluoroalkyl end-capped acrylic acid oligomers through the radical process as shown in Scheme 3.^{33~37)}



Scheme 3 Preparation of two fluoroalkyl end-capped acrylic acid oligomers

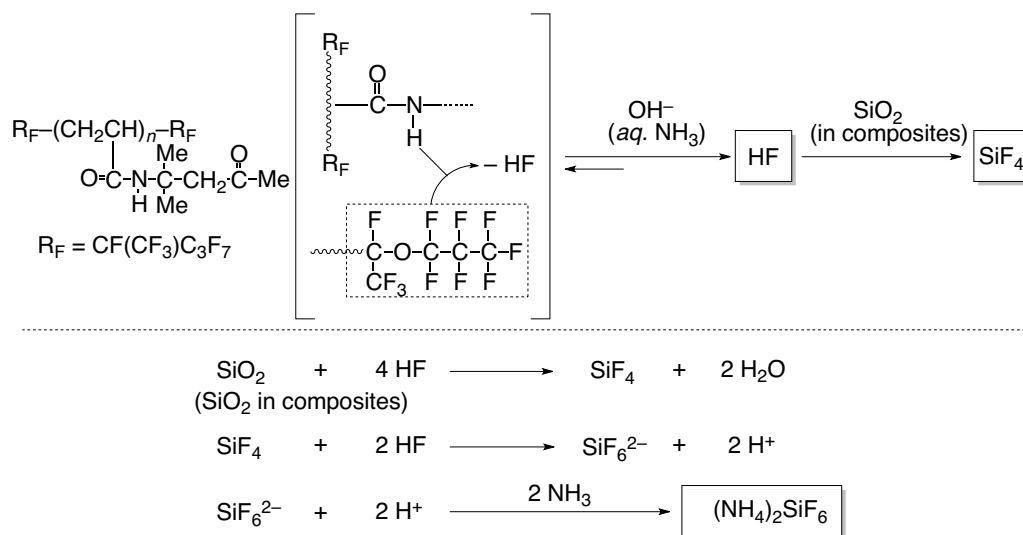
These fluorinated oligomers have a good solubility, significantly lowering the surface tension of water, quite similar to that of the low molecular weight fluorinated surfactants.^{33 ~ 37)}

Fluoroalkyl end-capped oligomers are applicable for the nanocomposite reactions with silica nanoparticles in the presence of tetraethoxysilane (TEOS) under alkaline conditions to afford the corresponding fluorinated oligomers/silica nanocomposites in good isolated yields.³⁸⁾ For example, fluoroalkyl end-capped *N*-(1,1-dimethyl-3-oxo-butyl)acrylamide oligomer [R_F-(DOBAA)_{*n*}-R_F] can react with TEOS in the presence of silica nanoparticles under alkaline conditions to afford the corresponding fluorinated oligomer/silica nanocomposites (see Scheme 4).³⁹⁾ Interestingly, R_F-(DOBAA)_{*n*}-R_F/SiO₂ nanocomposites can provide no weight loss behavior even after calcination at 800 °C; although polytetrafluoroethylene (PTFE), which has the highest heat resistance among organic polymers, has a perfect weight loss around 600 °C.^{40 ~ 42)}

Scheme 4 Preparation of $R_F-(DOBA)_{n-}R_F/SiO_2$ nanocomposites

Such no weight loss behavior is due to the formation of ammonium hexafluorosilicate, which

would be derived through the dehydrofluorination between the amide protons and fluorines in the oligomer catalyzed by ammonia in the presence of silica nanoparticles as the co-catalyst, and then reacting with silica nanoparticle as shown in the following Scheme 5.^{43 ~ 45)}



Scheme 5 Schematic illustration for the formation of ammonium hexafluorosilicate

On the other hand, fluoroalkyl end-capped acrylic acid oligomer/silica nanocomposites $[\text{R}_\text{F}-(\text{CH}_2\text{CHCOOH})_n-\text{R}_\text{F}/\text{SiO}_2]$ afford a usual weight loss characteristic, due to the no formation of ammonium hexafluorosilicate under similar conditions.^{43 ~ 45)} However, $\text{R}_\text{F}-(\text{CH}_2\text{CHCOOH})_n-\text{R}_\text{F}/\text{SiO}_2$ nanocomposites can be applicable to the surface modification of glass to afford the hydrophilic characteristic with a good oleophobicity on the modified surface.⁴⁶⁾ The creation of such hydrophilic surface at the interface with water would be due to the smooth replacement from hydrophobic fluoroalkyl groups to the hydrophilic carboxyl groups in the oligomer through the flip-flop motion between the fluoroalkyl and carboxyl

groups in the oligomers adapted to the environmental change on the modified surface as shown in Fig. 3.⁴⁶⁾

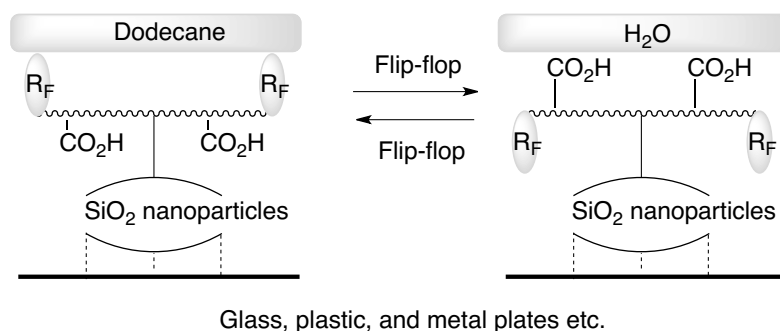


Fig. 3 Flip-flop motion between fluoroalkyl and carboxyl groups in the oligomers adapted to the environmental change on the modified glass surface

In this way, it has been shown that fluoroalkyl end-capped acrylic acid oligomer/silica nanocomposites have a unique surface active characteristic.⁴⁶⁾ Therefore, it is of particular interest to study on the nanocomposite reactions of not only $R_F-(CH_2CHCOOH)_n-R_F$ oligomers (R_F = perfluoro-oxa-alkyl groups) but also the corresponding monomeric carboxylic acids: $R_F-C(=O)OH$ and perfluoro-oxa-alkane diacid: $HO(O=)C-R_F-C(=O)OH$ (R_F = perfluoro-oxa-alkyl groups; $-R_F-$ = perfluoro-oxa-alkylene units) with TEOS in the presence of silica nanoparticles from the developmental viewpoint of new fluorinated nanocomposite materials.

4. Thesis outline

The direct introduction of perfluoro-oxa-alkylene unit into a variety of oligomeric main chains by using polymeric perfluoro-oxa-alkane diacyl peroxide will be discussed in this thesis. In addition, the properties of the obtained perfluoro-oxa-alkylene unit-containing oligomers are discussed. In this thesis, the preparation and properties of the monomeric $R_F-C(=O)OH/silica$ nanocomposites [R_F = perfluoro-oxa-alkyl group] and $HO(O=)C-R_F-C(=O)OH/silica$ nanocomposites [$-R_F-$ = perfluoro-oxa-alkylene unit] are also discussed, compared with those of the corresponding oligomeric silica nanocomposites [$R_F-(CH_2CHCOOH)_n-R_F/SiO_2$; R_F = perfluoro-oxa-alkyl group].

Chapter 1 demonstrates on the synthesis and thermal decomposition behavior of new polymeric perfluoro-oxa-alkane diacyl peroxide: $-[(O=)C-R_F-C(=O)OO]_n-$, which can be applied to the direct introduction of perfluoro-oxa-alkylene unit ($-R_F-$) into oligomer main chain through the carbon-carbon bond formation. In addition, the reactions of the polymeric perfluoro-oxa-alkane diacyl peroxide with acrylic acid to afford the corresponding perfluoro-oxa-alkylene unit-containing acrylic acid oligomers are discussed. The surface active property and anti-HIV-1 activity of the obtained fluorinated oligomers are also discussed.

In Chapter 2, new polymeric perfluoro-oxa-alkane diacyl peroxide will be applied to the direct introduction of perfluoro-oxa-alkylene unit into the cationic and anionic oligomer

main chains, respectively. Not only the surface active characteristic but also anti-HIV-1 and anti-bacterial activities of these obtained oligomers are discussed.

In Chapter 3, the monomeric fluorinated carboxylic acid: $R_F-C(=O)OH$ will be applied to the nanocomposite reactions with silica nanoparticles in the presence of tetraethoxysilane (TEOS) under alkaline conditions to afford the $R_F-C(=O)OH/SiO_2$ nanocomposites. In addition, thermal stability and surface active property of the obtained $R_F-C(=O)OH/SiO_2$ nanocomposites are also discussed, compared with those of the oligomeric silica nanocomposites $[R_F-(CH_2COOH)_n-R_F/SiO_2]$.

In Chapter 4, the monomeric perfluoro-oxa-alkane diacid: $HO(O=)C-R_F-C(=O)OH$ will be applied to the nanocomposite reactions with silica nanoparticles in the presence of TEOS under alkaline conditions to provide the $HO(O=)C-R_F-C(=O)OH/silica$ nanocomposites. Surface active characteristic of the obtained $HO(O=)C-R_F-C(=O)OH/silica$ nanocomposites will be also discussed in detail, compared with those of $R_F-C(=O)OH/silica$ nanocomposites and the perfluoro-oxa-alkylene unit-containing acrylic acid oligomer: $-R_F-(CH_2CHCOOH)_n-$.

References

- 1) V. Prakash Reddy, "Organofluorine Compounds in Biology and Medicine", Elsevier, Amsterdam (2015).

- 2) Y. Furuta, B. B. Gowen, K. Takahashi, K. Shiraki, D. F. Smee and D. L. Barnard, *Antiviral Research*, **100**, 446 (2013).
- 3) J. F. Liebman, A. Greenberg, and W. R. Dolbier Jr., "Fluorine-containing Molecules", VCH Publishers Inc., New York (1988).
- 4) W. R. Dolbier, *J. Fluorine Chem.*, **126**, 157 (2005).
- 5) T. Umemoto, *J. Soc. Syn. Org. Chem. Jpn.*, **41**, 251 (1983).
- 6) Y. Kobayashi and I. Kumadaki, *Tetrahedron Lett.*, **10**, 4095 (1969).
- 7) I. L. Knuyants and G. G. Yakobson, "Syntheses of Fluoroorganic Compounds", Springer-Verlag, Berlin (1985).
- 8) H. Sawada and M. Nakayama, *J. Jpn. Oil Chem. Soc.*, **38**, 985 (1989).
- 9) K. Uneyama, *J. Soc. Syn. Org. Chem. Jpn.*, **41**, 251 (1991).
- 10) G. J. Chen, L. S. Chen and K. C. Eapen, *J. Fluorine Chem.*, **63**, 113 (1993); **65**, 59 (1993).
- 11) J.-F. Berret, D. Calvet, A. Collet, and M. Viguier, *Curr. Opin. Colloid Interface Sci.*, **8**, 296 (2003).
- 12) T. Imae, *Curr. Opin. Colloid Interface Sci.*, **8**, 307 (2003).
- 13) T. Imae, H. Tabuchi, K. Funayama, A. Sato, T. Nakamura, and N. Amaya, *Colloid Surf. A: Physicochem. Eng. Aspects*, **167**, 73 (2000).
- 14) K. Jankova and S. Hvilsted, *J. Fluorine Chem.*, **126**, 241 (2005).

- 15) L. Andruzzi, E. Chiellini, G. Galli, X. Li, S. Kang, C. Ober, *J. Mater. Chem.*, **12**, 1684 (2002).
- 16) P. Lebreton, B. Ameduri, B. Boutevin and J. -M. Corpart, *Macromol. Chem. Phys.*, **203**, 522 (2002).
- 17) B. Ameduri and B. Boutevin, *J. Fluorine Chem.*, **104**, 53 (2000).
- 18) K. Johns and G. Stead, *J. Fluorine Chem.*, **104**, 5 (2000).
- 19) G. David, C. Boyer, J. Tonnar, B. Ameduri, P. Lacroix-Desmazes and B. Boutevin, *Chem. Rev.*, **106**, 3936 (2006).
- 20) Ameduri, B. *Chem. Rev.*, **109**, 6632 (2009).
- 21) F. Boschet and B. Ameduri, *Chem. Rev.*, **114**, 927 (2014).
- 22) P. Fabbri, M. Messori, M. Montecchi, S. Nannarore, L. Pasquali, F. Pilati, C. Tonelli, and M. Toseli, *Polymer*, **47**, 1055 (2006)
- 23) J. W. Cho and K. I. Sul, *Fiber Polym.*, **2**, 135 (2001).
- 24) J. Shim, D.W. Cho, W. Bae, and H. Kim, *Colloid Polym. Sci.*, **288**, 63 (2010).
- 25) M. Harmer, W. Farneth and Q. Sun, *J. Am. Chem. Soc.*, **118**, 7708 (1996).
- 26) S. Yano, N. Okubo, K. Takahashi, *Macromol. Symp.*, **108**, 270 (1996).
- 27) G. Yang, Z. Xue, Q. Zhuang, X. Liu, K. Zhang, and Z. Han, *Synth. Met.*, **175**, 112 (2013).
- 28) H. Sawada, *Chem. Rev.*, **96**, 1779 (1996).
- 29) H. Sawada and T. Kawase, *Kobunshi Ronbunshu*, **58**, 147 (2001).

- 30) H. Sawada and T. Kawase, *Kobunshi Ronbunshu*, **58**, 255 (2001).
- 31) H. Sawada, *J. Fluorine Chem.*, **105**, 219 (2000).
- 32) H. Sawada, *J. Fluorine Chem.*, **121**, 111 (2003).
- 33) H. Sawada, Y. –F. Gong, Y. Minoshima, T. Matsumoto, M. Nakayama, M. Kosugi and T. Migita, *J. Chem. Soc., Chem. Commun.*, 537 (1992).
- 34) H. Sawada, Y. Minoshima and H. Nakajima, *J. Fluorine Chem.*, **65**, 169 (1992).
- 35) H. Sawada, N. Itoh, T. Kawase, M. Mitani, H. Nakajima, M. Nishida and Y. Moriya, *Langmuir*, **10**, 994 (1994).
- 36) J. Nakagawa, K. Kamogawa, H. Sakai, T. Kawase, H. Sawada, J. Manosroi, A. Manosroi and M. Abe, *Langmuir*, **14**, 2055 (1998).
- 37) J. Nakagawa, K. Kamogawa, N. Momozawa, H. Sakai, T. Kawase, H. Sawada, Y. Sano and M. Abe, *Langmuir*, **14**, 2061 (1998).
- 38) H. Sawada, *Polym. Chem.*, **3**, 46 (2012).
- 39) H. Sawada, T. Narumi, A. Kajiwara, K. Ueno and K. Hamazaki, *Colloid Polym. Sci.*, **284**, 551 (2006).
- 40) H. Sawada, T. Narumi, S. Kodama, M. Kamijo, R. Ebara, M. Sugiya, and Y. Iwasaki, *Colloid Polym. Sci.*, **285**, 977 (2007).
- 41) H. Sawada, T. Tashima, and S. Kodama, *Polym. Adv. Technol.*, **19**, 739 (2008).
- 42) Y. –C. Chen, C. –C. Tsai and Y. –D. Lee, *J. Polym. Sci.: Part A: Polym. Chem.*, **42**, 1789 (2004).
- 43) H. Sawada, T. Tashima, H. Kakehi, Y. Nishiyama, M. Kikuchi, M. Miura, Y. Sato, and N. Isu, *Polym. J.*, **42**, 167 (2010).
- 44) H. Sawada, M. Kikuchi and M. Nishida, *J. Polym. Sci., Part A, Polym. Chem.*, **49**, 1070 (2011).

- 45) H. Sawada, T. Tashima, Y. Nishiyama, M. Kikuchi, G. Kostov, Y. Goto and B. Ameduri, *Macromolecules*, **44**, 1114 (2011).
- 46) H. Kakehi, M. Miura, N. Isu, and H. Sawada, *Polym, J.*, **11**, 1081 (2008).

CHAPTER 1

Synthesis and Surfactant Properties of Novel Acrylic Acid Oligomers Containing Perfluoro-oxa-alkylene Units: An Approach to Anti-human Immunodeficiency Virus Type-1 Agents

1.1 Introduction

In general, perfluoroalkylated compounds have various unique properties such as low surface tensions, high affinity for oxygen, high chemical and light resistance, excellent thermal properties and biological activities which cannot be achieved by the corresponding non-fluorinated materials.¹⁾ Usually, perfluoroalkyl groups are introduced into these materials through the ester bond, since the usual methods for alkylation cannot be applied to perfluoroalkylation due to the strong electronegativity of fluorine atoms, and these organofluorine compounds are unstable under acid or alkaline conditions because of the ester moieties. For this reason, it is most desirable to explore novel synthetic methodology for direct fluoroalkylation.

Reactions with perfluoroalkyl iodides, in particular copper induced Ullmann-type reactions, are a convenient strategy for the preparation of perfluoroalkylated compounds.²⁾ There have been active studies on the reaction behavior of a series of fluoroalkanoyl peroxides ($R_F\text{CO}_2\text{O}_2\text{CR}_F$, R_F = perfluoroalkyl, perfluoro-oxa-alkyl groups), which are useful reagents for the introduction of the corresponding fluoroalkyl group into arenes and olefins via a single-electron-transfer or a radical process. In particular, it has been demonstrated that perfluoro-oxa-alkylated compounds cause a considerable decrease in surface tension and exhibit new biological activities which cannot be achieved by the corresponding

perfluoroalkylated ones.³⁾ However, developments for the direct introduction of perfluoro-oxa-alkyl or perfluoro-oxa-alkylene units into various substrates have hitherto been very limited, despite these novel fluorinated compounds being the subject of considerable research of both a fundamental and an applied nature. An Ullmann-type perfluoro-oxa-alkylation with perfluoro-oxa-alkyl iodides has been reported by Eapen's group.⁴⁾ In contrast, there has been no report on the direct introduction of a perfluoro-oxa-alkylene unit into organic molecules with carbon-carbon bond formation.

Recently, much attention has been also focused on poly(anionic) derivatives such as dextran sulfate, heparin and pentosan polysulfate owing to their exhibiting antiviral activity, in particular anti-human immunodeficiency virus type-1 (anti-HIV-1) activity.⁵⁾ However, a clinical trial with dextran sulfate failed to demonstrate a therapeutic effect on acquired immunodeficiency syndrome (AIDS) patients due to its low oral bioavailability and rapid degradation of dextran sulfate in vivo because of the presence of ester moieties.⁶⁾ Hence, it is strongly desirable to explore novel polymeric inhibitors with high stability, potent antiviral activity and low toxicity.

This chapter shows that the synthesis and surfactant properties of various novel acrylic acid homo- and co-oligomers containing a perfluoro-oxa-alkylene groups using the polymeric perfluoro-oxa-alkane diacyl peroxide.⁷⁾ Furthermore, these fluoroalkylated oligomers have

been examined for their inhibitory effect on HIV-1 replication in vitro.

1.2 Experimental

1.2.1 Measurements

NMR spectra were measured using a JEOL-EX-270 FT-NMR (270 MHz) spectrometer. IR spectra were recorded on a HORIBA FT-300 FT-IR spectrophotometer. Molecular weights were calculated by using a JASCO 830-RI gel permeation chromatograph fitted with Shodex KF-804 and KF-8025 columns (calibrations based on polystyrene standards). The surface tensions and contact angles were measured at 25 °C using the Du Nöuy ring method and the goniometer type contact angle meter (ERMA G-I-1000) respectively, according to the previously reported method.⁸⁾

1.2.2 Materials

Polymeric perfluoro-oxa-alkane diacyl peroxide

$\{[-(\text{O})\text{C}(\text{CF}_3)\text{C}_\text{F}[\text{OCF}_2(\text{CF}_3)\text{CF}]_n\text{-O}(\text{CF}_2)_5\text{O}-[\text{CF}(\text{CF}_3)\text{CF}_2\text{O}]_m\text{CF}(\text{CF}_3)\text{C}(\text{:O})\text{OO}]_p\}$ was

prepared as follows. To a solution of potassium carbonate (2.7 g) in 16.2 g of water, 30% hydrogen peroxide (65.1 mmol) and then $\text{CF}_2\text{ClCFCl}_2$ (250 g) was added at 5 °C. The two-phase solution was cooled to −5 °C, stirred and the solution of the corresponding

perfluoro-oxa-alkane diacyl fluoride (18.6 mmol) in $\text{CF}_2\text{ClCFCl}_2$ (100 g) added drop by drop.

The reaction mixture was then kept at $-5\text{ }^\circ\text{C}$ for 1 h. The $\text{CF}_2\text{ClCFCl}_2$ layer was separated and the concentration of the peroxide determined iodometrically (yield, 52%). IR ν (cm^{-1}): 1857, 1828 ($\text{C}=\text{O}$). Because of its instability, the solution of the peroxide in $\text{CF}_2\text{ClCFCl}_2$ thus obtained was used without further purification.

The perfluoro-oxa-alkane diacyl fluoride

$$[\text{F}(\text{O})\text{C}(\text{CF}_3)\text{CF}[\text{OCF}_2(\text{CF}_3)\text{CF}]_n\text{O}(\text{CF}_2)_5\text{O}[\text{CF}(\text{CF}_3)\text{CF}_2\text{O}]_m\text{CF}(\text{CF}_3)\text{C}(\text{:O})\text{F}; (n + m) = 3]$$
used in the synthesis was supplied by PCR Inc. (Gainesville, FL, USA).

1.2.3 General procedure for the synthesis of acrylic acid oligomers containing the perfluoro-oxa-alkylene units

Polymeric perfluoro-oxa-alkane diacyl peroxide [0.5 mmol (calculated on the basis of the peroxidic monomer unit $\{-\text{C}(\text{:O})\text{R}_\text{F}\text{C}(\text{:O})\text{OO}-\}$ from iodometric titration)] in $\text{CF}_2\text{ClCFCl}_2$ solution (51.8 g) was added to a mixture of acrylic acid (28 mmol) and $\text{CF}_2\text{ClCFCl}_2$ (30 g). The solution was stirred at $45\text{ }^\circ\text{C}$ for 5 h under nitrogen. The white powder obtained was reprecipitated from methanol/ethyl acetate system to give the perfluoro-oxa-alkylene units-containing acrylic acid oligomers $[-\text{R}_\text{F}-(\text{CH}_2\text{CHCO}_2\text{H})_q]_p-$ $[-\text{R}_\text{F}- = (\text{CF}_3)\text{CF}[\text{OCF}_2(\text{CF}_3)\text{CF}]_n\text{O}(\text{CF}_2)_5\text{O}[\text{CF}(\text{CF}_3)\text{CF}_2\text{O}]_m\text{CF}(\text{CF}_3), n + m = 3]$ (1.44 g).

This oligomer exhibited the following spectral characteristics:

IR ν (cm^{-1}): 3080 (OH); 1724 (C=O); 1330 (CF_3); 1244 (CF_2). ^1H NMR (CD_3OD) δ : 1.41-2.11 ($-\text{CH}_2-$); 2.26-2.62 ($=\text{CH}-$) ppm. ^{19}F NMR (CD_3OD , ext. $\text{CF}_3\text{CO}_2\text{H}$) δ : -3.6 to 8.2 (21F); -46.3 (2F); -49.6 (10F); -69.0 (3F) ppm. ^{13}C NMR (CD_3OD) δ : 36.4; 42.9; 178.5 ppm. $\overline{\text{Mn}} = 12000$ ($\overline{\text{Mw}}/\overline{\text{Mn}} = 1.55$) (determined by gel permeation chromatography using standard polystyrenes for calibration).

The following spectral data were obtained for the other products studied.

$-\text{[R}_\text{F}\text{-(CH}_2\text{CHCO}_2\text{H)}_x\text{-(CH}_2\text{CHSiMe}_3\text{)}_y\text{]}_p-$: IR ν (cm^{-1}): 3120 (OH); 1709 (C=O); 1300 (CF_3); 1246 (CF_2). ^1H NMR (CD_3OD) δ : 0.05-0.25 ($-\text{CH}_3$); 1.35-2.85 ($-\text{CH}_2-$, $>\text{CH}-$) ppm. ^{19}F NMR (CD_3OD , ext. $\text{CF}_3\text{CO}_2\text{H}$) δ : -3.5 to 8.5 (21F); -46.0 (2F); -49.0 (10F); -68.0 (3F) ppm.

$-\text{[R}_\text{F}\text{-(CH}_2\text{CHCO}_2\text{H)}_x\text{-(CH}_2\text{CMeCO}_2\text{Me)}_y\text{]}_p-$: IR ν (cm^{-1}): 3120 (OH); 1734 (C=O); 1300 (CF_3); 1244 (CF_2). ^1H NMR (CD_3OD) δ : 1.00-2.85 ($-\text{CH}_3$, $-\text{CH}_2-$, $>\text{CH}-$); 3.60-3.85 ($-\text{CH}_3$) ppm. ^{19}F NMR (CD_3OD , ext. $\text{CF}_3\text{CO}_2\text{H}$) δ : -3.5 to 8.5 (21F); -46.0 (2F); -49.0 (10F); -68.5 (3F) ppm.

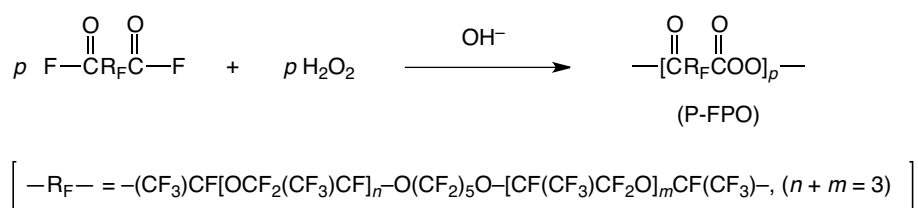
1.2.4 Antiviral assays

The antiviral activity of the compounds against HIV-I (HTLV-III_B strain) replication was based on the inhibition of virus-induced cytopathic effect in MT-4 cells as described

previously.⁹⁾ Briefly, MT-4 cells were suspended in a culture medium at 1×10^5 cells ml^{-1} and infected with HIV-1 at a multiplicity of infection of 0.2. Immediately after virus infection, the cell suspension (100 μl) was added to each well of a microtiter tray containing various concentrations of test compounds. After a 4-d incubation at 37 °C, the number of viable cells was determined by the 3-(4,5-dimethylthiazol-2-yl)-2,5-diphenyltetrazolium bromide (MTT) method.¹⁰⁾

1.3 Results and discussion

The polymeric perfluoro-oxa-alkane diacyl peroxide (P-FPO) was prepared by the reactions of the corresponding perfluoro-oxa-alkane diacid fluoride and hydrogen peroxide in $\text{CF}_2\text{ClCFCl}_2$ under alkaline conditions as shown in Scheme 1-1.



Scheme 1-1

The molecular mass of P-FPO could not be determined because of its thermal instability, but it has been succeeded in monitoring the thermal decomposition of P-FPO in

CF₂ClCFCl₂ by iodometry at various temperatures from 26 °C to 35 °C. The rate of decomposition of P-FPO was found to conform very well to a first-order equation, and the results obtained are listed in Table 1-1.

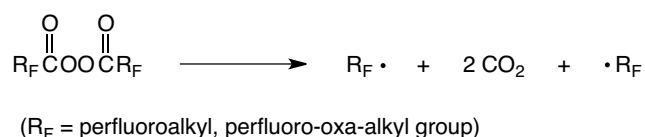
Table 1-1 Thermal decomposition of polymeric perfluoro-oxa-alkane diacyl peroxide and fluoroalkanoyl peroxides in CF₂ClCFCl₂

Peroxide	Temp. (°C)	k_d (s ⁻¹) × 10 ⁵	ΔE_a (kcal mol ⁻¹)
-[C(:O)R _F C(:O)OO] _p -	26	8.33 ± 0.04	21.9
	30	14.73 ± 0.52	
	35	25.27 ± 0.85	
(C ₇ F ₁₅ CO ₂) ₂ ^a	30	11.8	23.5
[C ₃ F ₇ OCF(CF ₃)CO ₂] ₂ ^b	30	19.6	23.9

^a See Ref. [11].

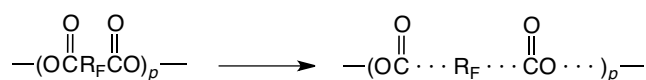
^b See Ref. [12].

The rate constants and activation parameters for the decomposition are quite similar to those for fluoroalkanoyl peroxides such as [C₃F₇OCF(CF₃)CO₂]₂ and (C₇F₁₅CO₂)₂, suggesting a concerted dissociation with three-bond hemolytic fission as previously reported (see Scheme 1-2).^{11, 12)}



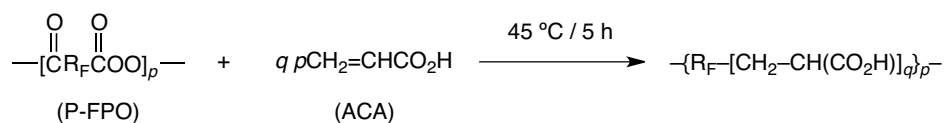
Scheme 1-2

These results indicate that P-FPO decomposes with simultaneous homolysis of the C-C (carbonyl carbon-fluoroalkyl carbon) and O-O peroxy bonds in the same manner as the perfluoroalkanoyl and perfluoro-oxa-alkanoyl peroxides $[(R_FCO_2)_2]$ which decompose homolytically with decarboxylation to afford $R_F\cdot$ radicals,^{11, 12)} and thereby provides a useful tool for the introduction of the perfluoro-oxa-alkylene units ($-R_F-$) into the oligomer main chain via a radical process (see Scheme 1-3).



Scheme 1-3

The reactions of P-FPO with acrylic acid were carried out for 5 h at 45 °C. The results are shown in Scheme 1-4 and Table 1-2.



Scheme 1-4

Table 1-2 Reactions of polymeric perfluoro-oxa-alkane diacyl peroxide (P-FPO) with acrylic acid

ACA (mmol)	ACA / P-FPO (mol / mol)	Yield (%) ^a	$-\{R_F-[CH_2-CH(CO_2H)]_q\}_p-$	
			\overline{M}_n (\overline{M}_w / \overline{M}_n)	Content of $-R_F-$ unit (wt. %) ^b
14	28	67	9900 (1.89)	8 (32) ^c
28	56	58	12000 (1.55)	7 (19)
35	117	77	13100 (1.51)	3 (10)
150	300	78	26300 (1.34)	2 (4)

^a Yields based on the starting material (acrylic acid) and the decarboxylated peroxide unit ($-R_F-$).

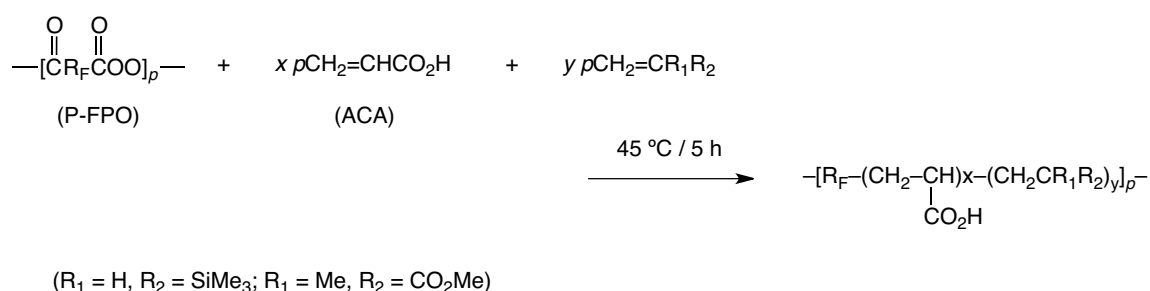
^b Content of $-R_F-$ unit in oligomer determined by ^{19}F NMR spectroscopy by comparing the peak area of the CF_3 groups of the oligomer with that of benzotrifluoride as the internal standard.

^c Theoretical $-R_F-$ unit content.

As shown in Table 1-2, the reactions of P-FPO with acrylic acid proceeded smoothly to afford in good yields acrylic acid oligomers containing the perfluoro-oxo-alkylene units. P-FPO has typical carbonyl bands around 1857 and 1828 cm^{-1} related to the $-R_F-C(=O)-$ unit. However, these absorption bands have been completely disappeared in the obtained $\{-[R_F-(CH_2CHCO_2H)_q]_p-\}$ oligomers, indicating that $-R_F-$ units should be introduced into the oligomer main chain through the carbon-carbon bond formation. The molecular weights of the oligomers obtained were found to be sensitive to the molar ratio of acrylic acid/P-FPO, increasing with higher acrylic acid to P-FPO ratios as is usual for radical oligomerizations. Furthermore, it was found that as the proportion of acrylic acid increased, the content of $-R_F-$ units decreased from 8% to 2% (mol/mol). If each oligomerization listed in Table 1-2 proceeded with 100% yield, the corresponding theoretical $-R_F-$ unit content would decrease from 32% to 4% (mol/mol). Hence, the $-R_F-$ unit was introduced into the acrylic acid

oligomers in only moderate yield. The reaction of P-FPO with acrylic acid is considered to be initiated by the radical addition of $-\text{[OC}(\cdot\text{O})\text{R}_\text{F}(\text{C}(\text{O})\text{O})\text{]}_r\text{-OC}(\cdot\text{O})\text{R}_\text{F}\cdot$ to acrylic acid. Perfluoro-oxa-alkylene units-containing acrylic acid oligomers $\{-[\text{R}_\text{F}-(\text{CH}_2\text{CHCO}_2\text{H})_q]_p\}$ are also useful for new fluorinated AB-type block co-oligomers since the molecular weight of the perfluoro-oxa-alkylene group is relatively high (MW of $-\text{R}_\text{F}-$ = 980).

Additionally, a series of acrylic acid co-oligomers containing the perfluoro-oxa-alkylene units have been prepared by the reactions of P-FPO with acrylic acid and trimethylvinylsilane or methyl methacrylate as shown in Scheme 1-5.



Scheme 1-5

Table 1-3 Reactions of P-FPO with acrylic acid and trimethylvinylsilane (or methyl methacrylate)

ACA / CH ₂ =CR ₁ R ₂ / P-FPO (mol / mol / mol)	-[R _F -(CH ₂ -CHCO ₂ H) _x -(CH ₂ CR ₁ R ₂) _y] _p -		
	Yield (%) ^a	\overline{M}_n (\overline{M}_w / \overline{M}_n)	x / y ^b
R ₁ = H, R ₂ = SiMe ₃			
70 / 100 / 1	9	2000 (1.36)	91:9
56 / 28 / 1	24	5980 (1.89)	98:2
272 / 56 / 1	16	4960 (1.68)	98:2
R ₁ = Me, R ₂ = CO ₂ Me			
56 / 56 / 1	9	16400 (3.02)	55:45
63 / 34 / 1	5	6060 (1.93)	90:10

^a Yields based on starting materials (acrylic acid, trimethylvinylsilane and methyl methacrylate) and the decarboxylated peroxide unit (-R_F-).

^b Co-oligomerization ratio determined by ¹H NMR spectroscopy.

Table 1-3 lists the results for the co-oligomerization of acrylic acid and trimethylvinylsilane (or methyl methacrylate) with P-FPO. Acrylic acid co-oligomers containing not only trimethylsilyl but also methyl ester moieties were obtained in 5% ~ 24% isolated yield. Co-oligomerization involving trimethylvinylsilane gave lower molecular weight oligomers. This may be due to the presence of trimethylvinylsilane being less capable of polymerization compared with methyl methacrylate. These novel fluoroalkylated cooligomers, in particular fluoroalkylated silicon cooligomers, should attract attention as useful functional materials in a variety of fields since there has been a great need for the development of new functional materials possessing the excellent properties imparted by both fluorine and silicon.¹³⁾

Interestingly, the series of acrylic acid homo- and co-oligomers containing the

perfluoro-oxa-alkylene units thus obtained were found to be readily soluble not only in water but also in water-soluble organic solvents such as methanol, ethanol and tetrahydrofuran. Hence, these oligomers are also applicable as new fluorinated surfactants. The surfactant properties of the fluorinated oligomers were evaluated by surface tension measurements of their aqueous solutions using the Du Nöuy ring method at 25 °C, and the results are shown in Table 1-4.

Table 1-4 Surface tensions (mN m⁻¹) of aqueous solutions of a series of acrylic acid oligomers containing the perfluoro-oxa-alkylene units

Oligomer [\overline{M}_n (x / y)]	Conc. of oligomer (g dm ⁻³)				
	10 ⁻³	10 ⁻²	10 ⁻¹	10 ⁰	10 ¹
-[R _F -(CH ₂ CHCO ₂ H) _q] _p - [9000]	72.6	72.4	67.0	43.9	32.0
-[R _F -(CH ₂ CHCO ₂ H) _x -(CH ₂ CHSiMe ₃) _y] _p - [2000 (91:9)]	72.6	72.4	59.2	44.8	—
R _F -(CH ₂ CHCO ₂ H) _n -R _F : [R _F = CF(CF ₃)OC ₃ F ₇] [12000 ($\overline{M}_w / \overline{M}_n$ = 1.54)]	72.6	71.6	29.8	17.8	17.6
-(CH ₂ CHCO ₂ H) _n - [2000]	72.6	72.2	66.2	57.5	44.9

As shown in Table 1-4, both acrylic acid homo- and co-oligomers containing the perfluoro-oxa-alkylene units were found to decrease the surface tension of water effectively compared with that of non-fluorinated poly(acrylic acid). On the other hand, an acrylic acid oligomer containing two perfluoro-oxa-alkylated end-groups [R_F-CH₂CHCO₂H]_n-R_F; R_F =

CF(CF₃)OC₃F₇], which was obtained by the oligomerization of acrylic acid with the corresponding (R_FCOO)₂,¹⁴⁾ was capable of reducing the surface tension of water more effectively than the acrylic acid homo- and co-oligomers containing the perfluoro-oxa-alkylene units. This finding indicates that since -[R_F-(CH₂CHCO₂H)_q]_p- is an AB-type block oligomer, the perfluoro-oxa-alkylene chains in the oligomer are not likely to be arranged regularly above the water surface compared with the perfluoro-oxa-alkyl chains in R_F-(CH₂CHCO₂H)_n-R_F oligomer.

In addition, the contact angles for water and dodecane on the modified glass treated with acrylic acid oligomers containing the perfluoro-oxa-alkylene units have been measured at 25 °C, and the results are listed in Table 1-5.

Table 1-5 Contact angles of dodecane on glass treated with $-\text{[R}_\text{F}-(\text{CH}_2\text{CHCO}_2\text{H})_q]_p-$ and $-\text{[R}_\text{F}-(\text{CH}_2\text{CHCO}_2\text{H})_x-(\text{CH}_2\text{CR}_1\text{R}_2)_y]_p-$

Oligomer	\overline{M}_n ($\overline{M}_w / \overline{M}_n$) [x:y]	Contact angle (°)
$-\text{[R}_\text{F}-(\text{CH}_2-\text{CHCO}_2\text{H})_q]_p-$	9900 (1.89)	54
	12000 (1.55)	52
	13100 (1.51)	51
	26300 (1.34)	46
$-\text{[R}_\text{F}-(\text{CH}_2-\text{CHCO}_2\text{H})_x-(\text{CH}_2\text{CR}_1\text{R}_2)_y]_p-$ ($\text{R}_1 = \text{H}$, $\text{R}_2 = \text{SiMe}_3$)	2000 (1.36) [91:9]	52
	5980 (1.89) [98:2]	45
	4960 (1.68) [98:2]	48
($\text{R}_1 = \text{Me}$, $\text{R}_2 = \text{CO}_2\text{Me}$)	16400 (3.02) [55:45]	54
	6060 (1.93) [90:10]	48
$\text{R}_\text{F}-[\text{CH}_2-\text{CH}(\text{CO}_2\text{H})]_n-\text{R}_\text{F}$: [$\text{R}_\text{F} = \text{CF}(\text{CF}_3)\text{OC}_3\text{F}_7$]	12000 (1.54)	60
$-\text{[CH}_2-\text{CH}(\text{CO}_2\text{H})]_n-$	2000	11

Since these oligomers are easily soluble in water, the contact angle of water was not able to be measured; however, the contact angles for dodecane on the modified glass were found to increase strongly in comparison to that of the non-fluorinated acrylic acid oligomers, indicating that fluorinated oligomers possessing higher contents of the $-\text{R}_\text{F}-$ unit (or lower molecular weight oligomers) confer a good oil repellency. In contrast, acrylic acid oligomers containing two perfluoro-oxa-alkylated end-groups showed a high contact angle (60°), higher than those of the corresponding acrylic acid homo- and co-oligomers containing the perfluoro-oxa-alkylene units. The contact angle measurements also strongly indicate that oligomer coatings containing the perfluoro-oxa-alkylene units, which shows strong oleophobic

properties, could not be oriented on the surface of glass slides, suggesting that the perfluoro-oxa-alkylene chains are approximately parallel to each other compared with $R_F-(CH_2CHCO_2H)_n-R_F$ oligomer.

Acrylic acid oligomers thus obtained by using the corresponding polymeric perfluoro-oxa-alkane diacyl peroxide are new compounds containing perfluoro-oxa-alkylene units, which were introduced into the oligomeric main chain through the carbon-carbon bond formation. Furthermore, these compounds have been demonstrated to have an excellent solubility in water and to reduce the surface tension of water effectively. Thus, these fluorinated oligomers are expected to become novel poly(anionic) inhibitors of HIV-1 with high stability and low toxicity. Such acrylic acid homo- and co-oligomers containing the perfluoro-oxa-alkylene units have been evaluated for activity against HIV-1 replication in MT-4 cells (see Table 1-6).

Table 1-6 Inhibitory effect of acrylic acid oligomers containing the perfluoro-oxa-alkylene unit on the replication of HIV-1 in MT-4 cells

Oligomer	\overline{M}_n ($\overline{M}_w / \overline{M}_n$)	x:y	EC_{50} ($\mu g\ ml^{-1}$) ^a	CC_{50} ($\mu g\ ml^{-1}$) ^b
$-[R_F-(CH_2-CHCO_2H)_q]_p-$	12000 (1.55)	—	> 100	> 100
$-[R_F-(CH_2-CHCO_2H)_x-(CH_2CR_1R_2)_y]_p-$ ($R_1 = H, R_2 = SiMe_3$)	2000 (1.36)	91:9	1.8	> 100
	5980 (1.89)	98:2	1.7	> 100
	4960 (1.68)	98:2	3.4	> 100
($R_1 = Me, R_2 = CO_2Me$)	16400 (3.02)	55:45	5.5	> 100
	6060 (1.93)	91:9	18	> 100
$R_F-[CH_2-CH(CO_2H)]_n-R_F$ [$R_F = CF(CF_3)[OCF_2CF(CF_3)]_3OC_3F_7$]	8800 (1.42)		6.2	> 100
Dextran sulfate (MW = 5000)			1.2	> 100

^a 50 % effective concentration, based on the inhibition of HIV-1-induced cytopathic effects in MT-4 cells.

^b 50 % cytotoxic concentration, based on the impairment of viability of mock-infected MT-4 cells.

As shown in Table 1-6, an acrylic acid homo-oligomer containing the perfluoro-oxa-alkylene units was found to be inactive. However, acrylic acid-trimethylvinylsilane and acrylic acid-methyl methacrylate co-oligomers containing the perfluoro-oxa-alkylene units were potent inhibitors of HIV-1 replication. These compounds showed a 50% effective concentration (EC_{50}) of $1.7 \sim 18 \mu\text{g ml}^{-1}$ whereas the 50% cytotoxic concentration (CC_{50}) was $>100 \mu\text{g ml}^{-1}$ in each case. Of these, $-\text{[R}_F\text{-(CH}_2\text{CHCO}_2\text{H)}_x\text{-(CH}_2\text{CHSiMe}_3\text{)}_y\text{]}_p\text{-}$ ($\overline{M}_n = 5980$; $x : y = 98 : 2$) was the most active, with a 50% effective concentration (EC_{50}) of $1.7 \mu\text{g ml}^{-1}$, a value similar to that of dextran sulfate, which has been considered to be a potent and selective polymeric inhibitor of HIV-1 replication in cell culture to date. It has been already reported that acrylic acid oligomers containing two perfluoro-oxa-alkylated end-groups proved to be effective against HIV-1 replication in MT-4 cells.⁹⁾ However, the present acrylic acid co-oligomers containing the perfluoro-oxa-alkylene unit as listed in Table 1-6 were shown to be more highly potent and selective inhibitors of HIV-1 replication in MT-4 cells compared with these two fluoroalkyl end-capped oligomers. It is suggested that dextran sulfate is easily degraded into inactive fragments by glycosidic cleavage since it is a polysaccharide,⁶⁾ and might be desulfated by sulfatase enzyme in vivo. In contrast, since the present acrylic acid co-oligomers containing

the fluoroalkylene units are structurally stable, these new fluorinated oligomers are expected to show distinct advantages over dextran sulfate.

1.4 Conclusions

A new polymeric perfluoro-oxa-alkane diacyl peroxide has been prepared by the reaction of the corresponding perfluoro-oxa-alkane diacid fluoride and hydrogen peroxide under alkaline conditions. The decomposition behavior of this peroxide was quite similar to those of the fluoroalkanoyl peroxides $[(R_F\text{COO}_2)_2]$; R_F = perfluoroalkyl and perfluoro-oxa-alkyl groups]. This peroxide decomposed homolytically with decarboxylation to afford the $-R_F-$ units and, in addition, was useful for the direct introduction of the perfluoro-oxa-alkylene ($-R_F-$) units into acrylic acid homo- and co-oligomer main chains through a radical process. These new acrylic acid oligomers containing the perfluoro-oxa-alkylene units were shown to be soluble in water, methanol, ethanol, and tetrahydrofuran and were not only able to reduce the surface tension of water effectively but also to confer good oil repellency. Furthermore, acrylic acid co-oligomers containing the perfluoro-oxa-alkylene units were found to be potent and selective inhibitors of human immunodeficiency virus type 1 (HIV-1) in vitro.

References

- 1) (a) J. F. Liebman, A. Greenberg, and W. R. Dolbier Jr. (eds.),

- “*Fluorine-containing Molecule*”, VCH, Weinheim/New York, (1988);
- (b) M. Kato, T. Takakura, M. Yamabe, K. Kataoka, Y. Sakurai, K. Imachi, and K. Atsumi, *Prog. Artif. Organs*, **2**, 858 (1983).
- 2) (a) V. C. R. McLoughlin and J. Thrower, *Tetrahedron*, **25**, 5921 (1969);
- (b) Y. Kobayashi and I. Kumadaki, *Tetrahedron Lett.*, 4095 (1969).
- 3) H. Sawada, *J. Fluorine Chem.*, **61**, 253 (1993), and references cited therein.
- 4) (a) G. J. Chen, L. S. Chen, and K. C. Eapen, *J. Fluorine Chem.*, **63**, 113 (1993);
- (b) G. J. Chen, L. S. Chen, and K. C. Eapen, *J. Fluorine Chem.*, **65**, 59 (1993).
- 5) (a) M. Ito, M. Baba, A. Sato, R. Pauwels, E. De Clercq, and S. Shigeta, *Antiviral Res.*, **7**, 361 (1987);
- (b) R. Ueno and S. Kuno, *Lancet*, 1379 (1987);
- (c) M. Baba, R. Pauwels, J. Balzarini, J. Arnout, J. Desmyter, and E. De Clercq, *Proc. Natl. Acad. Sci. USA*, **85**, 6132 (1988);
- (d) H. Mitsuya, D. J. Looney, S. Kuno, R. Ueno, F. Wong-Staal, and S. Broder, *Science*, **240**, 646 (1988).
- 6) N. R. Hartman, D. G. Johns, and H. Mitsuya, *AIDS Res. Human Retrovir.*, **6**, 805 (1990).
- 7) H. Sawada, E. Sumino, M. Oue, M. Mitani, H. Nakajima, M. Nishida, and Y. Moriya, *J. Chem. Soc., Chem. Commun.*, 143 (1994).

- 8) (a) M. Abe, K. Morikawa, K. Ogino, H. Sawada, T. Matsumoto, and M. Nakayama, *Langmuir*, **8**, 763 (1992);
- (b) H. Sawada, Y.-F. Gong, T. Matsumoto, M. Nakayama, M. Kosugi, and T. Migita, *J. Jpn. Oil Chem. Soc.*, **40**, 730 (1991).
- 9) M. Baba, T. Kira, S. Shigeta, T. Matsumoto, and H. Sawada, *J. Acquir. Immun. Defic. Syndr.*, **7**, 24 (1994).
- 10) R. Pauwels, J. Balzarini, M. Baba, R. Snoeck, D. Schols, P. Herdewijn, J. Desmyter, and E. De Clercq, *J. Virol. Methods*, **20**, 309 (1988).
- 11) H. Sawada, M. Nakayama, M. Yoshida, T. Yoshida, and N. Kamigata, *J. Fluorine Chem.*, **46**, 423 (1990).
- 12) H. Sawada and M. Nakayama, *J. Fluorine Chem.*, **51**, 117 (1991).
- 13) H. Sawada, N. Itoh, T. Kawase, M. Mitani, H. Nakajima, M. Nishida, and Y. Moriya, *Langmuir*, **10**, 994 (1994).
- 14) H. Sawada, Y.-F. Gong, Y. Minoshima, T. Matsumoto, M. Nakayama, M. Kosugi, and T. Migita, *J. Chem. Soc., Chem. Commun.*, 537 (1992).

CHAPTER 2

Synthesis and Properties of 2-Acryloyloxyethyltrimethylammonium Chloride and 2-(Methacryloyloxy)ethanesulfonic Acid Oligomers Containing Perfluoro-oxa-alkylene Groups

2.1 Introduction

It is well-known that fluoroalkyl end-capped oligomeric surfactants, of whose fluoroalkyl groups were introduced into the two end-sites of the oligomeric main chain through the direct carbon-carbon bond formation, can exhibit a variety of unique properties such as a good solubility in water and good surface active property, which can not be achieved in the corresponding randomly fluoroalkylated polymeric surfactants.^{1) , 2)} For example, two fluoroalkyl end-capped acrylic acid oligomers $[R_F-(CH_2CHCO_2H)_n-R_F]$ afford a good solubility toward water and can reduce the surface tension of water around to 15 mN m⁻¹ similar to that of the lower molecular-weight fluorinated surfactants.³⁾ These fluorinated oligomers can also exhibit a potent and selective anti-HIV activity in vitro system.⁴⁾ Fluoroalkyl end-capped 2-(methacryloxy)loxoethanesulfonic acid oligomers $[R_F-(CH_2CMeCO_2CH_2CH_2SO_3H)]_n-R_F]$ were reported to exhibit a higher anti-HIV activity than the corresponding oligomers containing carboxyl groups.⁵⁾ In contrast, fluoroalkyl end-capped oligomers containing trimethylammonium groups $[R_F-(CH_2CHCO_2CH_2CH_2N^+Me_3Cl)]_n-R_F]$ can exhibit a good antibacterial activity.⁶⁾

Perfluoro-oxa-alkylene units-containing acrylic acid oligomers $\{[-R_F-(CH_2-CHCO_2H)_q-]_p\}$ can be prepared by reaction of acrylic acid with fluorinated polymeric diacyl-type organic peroxide $\{[C(=O)R_FC(=O)OO]_p\}$.⁷⁾ These oligomers are water-soluble

and can reduce the surface tension of water, effectively.⁸ These fluorinated oligomers can exhibit a potent and selective anti-HIV activity, as well as that of two fluoroalkyl end-capped acrylic acid oligomers.⁸⁾ Thus, these fluorinated oligomers are suggested to have high potential as novel fluorinated functional materials.⁸⁾ This chapter shows on the synthesis and properties of the cationic- and anionic-type fluorinated oligomers, of whose perfluoro-oxa-alkylene units are directly introduced into the oligomer main chains, respectively, are described in this chapter.

2.2 Experimental

2.2.1. Measurements

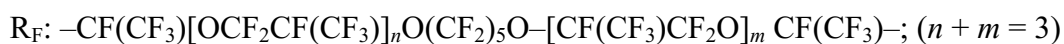
The IR spectra were recorded using an FT-300 FT-IR spectrometer (Horiba Ltd., Japan). The NMR spectra were recorded using a JEOL-EX-270 FT-NMR spectrometer (270 MHz, JEOL Ltd., Japan). The gel permeation chromatography (GPC) analysis was carried out using a Shodex A-80M x 2 column and *N,N*-dimethylformamide solution containing 0.5 M LiBr, and the molecular weight of the oligomer was calculated from the pullulan calibration curve. The surface tension was measured at 25 °C by the Du Nöuy method using an ST-1 DN tensiometer (Shimadzu Corporation, Japan).

2.2.2. Materials

Polymeric perfluoro-oxa-alkane diacyl peroxide was synthesized by the previously reported methods.^{7, 8)}

2.2.3. Synthesis of cationic- and anionic-type fluorinated oligomers containing perfluoro-oxa-alkylene groups

A mixture of fluorinated peroxide (0.2 mmol) and CF₂ClCFCl₂ (100 g) was added to an aqueous solution of 50% (w/w) 2-acryloyloxyethyltrimethylammonium chloride (AETM) (5 mmol), and the mixture was heated at 45 °C for 5 h under nitrogen atmosphere. After the reaction was completed, the solvent was removed under reduced pressure. The product was precipitated with a mixture of methanol/ethyl acetate and dried under reduced pressure, affording 0.24 g of the oligomer as a white powders as following:



The spectral data of the obtained oligomers are as follows:

$$\overline{M}_n = 7560$$

IR (KBr) cm⁻¹: 3444 (N⁺Me₃), 1733 (C=O), 1338 (CF₃), 1259 (CF₂);

¹H NMR (D₂O) δ: 1.51-2.12 (CH₂), 2.33-2.77 (CH), 3.22 (CH₃), 3.71-3.81 (CH₂),

4.40-4.71 (CH₂);

¹⁹F NMR (D₂O) δ: -3.3 to -6.2 (21F), -46.5 (12F), -69.0 (3F).

$$\overline{M}_n = 47900$$

IR (KBr) cm⁻¹: 3428 (N⁺Me₃), 1728 (C=O), 1330 (CF₃), 1267 (CF₂);

¹H NMR (D₂O) δ: 1.84-2.10 (CH₂), 2.20-2.43 (CH), 3.17 (CH₃), 3.59-3.90 (CH₂),

4.20-4.50 (CH₂);

¹⁹F NMR (D₂O) δ: -3.3 to -6.2 (21F), -46.5 (12F), -69.0 (3F).

$$\overline{M}_n = 26700$$

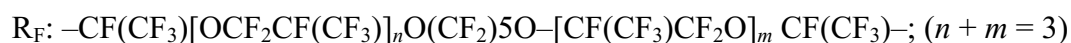
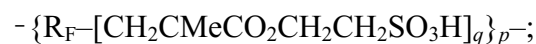
IR (KBr) cm⁻¹: 3437 (N⁺Me₃), 1724 (C=O), 1330 (CF₃), 1273 (CF₂);

¹H NMR (D₂O) δ: 1.73-2.06 (CH₂), 2.20-2.47 (CH), 3.01 (CH₃), 3.43-3.73 (CH₂),

4.20-4.47 (CH₂);

¹⁹F NMR (D₂O) δ: -3.3 to -6.2 (21F), -46.5 (12F), -69.0 (3F).

The fluorinated homo- and co-oligomers containing sulfo groups were synthesized under similar conditions, and the spectral data of each obtained product are as following:



$$\overline{M}_n = 10000$$

IR (KBr) cm⁻¹: 3420 (OH), 1718 (C=O), 1380 (CF₃), 1225 (CF₂), 1165 (SO₃H);

^1H NMR (D_2O) δ : 0.73-1.34 (CH_3), 1.81-2.24 (CH_2), 3.21-3.43 (CH_3), 4.18-4.51 (CH_2).

$$\overline{M}_n = 9250$$

IR (KBr) cm^{-1} : 3415 (OH), 1722 ($\text{C}=\text{O}$), 1398 (CF_3), 1221 (CF_2), 1167 (SO_3H);

^1H NMR (D_2O) δ : 0.69-1.46 (CH_3), 1.76-2.36 (CH_2), 3.17-3.59 (CH_3), 4.20-4.66 (CH_2).

$$\overline{M}_n = 15600$$

IR (KBr) cm^{-1} : 3433 (OH), 1718 ($\text{C}=\text{O}$), 1394 (CF_3), 1223 (CF_2), 1167 (SO_3H);

^1H NMR (D_2O) δ : 0.73-1.38 (CH_3), 1.80-2.17 (CH_2), 3.22-3.39 (CH_3), 4.16-4.44 (CH_2).

$$\overline{M}_n = 8750$$

IR (KBr) cm^{-1} : 3415 (OH), 1720 ($\text{C}=\text{O}$), 1315 (CF_3), 1250 (CF_2), 1161 (SO_3H);

^1H NMR (D_2O) δ : 0.80-1.38 (CH_3), 1.59-2.18 (CH_2), 3.20-3.38 (CH_3), 4.17-4.43 (CH_2).

$-\{\text{R}_F-[\text{CH}_2\text{CMeCO}_2\text{CH}_2\text{CH}_2\text{SO}_3\text{H}]_x-[\text{CH}_2\text{CHSiMe}_3]_y\}_p-$;

R_F : $-\text{CF}(\text{CF}_3)[\text{OCF}_2\text{CF}(\text{CF}_3)]_n\text{O}(\text{CF}_2)_5\text{O}-[\text{CF}(\text{CF}_3)\text{CF}_2\text{O}]_m\text{CF}(\text{CF}_3)-$; ($n + m = 3$)

$$\overline{M}_n = 6550$$

IR (KBr) cm^{-1} : 3415 (OH), 1718 ($\text{C}=\text{O}$), 1330 (CF_3), 1228 (CF_2), 1188 (SO_3H), 742

(Si-Me);

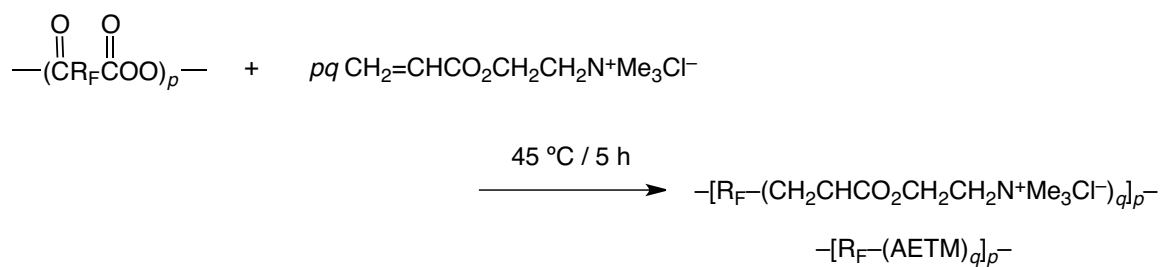
^1H NMR (D_2O) δ : 0.78-1.38 (CH_3 , CH), 1.61-2.30 (CH_2), 3.22-3.39 (CH_3), 4.22-4.50 (CH_2).

2.2.4. Anti-HIV and antibacterial activity of fluorinated oligomers

The anti-HIV and antibacterial activities were assayed by the previously reported methods.^{5, 6)}

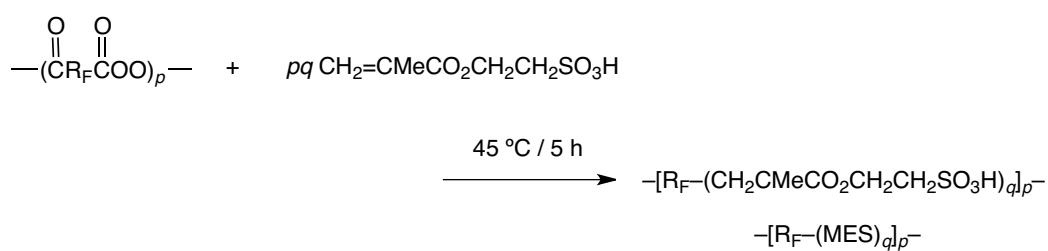
2.3 Results and discussion

Fluorinated polymeric peroxide $\{[\text{C}(=\text{O})-\text{R}_\text{F}\text{C}(=\text{O})\text{OO}]_p\}$,
 $-\text{R}_\text{F}- = -\text{CF}(\text{CF}_3)[\text{OCF}_2\text{CF}(\text{CF}_3)]_n\text{O}(\text{CF}_2)_5\text{O}-[\text{CF}(\text{CF}_3)\text{CF}_2\text{O}]_m\text{CF}(\text{CF}_3)-$ ($n + m = 3$) [PFPO]
reacted with 2-acryloyloxyethyltrimethylammonium chloride (AETM) under nitrogen atmosphere at 45 °C for 5 hrs to afford the corresponding oligomers containing perfluoro-oxa-alkylene and trimethylammonium segments (See Scheme 2-1).



Scheme 2-1

Similarly, PFPO was found to react with 2-methacryloyloxyethanesulfonic acid (MES) under similar conditions to provide the corresponding sulfonic acid oligomer containing perfluoro-oxa-alkylene units (See Scheme 2-2).



Scheme 2-2

Table 2-1 The reactions of P-FPO with AETM or MES

Monomer (mmol)	Monomer/ P-FPO (mol/mol)	Product	
		Yield (%) ^{a)}	$\overline{Mn}^b)$
AETM		$-[R_F-(AETM)_q]_p-$	
5	25	21	7560
10	50	69	47900
20	100	92	26700
MES		$-[R_F-(MES)_q]_p-$	
10	25	36	10000
10	50	12	9250
20	100	8	15600
60	500	1	8750

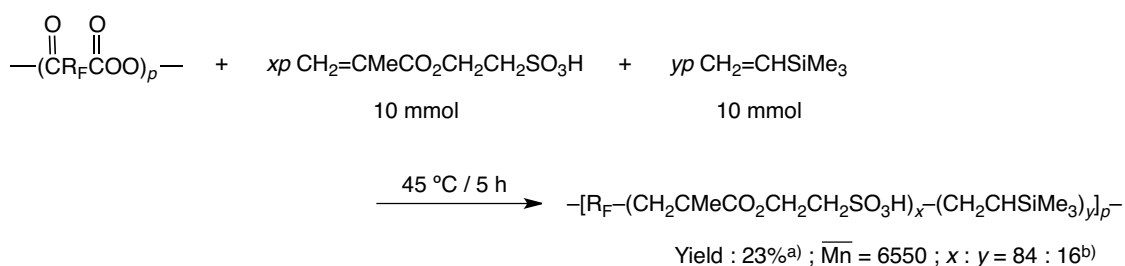
a) The yields are based on the starting material (AETM or MES) and the decarboxylated peroxide unit ($-R_F-$).

b) \overline{Mn} indicates the number-average molecular weight.

As shown in Table 2-1, the product yields were found to increase with the increase of the molar ratio of AETM in the AETM/PFPO, similar to the usual radical polymerization. On the other hand, in the reactions with MES, the product yields were found to decrease with the increase of the molar ratio of MES in the MES/PFPO. This is due to the presence of the strong acidic MES monomer, and such higher acidic monomer would induce the acidic decomposition of PFPO during the oligomerization process. The GPC analyses of the products show that the addition of salt to the eluent can afford the lower molecular weights of

the oligomers. This finding suggests that the oligomers containing perfluoro-oxa-alkylene units are likely to form the self-assembled molecular aggregates to provide the apparent molecular weights.

PFPO was applied to the cooligomerization of MES with trimethylvinylsilane, and the results are shown in Scheme 2-3.



a) The yields are based on the starting material (MES and trimethylvinylsilane) and the decarboxylated peroxide unit ($-\text{R}_\text{F}-$).

b) Co-oligomerization ratio was determined by ^1H NMR.

Scheme 2-3

The cooligomerization was found to proceed under mild reaction conditions to afford the corresponding cooligomers containing perfluoro-oxa-alkylene units, quite similar to those of the homooligomerizations illustrated in Schemes 2-1 and 2-2. In this way, this fluorinated cooligomer has high potential for new fluorinated silicon materials containing sulfo segments.

The oligomers containing fluoroalkylene units thus obtained were found to exhibit the

good solubility in both water and water-soluble polar organic solvents such as methanol, ethanol, tetrahydrofuran, and *N,N*-dimethylformamide. The cooligomers containing fluoroalkylene and trimethylsilyl groups also afforded the similar solubility to that of the corresponding homo-oligomers. It was previously reported that the solubility of two fluoroalkyl end-capped oligomers can significantly increase in organic solvents by the introduction of trimethylsilyl groups into the oligomeric side chains.⁹⁾ However, the present fluorinated cooligomers containing sulfo groups were enable to increase the solubility toward organic media. This would be due to the presence of polar sulfo groups in cooligomers.

A variety of the oligomers containing perfluoro-oxa-alkylene units provide a good solubility toward water. Therefore, the surfactant property of these oligomers was studied by measuring the surface tension of their aqueous solutions. The results are shown in Table 2-2.

Table 2-2 Surface tension of aqueous solutions of oligomers containing perfluoro-oxaalkylene units

Oligomer (\overline{Mn})	concentration (g dm ⁻³)				
	10 ⁻³	10 ⁻²	10 ⁻¹	10 ⁰	10
	Surface tensions (mN m ⁻¹)				
-[R _F -(AETM) _q] _p - (7560)	72.6	71.1	64.8	42.5	
-[R _F -(MES) _q] _p - (10000)	72.6	72.3	69.8	52.4	
R _F -(CH ₂ CHCO ₂ CH ₂ CH ₂ N ⁺ Me ₃ Cl ⁻) _n -R _F (6400) R _F = CF(CF ₃)OC ₃ F ₇	72.6	71.6	29.8	17.8	17.6 ^{a)}

a) See Ref. 6

The fluorinated oligomers containing trimethylammonium and sulfo groups can reduce the surface tension of water. However, their surface activity was poor compared with that of the corresponding fluoroalkyl end-capped oligomer containing trimethylammonium units. This can be attributed to a higher arrangement of the end-capped fluoroalkyl segments in the oligomer on the water surface than that of the corresponding fluorinated oligomer, of whose perfluoro-oxa-alkylene units are introduced into the oligomer main chain.

It has been already reported that the oligomers containing carboxyl or sulfo groups can exhibit a highly selective anti-HIV activity in vitro.^{4, 5)} Therefore, the anti-HIV activity of the present fluorinated oligomers containing sulfo and trimethylammonium units in MT-4 cells were studied, respectively, and the results are shown in Table 2-3.

Table 2-3 Inhibitory effect of oligomers containing perfluoro-oxaalkylene units on the replication of HIV-1 in MT-4 cells

Oligomer (\overline{Mn})	EC ₅₀ ($\mu\text{g ml}^{-1}$) ^{a)}	CC ₅₀ ($\mu\text{g ml}^{-1}$) ^{b)}
-[R _F -(MES) _q] _p - (9250)	0.71	> 100
-[R _F -(AETM) _q] _p - (47900)	> 3	3
(26700)	> 21	21
R _F -(MES) _n -R _F (12000) R _F = CF(CF ₃)[OCF ₂ CF(CF ₃)] ₂ OC ₃ F ₇	1.7 ^{c)}	> 100 ^{c)}
R _F -(CH ₂ CHCO ₂ H) _n -R _F (8800) R _F = CF(CF ₃)[OCF ₂ CF(CF ₃)] ₃ OC ₃ F ₇	6.2 ^{d)}	> 100 ^{d)}
Dextran sulfate	1.2	> 100

a) Fifty percent effective concentration, based on the inhibition of HIV-1-induced cytopathic effects in MT-4 cells.

b) Fifty percent cytotoxic concentration, based on the impairment of viability of mock-infected MT-4 cells.

c) See Ref. 5.

d) See Ref. 4.

The fluorinated oligomers containing sulfo groups showed a potent and selective anti-HIV activity: $EC_{50} = 0.71 \mu\text{g ml}^{-1}$, $CC_{50} > 100 \mu\text{g ml}^{-1}$. Particularly, the anti-HIV activity was higher than that of dextran sulfate, which is well-known as a potent polymeric anti-HIV drug. In addition, it was verified that this activity is also higher than that of the fluoroalkyl end-capped oligomers containing sulfo or carboxyl groups. This can be attributed to the adsorption inhibitory effect based on the effective electrostatic interaction between the positively charged gp 120 in HIV and the highly acidic sulfo groups in the perfluoro-oxa-alkylene units-containing oligomers.

In contrast, the fluorinated oligomers containing trimethylammonium segments cannot show a potent and selective anti-HIV activity. This would be due to the electrostatic repulsion between the positively charged gp 120 in HIV and the cationic segments in the oligomers. Especially, the cationic oligomers are effective for the replication of the normal cells, because their CC_{50} values are 3 and 21 $\mu\text{g/ml}$, respectively. Thus, the antibacterial activity against *Staphylococcus aureus* was studied for these cationic oligomers. The results are shown in Table 2-4.

Table 2-4 Antibacterial activity of cationic oligomers containing perfluoro-oxaalkylene units against *Staphylococcus aureus*

Oligomer (\overline{M}_n)	<i>Staphylococcus aureus</i>
none	2.0×10^8
$-\text{[R}_F\text{-(AETM)}_q\text{]}_p^-$ (47900)	1.2×10^7
(26700)	1.2×10^4

a) Concentration of oligomer : 1 mg/ml

The cationic oligomers containing fluoroalkylene groups were found to exhibit antibacterial activity. Particularly, the oligomer with a molecular weight of 26,700 can reduce the number of the colony to approximately 1/20,000. Thus, the oligomer has high potential as a new polymeric functional material possessing an antibacterial activity.

In this way, the perfluoro-oxa-alkylene units-containing oligomers possessing sulfo or trimethylammonium groups have great potential for applications in a variety of fields such as new fluorinated functional materials possessing not only surface active property but also anti-HIV and antibacterial activities.

2.4 Conclusions

A series of 2-acryloyloxyethyltrimethylammonium chloride and 2-(methacryloyloxy)ethanesulfonic acid oligomers containing perfluoro-oxa-alkylene groups were prepared by reaction of the polymeric perfluoro-oxa-alkane diacyl peroxide and the

corresponding monomers under moderate reaction conditions. The oligomers were soluble in both water and water-soluble polar organic solvents such as methanol, ethanol, tetrahydrofuran, and *N,N*-dimethylformamide. The oligomers containing either trimethylammonium or sulfo groups were able to reduce the surface tension of water, effectively, and are applicable to new fluorinated polymeric surfactants. In addition, the fluorinated oligomers containing sulfo groups were shown to exhibit anti-HIV activity. On the other hand, the oligomers containing trimethylammonium groups were clarified to possess antibacterial activity against *Staphylococcus aureus*.

References

- 1) D. Cochin, P. Hendlinger, and A. Laschewsky, *Colloid Polym. Sci.*, **273**, 1138 (1995).
- 2) H. Sawada, *Chem. Rev.*, **96**, 1779 (1996).
- 3) a) H. Sawada, Y.-F. Gong, Y. Minoshima, T. Matsumoto, M. Nakayama, M. Kosugi, and T. Migita, *J. Chem. Soc., Chem. Commun.*, 537 (1992);
b) H. Sawada, Y. Minoshima, and H. Nakajima, *J. Fluorine Chem.*, **65**, 169 (1993).
- 4) M. Baba, T. Kira, S. Shigeta, T. Matsumoto, and H. Sawada, *J. Acquir. Immune Defic. Syndr.*, **7**, 24 (1994).
- 5) H. Sawada, A. Ohashi, M. Baba, T. Kawase, and Y. Hayakawa, *J. Fluorine Chem.*, **79**, 149 (1996).

- 6) H. Sawada, S. Katayama, M. Oue, T. Kawase, Y. Hayakawa, M. Baba, T. Tomita, and M. Mitani, *J. Jpn. Oil Chemists' Soc.*, **45**, 161 (1996).
- 7) H. Sawada, E. Sumino, M. Oue, M. Mitani, H. Nakajima, M. Nishida, and Y. Moriya, *J. Chem. Soc., Chem. Commun.*, 143 (1994).
- 8) H. Sawada, E. Sumino, M. Oue, M. Baba, T. Kira, S. Shigeta, M. Mitani, H. Nakajima, M. Nishida, and Y. Moriya, *J. Fluorine Chem.*, **74**, 21 (1995).
- 9) H. Sawada, N. Itoh, T. Kawase, M. Mitani, H. Nakajima, M. Nishida, and Y. Moriya, *Langmuir*, **10**, 994 (1994).

CHAPTER 3

Preparation and Properties of Fluorinated Carboxylic Acid/Silica Nanocomposite-Encapsulated Low Molecular Weight Compounds

3.1 Introduction

Partially longer fluoroalkylated polymers are useful class of materials due to their unique balance of properties such as low surface free energy, low coefficient of friction, and solvent and chemical resistance, which cannot be achieved by the corresponding non-fluorinated polymers.^{1 ~ 15)} In comprehensive studies of longer fluoroalkylated polymers, it has been already reported that fluoroalkyl end-capped oligomers exhibit a variety of unique properties such as high solubility, surface active properties, antibacterial activity, anti-HIV-1 activity, and the formation of nanometer size controlled self-assembled molecular aggregates with the aggregations of terminal fluoroalkyl groups, which cannot be achieved by the corresponding randomly fluoroalkylated polymers and fluoroalkylated block polymers.^{16 ~ 22)} There have been hitherto numerous reports on the surface modification of silica nanoparticles by chemical bound polymers due to their potential applications in a wide variety of fields such as coatings, electronics, catalyst, and diagnostics.^{23 ~ 44)} Therefore, it is of particular interest to explore novel fluorinated polymers, especially partially longer fluoroalkylated polymers/silica nanocomposites from the developmental viewpoints of new functional materials imparted by both fluorine and silica nanoparticles.^{45 ~ 50)} In

fact, fluoroalkyl end-capped acrylic acid homooligomer [$R_F-(CH_2CHCOOH)_n-R_F$; $R_F=CF(CF_3)OC_3F_7$; $R_F-(ACA)_n-R_F$] was applied to the preparation of the corresponding fluorinated oligomer/silica nanocomposite.^{51, 52)} This fluorinated nanocomposite was also applied to the encapsulation of low molecular weight aromatic compounds such as bisphenol AF into the composite cores. Interestingly, these encapsulated aromatic compounds were found to exhibit nonflammable characteristic in the composite cores even after calcination at 800 °C, although the parent $R_F-(ACA)_n-R_F$ oligomer exhibits a perfectly flammable characteristic in the composite cores under the same calcination conditions.⁵³⁾ In order to clarify this interesting thermal decomposition behavior in the silica gel matrices, it is very important to study the preparation and thermal stability of the corresponding low molecular weight fluorinated carboxylic acid [R_F-CO_2H ; $R_F=CF(CF_3)OC_3F_7$]/silica nanocomposites including the encapsulation of the low molecular weight compounds into such fluorinated silica composite cores. This chapter shows on the preparation and the thermal stability of fluorinated carboxylic acid/silica nanocomposites including the encapsulation of aromatic compounds into these composite cores.

3.2 Experimental

3.2.1. Measurements

^1H magic-angle spinning (MAS) NMR spectra were measured at room temperature using Varian Unity INOVA 300 (Tokyo, Japan). Thermal analyses were recorded by raising the temperature around 800 °C (the heating rate, 10 °C/min) under atmospheric conditions by the use of Bruker axis TGDTA2000SA differential thermo balance (Kanagawa, Japan). Size [number-average diameter (average hydrodynamic diameter)] of nanocomposites was measured by using Otsuka Electronics DLS-7000 HL (Tokyo, Japan). Field emission scanning electron micrographs (FE-SEM) were obtained using JEOL JSM-7000F (Tokyo, Japan). Contact angles were measured using a Kyowa Interface Science Drop Master 300 (Saitama, Japan). Ultraviolet–visible (UV–vis) spectra were carried out using a UV–vis spectrophotometer (UV-1800, Shimadzu, Japan). The pH measurement was performed by using a pH meter (PH-02, AS ONE, Japan). The zeta potential was assessed by the use of Microtec Niton ZEECOM/ZC- 2000 (Chiba, Japan).

3.2.2. Materials

Perfluoro-2-methyl-3-oxahexanoyl fluoride was used as received Hydrus Chemical Inc. (Tokyo, Japan). Silica-nanoparticle methanol solution [30 % (wt.): average particle size: 11 nm (Methanol Silica-solTR)] was supplied by Nissan Chemical Industrials Ltd. (Tokyo, Japan). Bisphenol A [BPA], bisphenol AF [BPAF], 4,4'-biphenol [BPOH], octafluoro-4, 4'-biphenol [FBPOH], α -cyclodextrin (α -CD), β -cyclodextrin (β -CD), and γ -cyclodextrin (γ -CD) were purchased from Tokyo Chemical Industrial Co., Ltd. (Tokyo, Japan). 4,4'-Bis(triethoxysilyl)-1,1'-biphenyl [BTBSP] and 3-(trihydroxysilyl)propane-1-sulfonic acid [THSP] were received from Sigma-Aldrich Japan Co. (Tokyo, Japan) and Azmax Co., Ltd. (Chiba, Japan), respectively. Aqueous ammonia was purchased from Wako Pure Chemical Industries, Ltd. (Osaka, Japan). Perfluoro-2-methyl-3-oxahexanoic acid (bp, 60 °C/10 mm) was prepared by the hydrolysis of perfluoro-2-methyl-3-oxahexanoyl fluoride. Fluoroalkyl end-capped acrylic acid oligomer [$R_F-(CH_2CHCO_2H)_n-R_F$; $R_F = CF(CF_3)OC_3F_7$; $M_n = 2770$] was prepared by reaction of fluoroalkanoyl peroxide with the corresponding monomer according to the previously reported methods.⁵⁴⁾

3.2.3. Preparation of perfluoro-2-methyl-3-oxahexanoic acid/silica gel

nanocomposites

To a methanol solution (20 ml) of perfluoro-2-methyl-3-oxahexanoic acid [$\text{C}_3\text{F}_7\text{OCF}(\text{CF}_3)\text{C}(=\text{O})\text{OH}$: 250 mg] were added tetraethoxysilane (TEOS, 0.25 ml), silica-nanoparticle methanol solution [30 % (wt): 1.67 g] and 25 % aqueous ammonia solution (0.25 ml). The mixture was stirred with a magnetic stirring bar at room temperature for 5 hrs. After the solvent was evaporated off, to the obtained crude products was added methanol (15 ml). The methanol solution was stirred with magnetic stirring bar at room temperature for 1 day, and then was centrifuged for 30 min. The expected fluorinated nanocomposites were easily separated from the methanol solution, and then were washed with methanol in several times. Fluorinated nanocomposites powders thus obtained were dried in vacuo at 50 °C for 2 days to afford purified particle powders (538 mg).

3.2.4. Preparation of perfluoro-2-methyl-3-oxahexanoic acid/silica gel nanocomposite-encapsulated bisphenol A

To a methanol solution (20 ml) of perfluoro-2-methyl-3-oxahexanoic acid

[C₃F₇OCF(CF₃)C(=O)OH: 250 mg] were added bisphenol A (BPA: 250 mg), tetraethoxysilane (TEOS: 0.25 ml), silica-nanoparticle methanol solution [30 % (wt): 1.67 g], and 25 % aqueous ammonia solution (0.25 ml). The mixture was stirred with a magnetic stirring bar at room temperature for 5 hrs. After the solvent was evaporated off, to the obtained crude products was added methanol (25 ml). The methanol solution was stirred with magnetic stirring bar at room temperature for 1 day, and then was centrifuged for 30 min. The expected fluorinated nanocomposite-encapsulated BPA was easily separated from the methanol solution, and then was washed with methanol in several times. Fluorinated nanocomposite-encapsulated BPA powders thus obtained were dried in vacuo at 50 °C for 2 days to afford purified particle powders (530 mg). Fluorinated nanocomposite-encapsulated other low molecular weight aromatic and aliphatic compounds were also prepared under similar conditions.

3.2.5. Preparation of modified glass treated with perfluoro-2-methyl-3-oxahexanoic acid/silica nanocomposites by dipping method

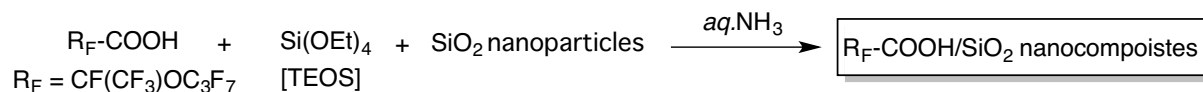
To a methanol solution (20 ml) containing perfluoro-2-methyl-3-oxahexanoic

acid (250mg) were added tetraethoxysilane (0.25 ml) and 25 wt% aqueous ammonia solution (0.25 ml). The mixture was stirred with a magnetic stirring bar at room temperature for 5 hrs. The glass plate (18×18 mm² pieces) was dipped into the methanol solution of fluorinated nanocomposites at room temperature and left for 1 min. This was lifted from the solution at constant rate and dried at room temperature for 1 day under vacuum to afford the modified glass.

3.3 Results and discussion

Sol–gel reactions of tetraethoxysilane in the presence of perfluoro-2-methyl-3-oxahexanoic acid [$R_F\text{-CO}_2\text{H}$] were found to proceed smoothly under alkaline conditions to give the corresponding fluorinated carboxylic acid/silica nanocomposites in 41~79 % isolated yields as shown in Scheme 3-1 and Table 3-1.

The obtained fluorinated nanocomposites have a good dispersibility and stability in methanol, ethanol, 2-propanol, and water. Thus, the size of these composites in methanol by dynamic light-scattering (DLS) measurements at 25 °C has been measured, and the results are also shown in Table 3-1.



Scheme 3-1 Preparation of R_F-COOH/SiO₂ nanocomposites

Table 3-1 Preparation of R_F-COOH/SiO₂ nanocomposites

Run	R _F -COOH (mg)	TEOS (mL)	SiO ₂ (mg)	25 wt% aq. NH ₃ (mL)	Yield ^{a)} (%)	Size of composites ^{b)} (nm)
1	125	0.25	500	0.25	79	26.5 ± 5.5
2	250	0.25	500	0.25	66	38.1 ± 7.5
3	500	0.25	500	0.25	41	42.3 ± 10.6

a) Yield was based on R_F-COOH, TEOS and SiO₂

b) Determined by dynamic light scattering in methanol solution

Fluorinated composites in Table 3-1 were nanometer size-controlled very fine nanoparticles from 27 to 42 nm. In order to clarify the formation of fluorinated nanocomposite particles, the field emission scanning electron micrograph (FE-SEM) of methanol solutions of R_F-CO₂H/SiO₂ nanocomposites before and after calcination at 800 °C has been measured, and the results were shown in Fig. 3-1.

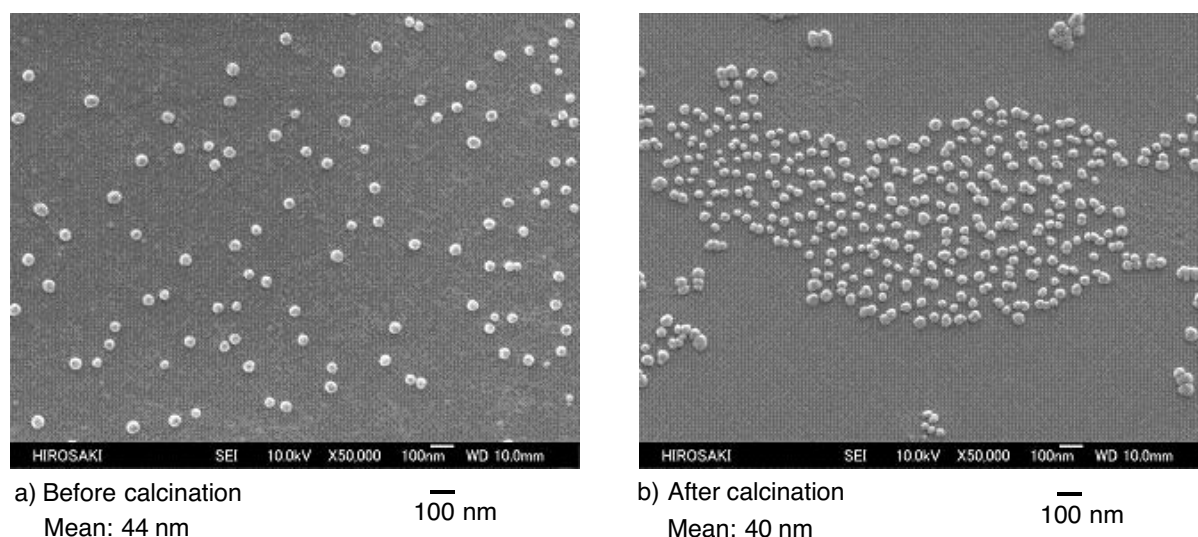


Fig. 3-1 FE-SEM image of $R_F\text{-CO}_2\text{H/SiO}_2$ nanocomposites (Run 2 in Table 1) before and after calcination at 800 °C [$R_F = \text{CF}(\text{CF}_3)\text{OC}_3\text{F}_7$]

Electron micrographs also showed the formation of fluorinated composite fine particles with a mean diameter of 44 nm (Fig. 3-1-a): before calcination), and the similar size value as that (38 nm) of DLS was obtained in FE-SEM measurements. The similar size fine particles (a mean diameter: 40 nm) was observed after calcination at 800 °C (see Fig. 3-1-b)). In addition, it was demonstrated that the appearance of white colored nanocomposite powders did not change at all before and after calcination at 800 °C.

Thermal stability of these fluorinated nanocomposites was studied by the use of thermogravimetric analyses (TGA), in which the weight loss of these nanocomposites was measured by raising the temperature around 800 °C at a 10 °C/min heating rate under air atmospheric conditions, and the results were shown in Fig. 3-2.

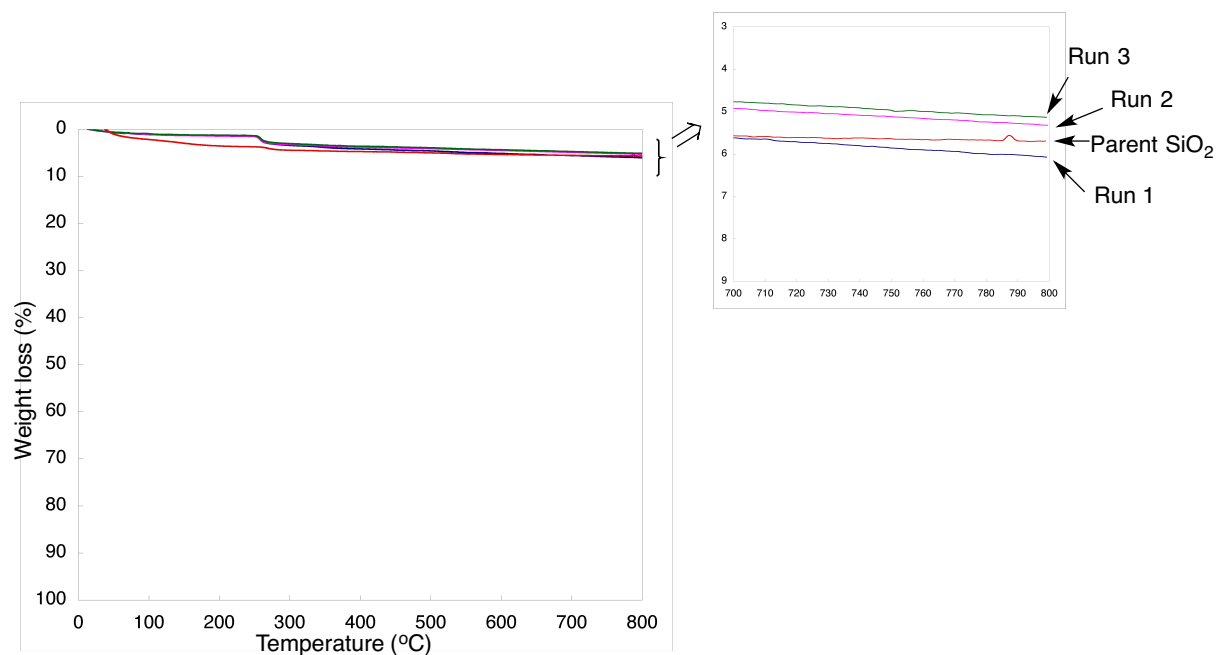


Fig. 3-2 Thermogravimetric analyses (TGA) of $R_F\text{-COOH/SiO}_2$ nanocomposites

Fig. 3-2 shows the TGA curves of $R_F\text{-CO}_2\text{H/SiO}_2$ nanocomposites, and each nanocomposite was found to give no weight loss even after calcination at 800 °C as well as that of original silica gel nanoparticles, although the theoretical contents of $R_F\text{-CO}_2\text{H}$ in the composites are 18~47 %. In order to clarify the presence of $R_F\text{-CO}_2\text{H}$ in the composites before calcination, the mean zeta potential of well-dispersed aqueous solution based on $R_F\text{-CO}_2\text{H/SiO}_2$ nanocomposites (Run 2 in Table 3-1) has been measure, and the results were shown in Table 3-2.

Table 3-2 Zeta potential of R_F -COOH/SiO₂ nanocomposites
($R_F = CF(CF_3)OC_3F_7$)

		Zeta potential (mV)
Original SiO ₂ Particle ^{a)}	Before Calcination	-23.2
	After Calcination	-22.2
Run 2 in Table 1	Before Calcination	-33.2
	After Calcination	-52.0

Concentration of SiO₂ and nanocomposites is 0.01 g/dm³

a) Prepared by TEOS

The mean zeta potential of R_F -CO₂H/SiO₂ nanocomposites before calcination had a negatively enhanced charge (−33.2 mV) compared with that of the original silica nanoparticle (−23.2 mV), indicating that negatively charged carboxyl groups in fluorinated carboxylic acids should be arranged on the composite particle surface through the nanocomposite reaction in Scheme 3-1. A similar negatively enhanced charge (−52.0 mV) after calcination, compared with that (−22.2 mV) of the original silica nanoparticles after calcination, suggests that fluorinated carboxylic acid can exhibit a nonflammable characteristic in the composites even after calcination. Especially, the zeta potential of R_F -CO₂H/SiO₂ nanocomposites after calcination had a negatively enhanced charge (−52.0 mV), compared with that (−33.2 mV) of the nanocomposites before calcination. This finding would be due to the formation of the silyl esters: $R_F-C(=O)-OSi\equiv$ in the silica nanocomposite cores as the byproducts in

the sol–gel reaction illustrated in Scheme 3-1, and the silyl esters thus obtained could produce the $R_F\text{-CO}_2\text{H}$ in the composites during the calcination process to afford the negatively enhanced zeta potential value. Hitherto, it has been reported that fluoroalkyl end-capped *N*-(1,1-dimethyl-3-oxobutyl)acrylamide oligomer $[R_F\text{-(DOBAA)}_n\text{-}R_F]/\text{SiO}_2$ nanocomposites, which were prepared by the sol–gel reaction under alkaline conditions, exhibit no weight loss characteristic even after calcination at 800 °C.^{55, 56)} It is suggested that ammonium hexafluorosilicate is formed through the dehydrofluorination between the amido protons and fluorines in oligomer during the nanocomposite reactions, and the effective interaction between ammonium hexafluorosilicate and $R_F\text{-(DOBBA)}_n\text{-}R_F$ oligomer in silica gel matrices should afford a nonflammable characteristic for this fluorinated oligomer.^{55 ~ 58)} On the other hand, fluoroalkyl end-capped acrylic acid oligomer/silica nanocomposites $[R_F\text{-(CH}_2\text{CHCOOH)}_n\text{-}R_F/\text{SiO}_2$; $R_F=\text{CF}(\text{CF}_3)\text{OC}_3\text{F}_7]$, which were prepared under similar sol–gel reactions, exhibit the usual flammable characteristic corresponding to the oligomer in the composite cores after calcination at 800 °C.^{55, 56)} This finding would be due to the no formation of ammonium hexafluorosilicate through the dehydrofluorination between the fluorines and hydrogens in oligomer during the nanocomposite reaction under alkaline conditions.^{55 ~ 58)} Dehydrofluorination between

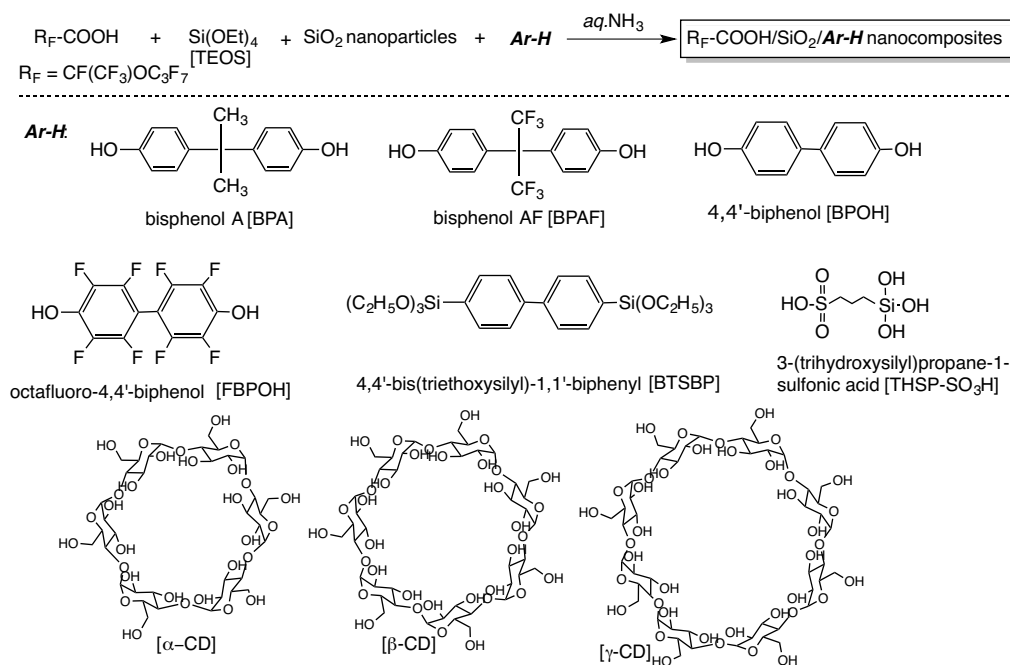
fluorines and higher acidic protons in $R_F\text{-CO}_2\text{H}$ should proceed under alkaline conditions (aqueous ammonia) in the presence of silica nanoparticles as a co-catalyst to give tetrafluorosilane, and finally, ammonium hexafluorosilicate, since the pH value (2.15) of $R_F\text{-CO}_2\text{H}$ is smaller than that (3.26) of $R_F\text{-(CH}_2\text{CHCOOH)}_n\text{-R}_F$ oligomer [$R_F=\text{CF}(\text{CF}_3)\text{OC}_3\text{F}_7$; $M_n=2770$]. The formation of the ammonium hexafluorosilicate enables $R_F\text{-CO}_2\text{H}$ in the silica nanocomposite cores to give a nonflammable characteristic even after calcination. In contrast, the higher pH value of $R_F\text{-(CH}_2\text{CHCOOH)}_n\text{-R}_F$ oligomer cannot cause such dehydrofluorination to give the nonflammable characteristic for the oligomer in the silica nanocomposites.^{55 ~ 58)}

$R_F\text{-(CH}_2\text{CMeCO}_2\text{CH}_2\text{CH}_2\text{SO}_3\text{H)}_n\text{-R}_F$ oligomer possessing a similar pH value (2.71) to that (2.15) of $R_F\text{-CO}_2\text{H}$ has been shown to have a nonflammable characteristic in silica nanocomposite cores even after calcination at 800 °C.⁵⁷⁾

In addition, present $R_F\text{-CO}_2\text{H/SiO}_2$ nanocomposites (Run 2 in Table 3-1) were applied to the surface modification of glass to exhibit not only a higher oleophobicity imparted by longer fluoroalkyl groups (dodecane contact angle value, 73°) but also a superhydrophilicity related to the carboxylic groups in $R_F\text{-CO}_2\text{H}$ (water contact angle value, 0°) in order to clarify the presence of fluorinated carboxylic acid in the composites; although the dodecane and water contact angle values of the non-treated

glass surface are 0° and 47° , respectively. This finding also suggests the nonflammable characteristic of $R_F\text{-CO}_2\text{H}$ in the composite cores even after calcination.

The encapsulation of a variety of low molecular weight aromatic and aliphatic compounds (*Ar-H*) such as bisphenol A [BPA], bisphenol AF [BPAF], 4,4'-biphenol [BPOH], octafluoro-4,4'-biphenol [FBPOH], 4,4'-bis(triethoxysilyl)-1,1'-biphenyl [BTSBP], 3-(triethoxysilyl)propane-1-sulfonic acid [THSP], α -cyclodextrin (α -CD), β -cyclodextrin (β -CD), and γ -cyclodextrin (γ -CD) into $R_F\text{CO}_2\text{H}/\text{SiO}_2$ nanocomposite cores has been studied, and the results are shown in Scheme 3-2 and Table 3-3.



Scheme 3-2 Preparation of $R_F\text{-COOH}/\text{SiO}_2/\text{Ar-H}$ nanocomposites

Table 3-3 Preparation of R_F-COOH/SiO₂/*Ar-H* nanocomposites [R_F=CF(CF₃)OC₃F₇]

Run	R _F -COOH (mg)	<i>Ar-H</i> (mg)	TEOS (ml)	SiO ₂ (g)	MeOH (ml)	25 wt% NH ₃ (ml)	Product yield ^{a)} (%)	Size of dispersed particles ^{b)} (nm)
BPAF								
1	250	150	0.25	0.5	20	0.25	64	167.2 ± 26.2
2	250	250	0.25	0.5	20	0.25	49	636.6 ± 126.9
3	250	350	0.25	0.5	20	0.25	51	33.2 ± 7.7
BPA								
4	250	150	0.25	0.5	20	0.25	67	519.1 ± 101.7
5	250	250	0.25	0.5	20	0.25	53	297.6 ± 74.8
6	250	350	0.25	0.5	20	0.25	60	280.4 ± 59.1
BPOH								
7	250	250	0.25	0.5	20	0.25	38	50.7 ± 12.2
FBPOH								
8	250	250	0.25	0.5	20	0.25	60	83.1 ± 19.3
BTSBP								
9	250	250	0.25	0.5	20	0.25	76	125.5 ± 23.5
THSP								
10	250	250	0.25	0.5	20	0.25	69	162.8 ± 35.5
α-CD								
11	100	25	0.1	0.2	8.0	0.1	87	51.0 ± 12.3
12	100	50	0.1	0.2	8.0	0.1	81	36.3 ± 9.0
13	100	100	0.1	0.2	8.0	0.1	83	255.0 ± 52.8
β-CD								
14	100	25	0.1	0.2	8.0	0.1	98	63.5 ± 11.7
15	100	50	0.1	0.2	8.0	0.1	99	47.1 ± 10.4
16	100	100	0.1	0.2	8.0	0.1	84	221.6 ± 40.4
γ-CD								
17	100	25	0.1	0.2	8.0	0.1	96	47.2 ± 7.9
18	100	50	0.1	0.2	8.0	0.1	86	83.3 ± 17.7
19	100	100	0.1	0.2	8.0	0.1	85	47.3 ± 12.9

a) Yields were based on R_F-COOH, *Ar-H*, TEOS, and SiO₂

b) Determined by dynamic light scattering measurements in methanol solution

As shown in Scheme 3-2 and Table 3-3, encapsulation of *Ar-H* into R_F-CO₂H/SiO₂ nanocomposite cores was found to proceed smoothly to afford the expected R_FCO₂H/SiO₂ composites-encapsulated *Ar-H* in 38~99 % isolated yields.

These fluorinated nanocomposites-encapsulated *Ar-H* were found to exhibit good dispersibility and stability in methanol, ethanol, and 2-propanol. Thus, the size of these fluorinated composites in methanol has been measured by using DLS measurements at 25 °C. Fluorinated composites in Table 3-3 were nanometer size-controlled very fine nanoparticles from 33 ~ 637 nm. In order to clarify the formation of fluorinated nanocomposite particles, the field-emission scanning electron micrograph (FE-SEM) of methanol solutions of $R_F\text{-CO}_2\text{H/SiO}_2$ nanocomposite-encapsulated BPA (Run 4 in Table 3-3) have been studied, and the results are shown in Fig. 3-3.

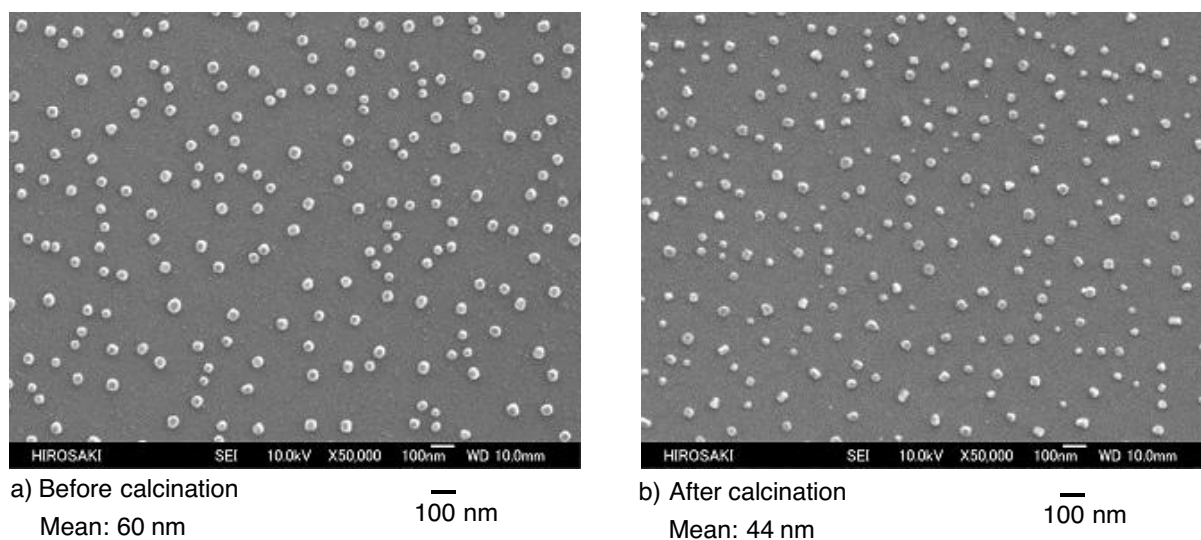


Fig. 3-3 FE-SEM image of $R_F\text{-COOH/SiO}_2$ /BPA nanocomposites before and after calcination at 800 °C (Run 4 in Table 2) [$R_F=\text{CF}(\text{CF}_3)\text{OC}_3\text{F}_7$]

FE-SEM images for $R_F\text{-CO}_2\text{H/SiO}_2$ /BPA nanocomposites also show the

formation of fluorinated composite fine particles with mean diameter of 60 nm.

Similar size-controlled fine particles (44 nm) were observed by FE-SEM measurements of $R_F\text{-CO}_2\text{H/SiO}_2\text{/BPA}$ nanocomposites after calcination.

The thermal stability of $R_F\text{-CO}_2\text{H/SiO}_2$ nanocomposite-encapsulated *Ar-H* possessing acidic phenol-type hydroxyl groups was studied by the use of thermogravimetric analyses (TGA), in which the weight loss of these nanocomposites was measured by raising the temperature around 800 °C at a 10 °C/min heating rate under air atmospheric conditions, and the results are shown in Figs. 3-4 ~ 3-7.

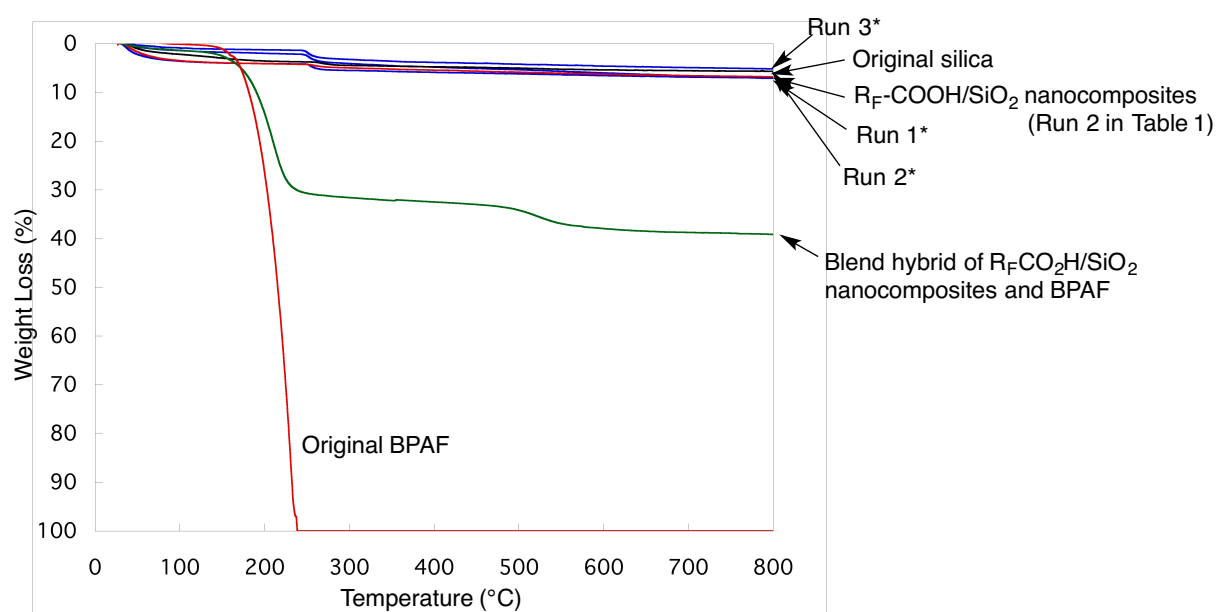


Fig. 3-4 Thermogravimetric analyses of $R_F\text{-COOH/SiO}_2\text{/BPAF}$ nanocomposites [$R_F=\text{CF}(\text{CF}_3)\text{OC}_3\text{F}_7$]
 *Each Run No corresponds to that of Table 2

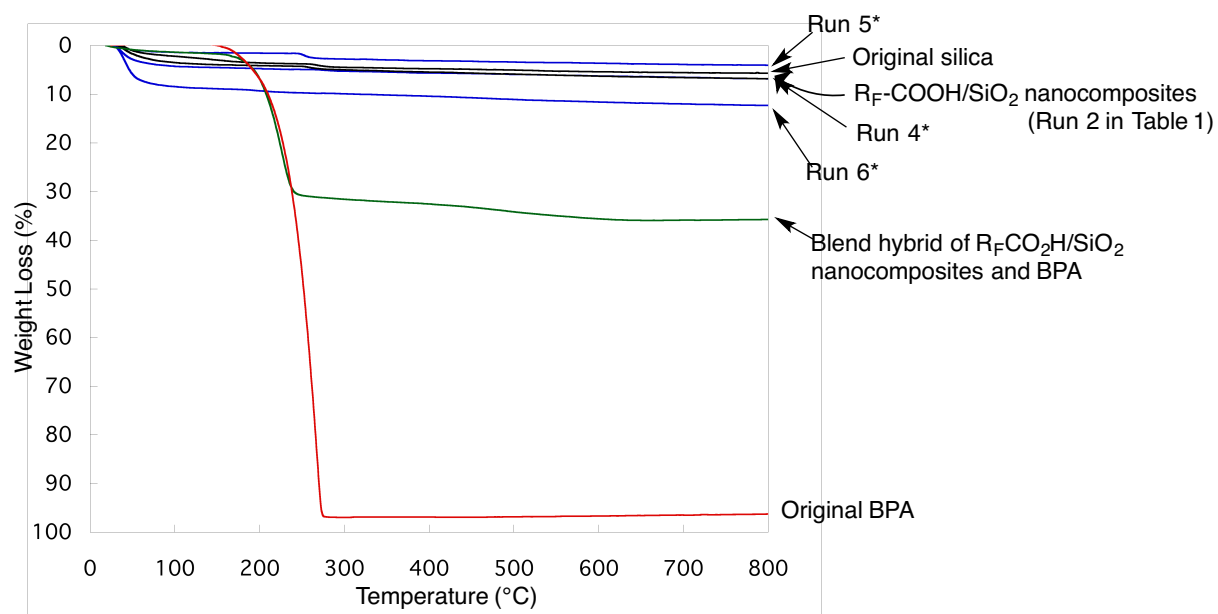


Fig. 3-5 Thermogravimetric analyses of R_F -COOH/ SiO_2 /BPA nanocomposites [$R_F=CF(CF_3)OC_3F_7$]
 *Each Run No corresponds to that of Table 2

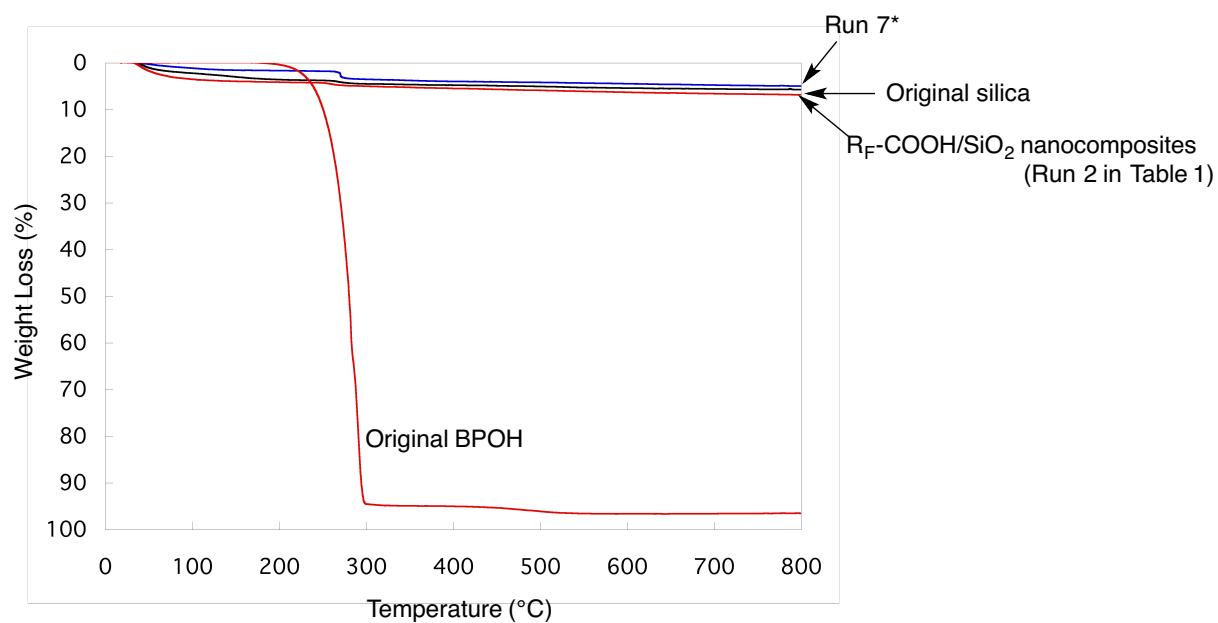


Fig. 3-6 Thermogravimetric analyses of R_F -COOH/ SiO_2 /BPOH nanocomposites [$R_F = CF(CF_3)OC_3F_7$]
 *Each Run No corresponds to that of Table 2

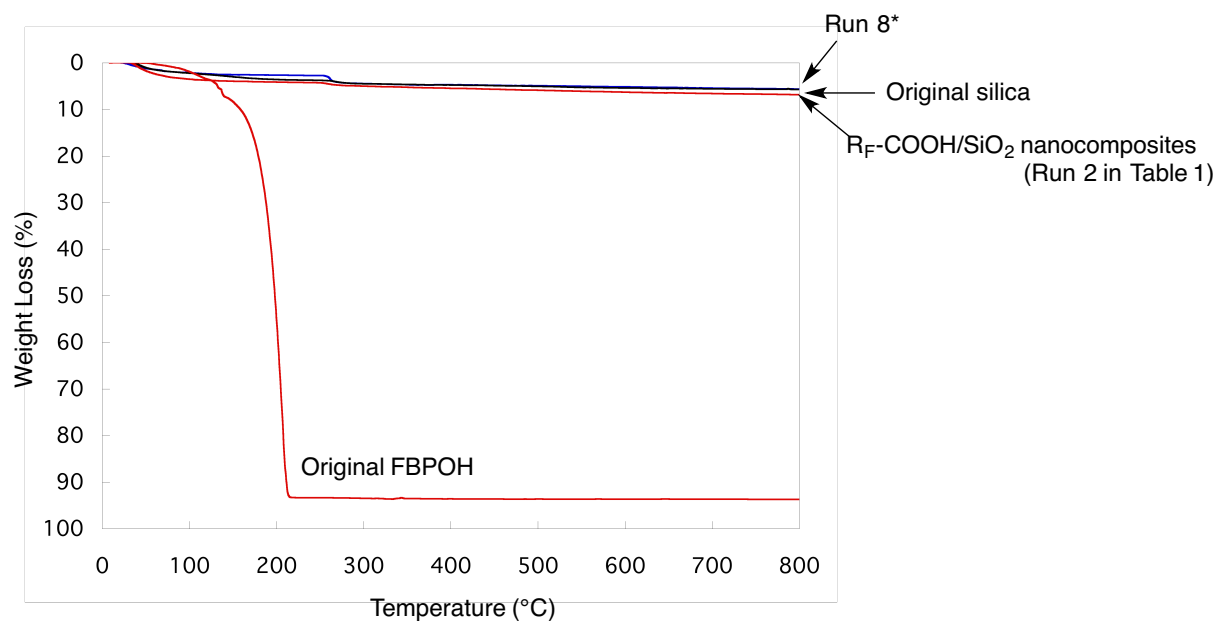


Fig. 3-7 Thermogravimetric analyses of R_F-COOH/SiO₂ /FBPOH nanocomposites [R_F = CF(CF₃)OC₃F₇]
 *Each Run No corresponds to that of Table 2

As shown in Figs. 3-4~3-7, encapsulated *Ar-H* possessing acidic phenol-type hydroxyl groups were found to exhibit no weight loss even after calcination at 800 °C as well as that of the original silica nanoparticles or R_F-CO₂H/SiO₂ nanocomposites, although the theoretical contents of *Ar-H* in the composites are 15~30 %, and original BPAF decomposed completely around 230 °C. On the other hand, the hybrid based on the blend of R_F-CO₂H/SiO₂ nanocomposites (Run 2 in Table 3-1) and original BPAF [content of BPAF in hybrid, 30 %] showed a clear weight loss at 800 °C, which corresponds well to the content of BPAF in the hybrid. A similar result was obtained in the blend hybrid of R_F-CO₂H/SiO₂ nanocomposites and original BPA (see Fig. 3-5). These findings suggest that R_F-CO₂H/SiO₂ nanocomposites can encapsulate *Ar-H*

possessing acidic phenol-type hydroxyl groups as guest molecules into fluorinated silica gel matrices in theoretical encapsulated ratios: 15 ~ 30 % to afford a nonflammable characteristic toward encapsulated *Ar-H*.

UV-vis spectra of well-dispersed $R_F\text{-CO}_2\text{H/SiO}_2$ nanocomposite-encapsulated BPAF, BPA, BPOH, and FBPOH methanol solutions have been measured to verify the presence of encapsulated *Ar-H* in the composites before and after calcination at 800 °C, and the results are shown in Figs. 3-8 ~ 3-11.

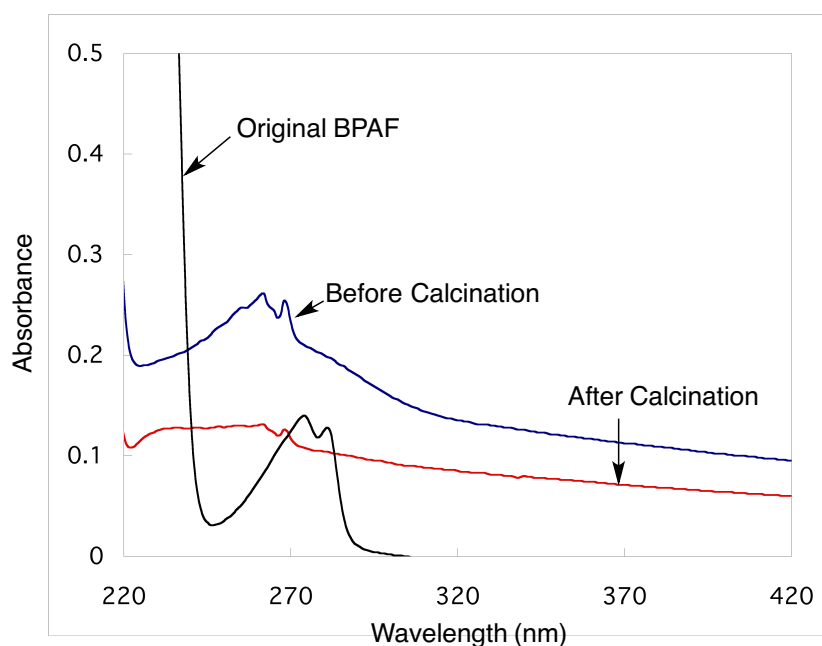


Fig. 3-8 UV-vis spectra of $R_F\text{-COOH/SiO}_2\text{/BPAF}$ nanocomposites (Run 2 in Table 2) before and after calcination at 800 °C in methanol [$R_F = \text{CF}(\text{CF}_3)\text{OC}_3\text{F}_7$]: Concentration of $R_F\text{-COOH/SiO}_2\text{/BPAF}$ nanocomposites: 100 mg/dm³; original BPAF: 20.2 mg/dm³

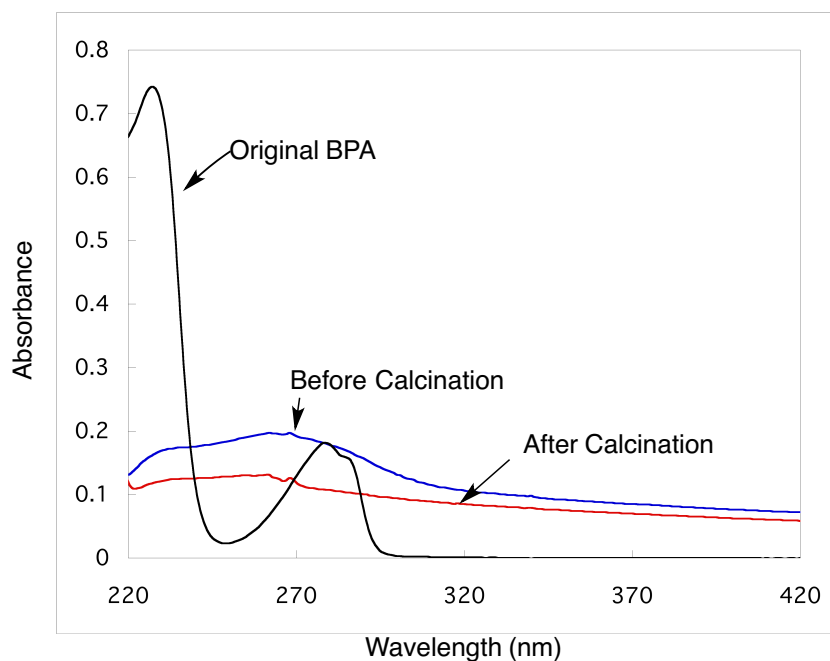


Fig. 3-9 UV-vis spectra of R_F -COOH/SiO₂/BPA nanocomposites (Run 5 in Table 2) before and after calcination at 800 °C in methanol [$R_F = CF(CF_3)]OC_3F_7$]: Concentration of R_F -COOH/SiO₂/BPA nanocomposites: 100 mg/dm³; original BPA: 11.4 mg/dm³

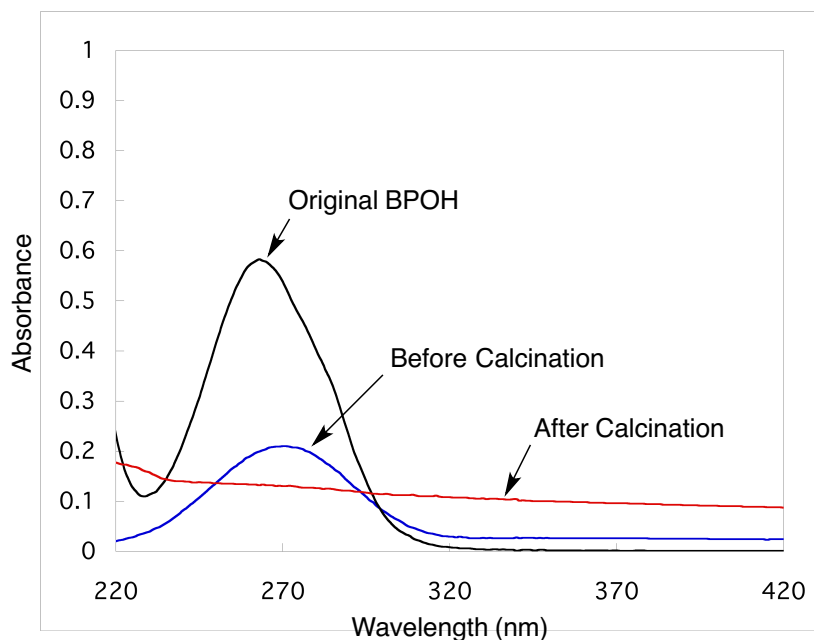


Fig. 3-10 UV-vis spectra of R_F -COOH/SiO₂/BPOH nanocomposites (Run 7 in Table 2) in methanol before and after calcination at 800 °C [$R_F = CF(CF_3)]OC_3F_7$]:
 R_F -COOH/SiO₂/BPOH nanocomposites before calcination at 800 °C (50 mg/dm³)
 R_F -COOH/SiO₂/BPOH nanocomposites after calcination at 800 °C (100 mg/dm³)
 Original BPOH (5 mg/dm³)

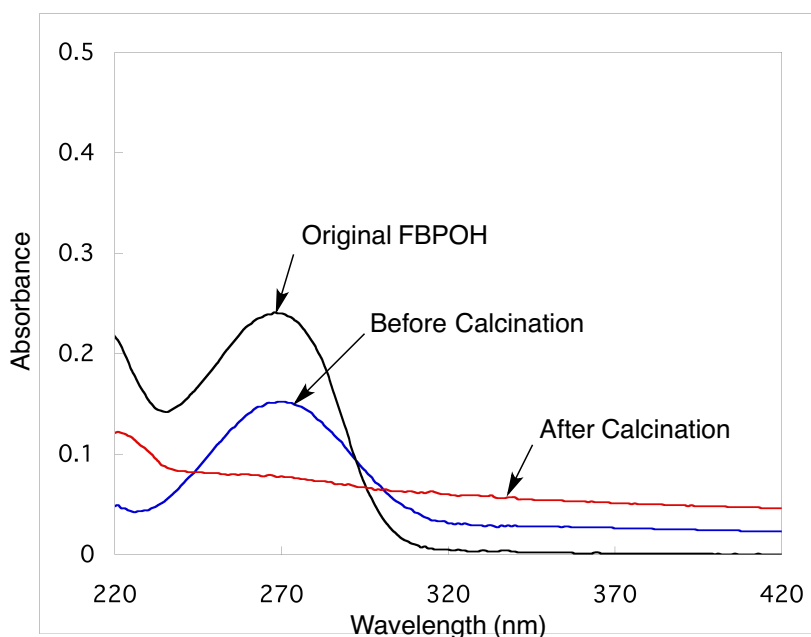


Fig. 3-11 UV-vis spectra of R_F -COOH/SiO₂/FBPOH nanocomposites (Run 8 in Table 2) in methanol before and after calcination at 800 °C [$R_F = \text{CF}(\text{CF}_3)\text{OC}_3\text{F}_7$]:

R_F -COOH/SiO₂/FBPOH nanocomposites before calcination at 800 °C: 50 mg/dm³

R_F -COOH/SiO₂/FBPOH nanocomposites after calcination at 800 °C: 100 mg/dm³

Original FBPOH: 5 mg/dm³

R_F -CO₂H/SiO₂ nanocomposite-encapsulated BPAF before calcination were found to exhibit a clear absorption band around 250 nm related to the encapsulated BPAF, of whose peak was slightly blue-shifted compared with that of the parent BPAF. The encapsulated ratios (based on the theoretical content of BPAF in the composites) of BPAF in the nanocomposites (Run 2 in Table 3-3) before and after calcination were estimated by the use of the molar absorption coefficient of BPAF in methanol to be 58 and 19 %, respectively. Therefore, BPAF can be encapsulated into R_F -CO₂H/SiO₂ nanocomposite cores in excellent to moderate encapsulated ratios

before and even after calcination. A similar result was obtained in the encapsulated BPA in $R_F\text{-CO}_2\text{H/SiO}_2$ nanocomposite cores before and after calcination [encapsulation ratios of BPA in the composites: 31 % (before calcination); 12 % (after calcination): see Fig. 3-9]. In the cases of encapsulated BPOH and FBPOH in $R_F\text{-CO}_2\text{H/SiO}_2$ nanocomposite cores before calcination, the relatively good encapsulated ratios can be observed: 14 and 21 % , respectively; however, the UV-vis absorption peaks related to the encapsulated BPOH and FBPOH in $R_F\text{-CO}_2\text{H/SiO}_2$ nanocomposites after calcination were not observed after calcination at 800 °C, indicating that these encapsulated guest molecules cannot be easily released into methanol through the alcoholysis due to the tight fluorinated silica gel matrices after calcination (see Figs. 3-10 and 3-11). These findings suggest that BPAF, BPA, BPOH, and FBPOH can be encapsulated into $R_F\text{-CO}_2\text{H/SiO}_2$ nanocomposites through the sol-gel reactions illustrated in Scheme 3-2, and these encapsulated guest molecules should exhibit a nonflammable characteristic in the $R_F\text{-CO}_2\text{H/SiO}_2$ nanocomposite cores even after calcination at 800 °C.

^1H magic-angle spinning (MAS) NMR of $R_F\text{-CO}_2\text{H/SiO}_2$ nanocomposite-encapsulated BPAF and BPA were measured to verify the presence of guest molecules in the nanocomposites before and after calcination at 800 °C, and the

results were shown in Figs. 3-12 and 3-13.

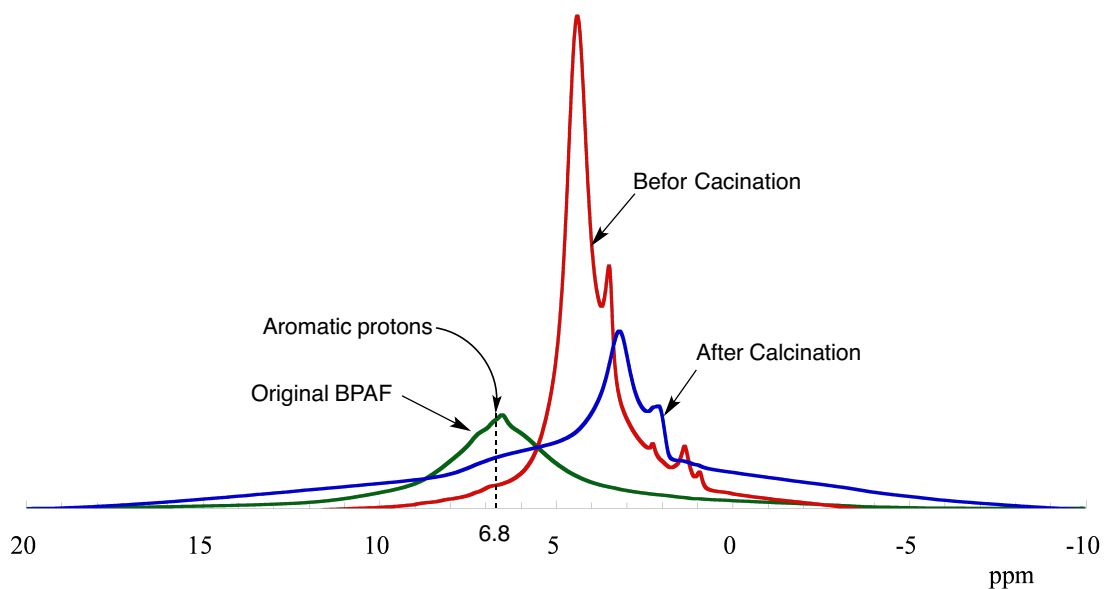


Fig. 3-12 ^1H MAS (Magic Angle Spinning) NMR spectra of $\text{R}_\text{F}\text{-COOH/SiO}_2\text{/BPAF}$ nanocomposites (Run 2 in Table 2) before and after calcination at $800\text{ }^\circ\text{C}$ [$\text{R}_\text{F} = \text{CF}(\text{CF}_3)\text{OC}_3\text{F}_7$]

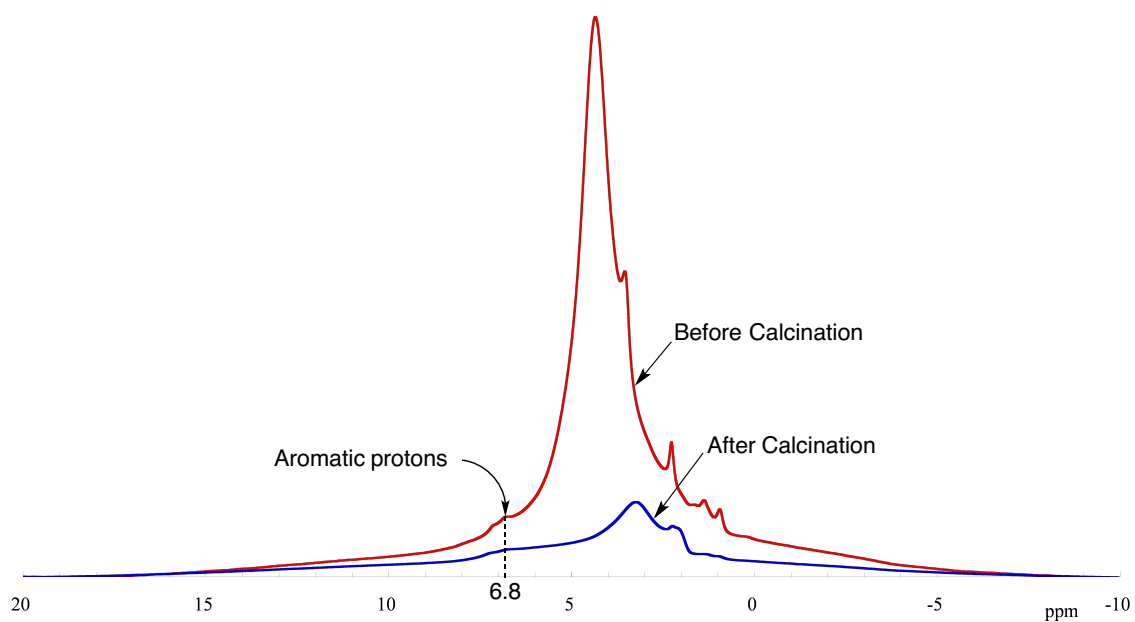


Fig. 3-13 ^1H MAS (Magic Angle Spinning) NMR spectra $\text{R}_\text{F}\text{-COOH/SiO}_2\text{/BPA}$ nanocomposites (Run 5 in Table 2) before and after calcination at $800\text{ }^\circ\text{C}$ [$\text{R}_\text{F} = \text{CF}(\text{CF}_3)\text{OC}_3\text{F}_7$]

As shown in Figs. 3-12 and 3-13, relatively sharp peaks are observed around 1~9 ppm related to the presence of not only aromatic protons in BPAF and BPA but also ethoxysilyl protons, which would be produced by the sol-gel reactions with tetraethoxysilane and silica nanoparticles under alkaline conditions as in Scheme 3-2. Peaks (~ 4 ppm) related to ethoxysilyl protons in the composites have been completely disappeared by calcination at 800 °C; however, aromatic protons were observed around 7 ppm related to the encapsulated guest molecules, suggesting that encapsulated BPA and BPAF should exhibit a nonflammable characteristic in the fluorinated silica gel matrices even after calcination.

Additionally, the modified glasses treated with $R_F\text{-CO}_2\text{H/SiO}_2$ nanocomposite-encapsulated BPAF, BPA, BPOH, and FBPOH have been prepared, and the contact angle values of water and dodecane on the surface of these modified glasses were measured at room temperature by the use of goniometer-type contact angle measurements. These results are shown in Table 3-4.

Table 3-4 Contact angles of water and dodecane on the modified glass surface treated with R_F -COOH/SiO₂/**Ar-H** nanocomposites [$R_F = CF(CF_3)OC_3F_7$]

Run*	Ar-H	Contact angle (degree)	
		Dodecane	Water**
non-treated glass	—	0	43
R_F -COOH/SiO ₂ nanocomposites***	—	73	0

	BPA		
1		39	0
2		48	0
3		29	0

	BPAF		
4		60	0
5		48	0
6		64	0

	BPOH		
7		65	0

	FBPOH		
8		66	0

*Each Run No corresponds to that of Table 2

**Water contact angle value after 3 min after adhesion of the water droplet on the modified glass surface

***Used composites: Run 2 in Table 1

As shown in Table 3-4, dodecane contact angle values (29~65) were found to decrease by the encapsulation of aromatic compounds into R_F -CO₂H/SiO₂ composite cores, compared with that (73) of R_F -CO₂H/SiO₂, although the water contact angle value is 0° in each case as well as that of R_F -CO₂H/SiO₂ nanocomposites. This suggests that aromatic compounds such as BPAF, BPA, BPOH, and FBPOH should be effectively encapsulated into the R_F -CO₂H/SiO₂ nanocomposite cores to decrease the dodecane contact angle values.

In the present nanocomposite reactions of R_F -CO₂H with tetraethoxysilane and

silica nanoparticles in the presence of guest molecules possessing acidic phenol-type hydroxyl groups illustrated in Scheme 3-2, ammonium hexafluorosilicate would be formed by the smooth dehydrofluorination of phenol-type acidic protons in BPAF, BPA, BPOH, and FBPOH with fluorines in $R_F\text{-CO}_2\text{H}$ catalyzed by both ammonia and silica nanoparticles to give a nonflammable characteristic toward these encapsulated compounds, as well as that of $R_F\text{-(DOBAA)}_n\text{-R}_F/\text{SiO}_2$ nanocomposites possessing no weight loss characteristic even after calcination at 800 °C.^{55 ~ 58)}

Low molecular weight compounds such as 4,4'-bis(triethoxysilyl)-1,1'-biphenyl [BTSBP], 3-(trihydroxysilyl)-propane-1-sulfonic acid [THSP], α -cyclodextrin (α -CD), β -cyclodextrin (β -CD), and γ -cyclodextrin (γ -CD) have no acidic phenol-type hydroxyl groups. Thus, it is suggested that these compounds should exhibit a flammable characteristic in $R_F\text{-CO}_2\text{H}/\text{SiO}_2$ nanocomposite matrices, due to the formation of no ammonium hexafluorosilicate through the dehydrofluorination as mentioned above. In fact, $R_F\text{-CO}_2\text{H}/\text{SiO}_2$ nanocomposite-encapsulated these guest molecules have been prepared illustrated in Scheme 3-2 and Table 3-3.

As shown in Scheme 3-2 and Table 3-3, BTSBP, THSP, α -CD, β -CD, and γ -CD were effectively encapsulated as guest molecules into $R_F\text{-CO}_2\text{H}/\text{SiO}_2$ nanocomposite cores to give the expected $R_F\text{-CO}_2\text{H}/\text{SiO}_2$ nanocomposites

encapsulated the corresponding low molecular weight compounds in 69~99 % isolated yields. These composites thus obtained were found to exhibit a good dispersibility and stability in methanol, ethanol, and 2-propanol. Thus, the size of these composites in methanol has been measured by using DLS at 25 °C, and the size of these composites was nanometer size-controlled: 59~433 nm. FE-SEM images of R_F -CO₂H/SiO₂ nanocomposites-capsulated α -CD show the very fine nanoparticles with mean diameter: 47 nm (see Fig. 3-14).

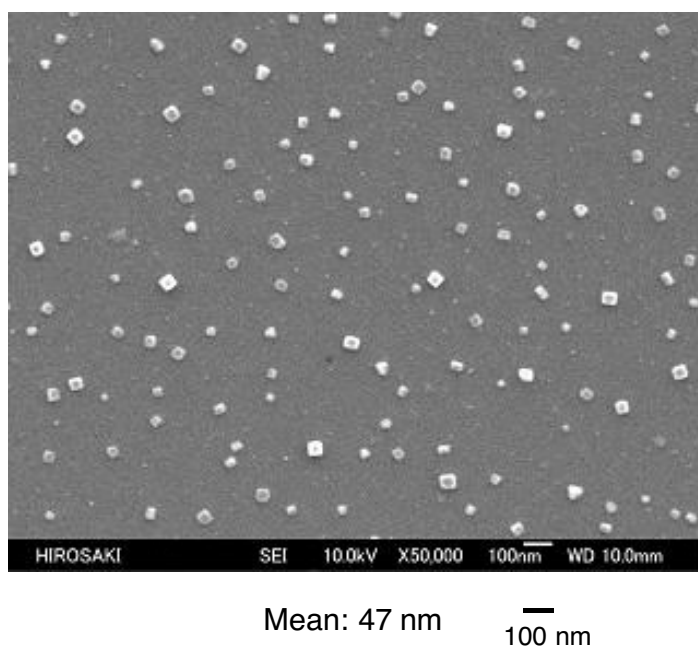


Fig. 3-14 FE-SEM image of R_F -COOH/SiO₂/ α -CD nanocomposites (Run 11 in Table 2)
[$R_F = CF(CF_3)OC_3F_7$]

The thermal stability of these fluorinated nanocomposites has been studied by

the use of TGA measurements under similar conditions to those of Figs. 3-2 and 3-4, and the results were shown in Fig. 3-15~3-19.

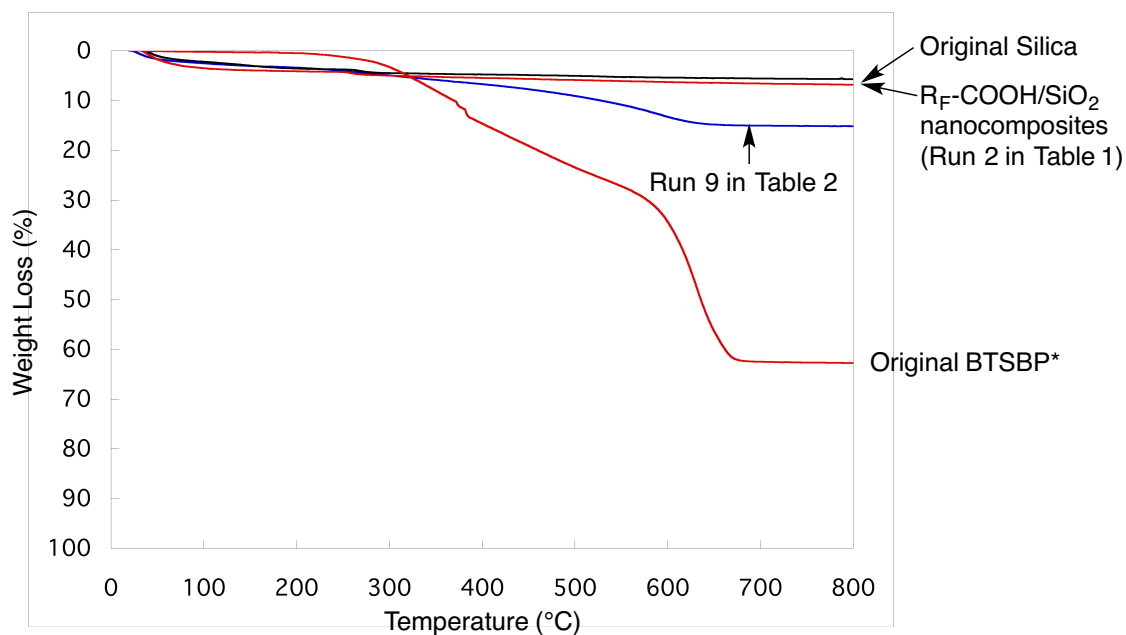


Fig. 3-15 Thermogravimetric analyses of R_F-COOH/SiO₂/BTSBP nanocomposites [R_F=CF(CF₃)OC₃F₇]
*Silica composite particles which were prepared by the sol-gel reaction of original BTSBP under alkaline onditions

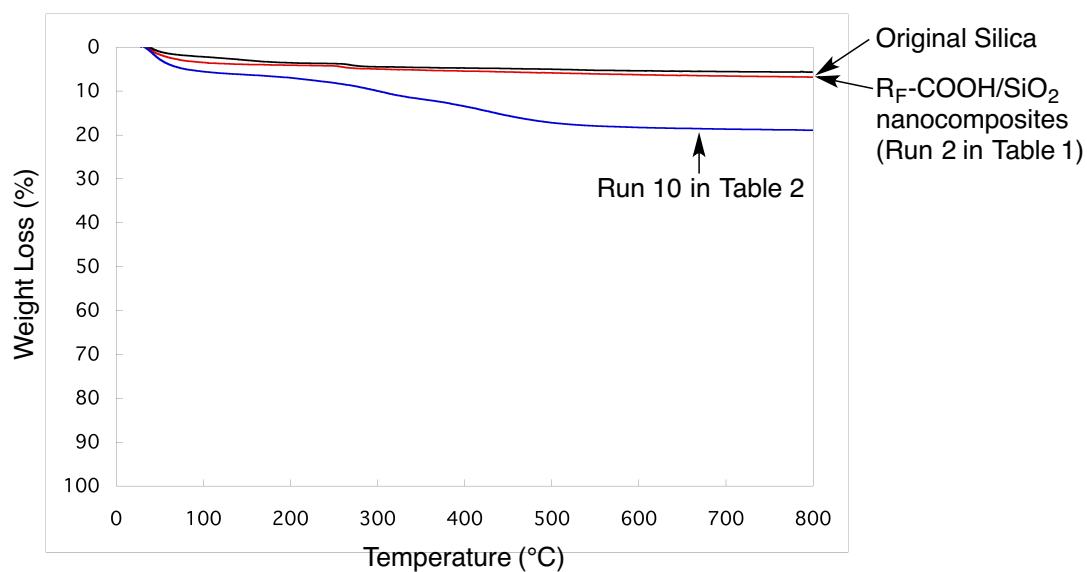


Fig. 3-16 Thermogravimetric analyses of R_F-COOH/SiO₂/THSP nanocomposites [R_F=CF(CF₃)OC₃F₇]

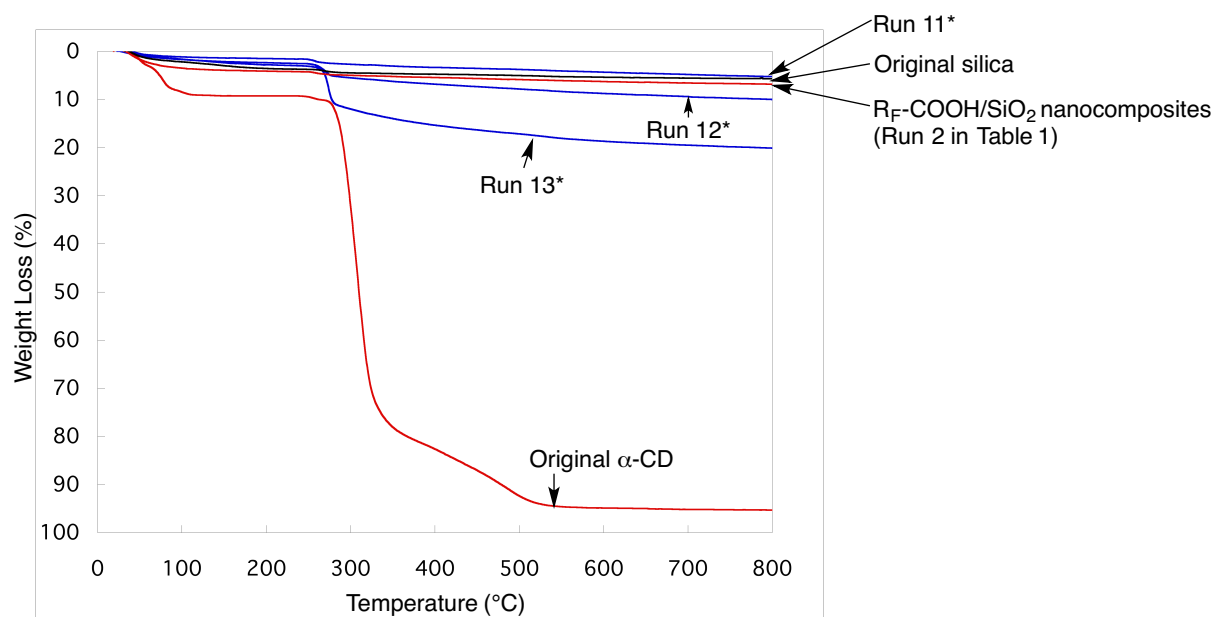


Fig. 3-17 Thermogravimetric analyses of $R_F\text{-COOH/SiO}_2/\alpha\text{-CD}$ nanocomposites [$R_F=\text{CF}(\text{CF}_3)\text{OC}_3\text{F}_7$]
 *Each Run No corresponds to that of Table 2

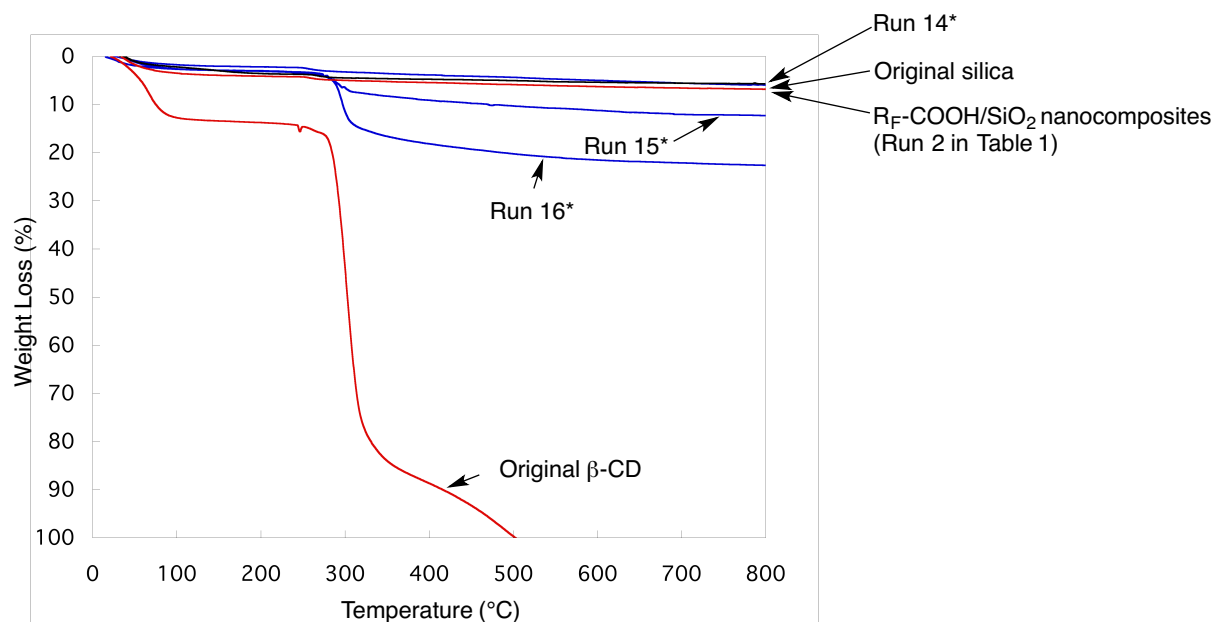


Fig. 3-18 Thermogravimetric analyses of $R_F\text{-COOH/SiO}_2/\beta\text{-CD}$ nanocomposites [$R_F=\text{CF}(\text{CF}_3)\text{OC}_3\text{F}_7$]
 *Each Run No corresponds to that of Table 2

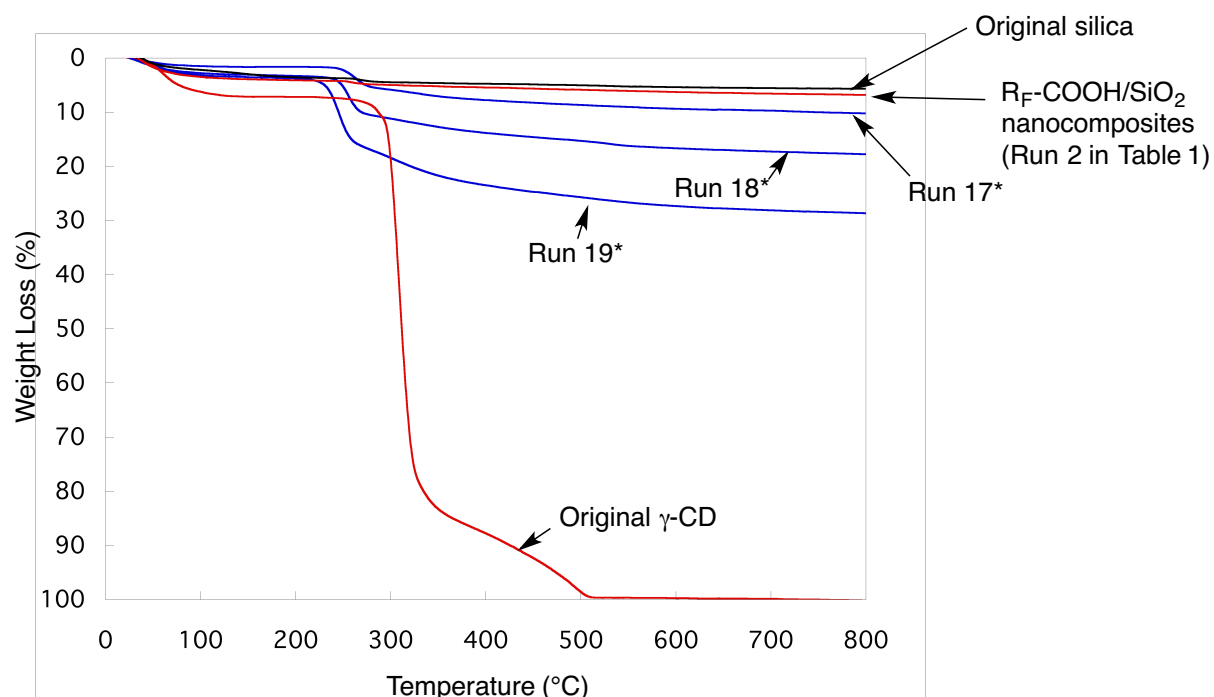


Fig. 3-19 Thermogravimetric analyses of R_F-COOH/SiO₂/γ-CD nanocomposites [R_F=CF(CF₃)OC₃F₇]
 *Each Run No corresponds to that of Table 2

R_F-CO₂H/SiO₂ nanocomposite-encapsulated BTSBP, THSP, α-CD, β-CD, and γ-CD were found to exhibit a clear weight loss corresponding to the contents of encapsulated low molecular weight compounds after calcination at 800 °C, quite different from that of R_F-CO₂H/SiO₂ nanocomposites-encapsulated BPAF, BPA, BPOH, and FBPOH. This finding would be due to the absence of acidic phenol-type hydroxyl groups in these encapsulated guest molecules. Especially, no dehydrofluorination between BTSBP, THSP, α-CD, β-CD, or γ-CD and fluorines in R_F-CO₂H under alkaline conditions in the presence of silica nanoparticles as a cocatalyst would give a weight loss behavior. Thus, encapsulated BTSBP, THSP,

α -CD, β -CD, and γ -CD can give a flammable characteristic in $R_F\text{-CO}_2\text{H/SiO}_2$ nanocomposites under such conditions. Hexafluorosilicate anions obtained in the nanocomposite reactions in the presence of guest molecules possessing acidic phenol-type hydroxyl groups would afford the synergistic interactions derived from not only hydrogen bonding interaction between the fluorines in hexafluorosilicate and hydrogen atoms in the guest molecules but also noncovalent $\text{Si}\cdots\text{F}$ interactions between the silica gel in the composites and hexafluorosilicate,^{59 ~ 67)} and such effective interactions should enable encapsulated guest molecules to exhibit a perfectly nonflammable characteristic at 800 °C.

3.4 Conclusions

It was demonstrated that $R_F\text{-CO}_2\text{H/SiO}_2$ nanocomposites were prepared by the sol–gel reactions of tetraethoxysilane in the presence of the corresponding fluorinated carboxylic acid and silica nanoparticles under alkaline conditions. $R_F\text{-CO}_2\text{H/SiO}_2$ nanocomposites thus obtained afforded no weight loss in proportion to the contents of $R_F\text{-CO}_2\text{H}$ in the composites even after calcination at 800 °C. Modified glass surface treated with $R_F\text{-CO}_2\text{H/SiO}_2$ nanocomposites were found to exhibit good oleophobicity

with superhydrophilicity imparted by fluorinated carboxylic acid in the composites on the surface. $R_F\text{-CO}_2\text{H/SiO}_2$ nanocomposites were also applied to the encapsulation of low molecular weight aromatic compounds possessing acidic phenol-type hydroxyl groups such as BPAF, BPA, BPOH and FBOH. $R_F\text{-CO}_2\text{H/SiO}_2$ nanocomposite-encapsulated these guest molecules were found to exhibit no weight loss corresponding to the contents of these molecules in the composites even after calcination at 800 °C. On the other hand, $R_F\text{-CO}_2\text{H/SiO}_2$ nanocomposite-encapsulated low molecular weight compounds possessing no such acidic hydroxyl groups afforded a clear weight loss corresponding to the contents of these encapsulated compounds in the composites after calcination at 800 °C.

Reference

- 1) A.-M. Caminade, C.-O. Turrin, P. Sutra, J.-P. Majoral, *Curr. Opin, Colloid Interface Sci.* **8**, 282 (2003).
- 2) T. Imae, *Curr. Opin, Colloid Interface Sci.* **8**, 307 (2003).
- 3) A. Zaggia and B. Ameduri, *Curr. Opin, Colloid Interface Sci.* **17**, 188 (2012).
- 4) B. Ameduri and B. Boutevin, "Well-architected fluoropolymers: Synthesis,

- Properties and Applications”, Elsevier, Amsterdam, 231 (2004).
- 5) J.-F. Berret, D. Calvet, A. Collet and M. Viguier, *Curr. Opinion Colloid Interface Sci.*, **8**, 296 (2003).
 - 6) T. Imae, H. Tabuchi, K. Funayama, A. Sato, T. Nakamura and N. Amaya, *Colloids Surfaces A: Physicochem. Eng. Aspects*, **167**, 73 (2000).
 - 7) P. Lebreton, B. Ameduri, B. Boutevin, and J. M. Corpart, *Macromol. Chem. Phys.*, **203**, 522 (2002).
 - 8) M. J. Monteiro, M. M. Adamy, B. J. Leeuwen, A. M. Van Herk and M. Destarac, *Macromolecules*, **38**, 1538 (2005).
 - 9) A. E. Feiring, E. R. Wonchoba, F. Davdson, V. Percec and B. Barboiu, *J. Polym. Sci. Part A: Polym. Chem.*, **38**, 3313 (2000).
 - 10) M. Destarac, K. Matyjaszewski, E. Silverman, B. Ameduri and B. Boutevin, *Macromolecules*, **33**, 4613 (2000).
 - 11) Z. Shi and S. Holdcroft, *Macromolecules*, **38**, 4193 (2005).
 - 12) K. Jankova and S. Hvilsted, *J. Fluorine Chem.*, **126**, 241 (2005).
 - 13) G. Laruelle, E. Nicol, B. Ameduri, J.-F. Tassin and N. Ajellal, *J. Polym. Chem. Sci. Part A: Polym. Chem.*, **49**, 3960 (2011).
 - 14) Y. Patil, B. Ameduri, *Polym. Chem.*, **4**, 2783 (2013).

- 15) F. Boschet, G. Kostov, B. Ameduri, A. Jackson and B. Boutevin, *Polym. Chem.*, **3**, 217 (2012).
- 16) H. Sawada, *Chem. Rev.*, **96**, 1779 (1996).
- 17) H. Sawada and T. Kawase, *Kobunshi Ronbunshu*, **58**, 147 (2001).
- 18) H. Sawada and T. Kawase, *Kobunshi Ronbunshu*, **58**, 255 (2001).
- 19) H. Sawada, *J. Fluorine Chem.*, **105**, 219 (2000).
- 20) H. Sawada, *Prog. Polym. Sci.*, **32**, 509 (2007).
- 21) H. Sawada, *Polym. Chem.*, **3**, 46 (2012).
- 22) H. Sawada, *J. Fluorine Chem.*, **121**, 111 (2003).
- 23) P. Gomez-Romero and C. Sanchez (eds.), *Functional hybrid materials*, Wiley-VCH, Weinheim, 2004.
- 24) P. Judeinstein and C. Sanchez, *J. Mater. Chem.*, **6**, 511 (1996).
- 25) J. Wen and G. L. Wilkes, *Chem. Mater.*, **8**, 1667 (1996).
- 26) C. J. Brinker and G. W. Scherer, *Sol-gel science*, Academic Press, Boston, (1990).
- 27) Z. Hua and K.-Y. Qiu, *Polymer*, **31**, 521 (1997).
- 28) M. A. S. Pedroso, M. L. Dias, R. A. S. San Gil and C. G. Mothe, *Colloid Polym. Sci.*, **281**, 19 (2003).

- 29) A. Bandyopadhyay, M. D. Sarkar and A. K. Bhowmick, *J. Polym. Sci.: Part B: Polym Phys.*, **43**, 2399 (2005).
- 30) S. Li, Z. Zhou, H. Abernathy, M. Liu, W. Li, J. Ukai, K. Hase, and M. Nakanishi, *J. Mater. Chem.*, **16**, 858 (2006).
- 31) P. Hajji, L. David, J. F. Gerard, J. P. Pascault and G. Vigier, *J. Polym. Sci.: Part B: Polym. Phys.*, **37**, 3172 (1999).
- 32) O. Prucker and J. Ruhe, *Macromolecules*, **31**, 592 (1998).
- 33) B. De Boer, H. K. Simon, M. L. P. Werts, E. W. van Der and G. Hadziioannou, *Macromolecules*, **33**, 349 (2000).
- 34) B. Zhao and W. J. Brittain, *J. Am. Chem. Soc.*, **121**, 3557 (1999).
- 35) R. Jordan, A. Ulma, J. F. Kang, M. H. Rafailovich and J Sokolov, *J. Am. Chem. Soc.*, **121**, 1016 (1999).
- 36) S.-W. Zhang, S.-X. Zhou, Y.-M. Weng and L.-M. Wu, *Langmuir*, **21**, 2124 (2005).
- 37) R. Ranjan and W. J. Brittain, *Macromol. Rapid Commun.*, **29**, 1104 (2008).
- 38) Y. Li and B. C. Benicewicz, *Macromolecules*, **41**, 7986 (2008).
- 39) C.-H. Liu and C.-Y. Pan, *Polymer*, **48**, 3679 (2007).
- 40) D. H. Nguyen and P. Vana, *Polym. Adv. Technol.*, **17**, 625 (2006).
- 41) C. Bartholome, E. Beyou, E. Bourgeat-Lami, P. Chumont and N. Zydowicz,

- Macromolecules*, **36**, 7946 (2003).
- 42) M. Husseman, E. E. Maalmstrom, M. McNamara, M. Mate, D. Mecerreyes, D. G. Benoit, J. L. Hedrick, P. Mansky, E. Huang, T. P. Russell and C. J. Hawker, *Macromolecules*, **32**, 1424 (1999).
- 43) K. Ueno, A. Inaba, M. Kondoh and M. Watanabe, *Langmuir*, **24**, 5253 (2008).
- 44) K. Matyjaszewski and J. Xia, *Chem Rev.*, **101**, 2921 (2001).
- 45) Y.-L. Liu and S.-H. Li, *Macromol. Rapid Commun.*, **25**, 1392 (2004).
- 46) G. Schmid, *Nanoparticles*, Wiley-VCH, Weinheim, (2004)
- 47) L. Matejka and J. Plestil, *Macromol. Symp.*, **122**, 191 (1997).
- 48) N. Juangvanich and K. A. Maurite, *J. Appl. Polym. Sci.*, **67**, 1799 (1998).
- 49) A. M. Granville and W. J. Brittain, *Macromol. Rapid Commun.*, **25**, 1298 (2004).
- 50) L. Andruzzi, A. Hexemer, X. Li, C. K. Ober, E. J. Krmaer, G. Galli, E. Chiellini and D. A. Fischer, *Langmuir*, **20**, 10498 (2004).
- 51) H. Sawada, T. Narumi, A. Kajiware, K. Ueno and K. Hamazaki, *Colloid Polym. Sci.*, **284**, 551 (2006).
- 52) H. Sawada, T. Narumi, S. Kodama, M. Kamijo, R. Ebara, M. Sugiyama and Y. Iwasaki, *Colloid Polym. Sci.*, **285**, 977 (2007).
- 53) H. Sawada, M. Kikuchi and M. Nishida, *J. Polym. Sci. Part A: Polym. Chem.*, **49**,

- 1070 (2011).
- 54) H. Sawada, Y.-F. Gong, Y. Minoshima, T. Matsumoto, M. Nakayama, M. Kosugi and T. Migita, *J. Chem. Soc. Chem. Commun.*, 537 (1992).
- 55) H. Sawada, T. Tashima and S. Kodama, *Polym. Adv. Technol.*, **19**, 739 (2008).
- 56) H. Sawada, H. Kakehi, T. Tashima, Y. Nishiyama, M. Miura and N. Isu, *J. Appl. Polym. Sci.*, **112**, 3482 (2009).
- 57) H. Sawada, T. Tashima, H. Kakehi, Y. Nishiyama, M. Kikuchi, M. Miura, Y Sato and N. Isu, *Polym. J.*, **42**, 167 (2010).
- 58) H. Sawada, T. Tashima, Y. Nishiyama, M. Kikuchi, G. Kostov, Y. Goto and B. Ameduri, *Macromolecules*, **44**, 1114 (2011).
- 59) A. Saxena, R. Rai, S.-Y. Kim, M. Fujiki, M. Naito, K. Okoshi and G. J. Kwak, *Polym. Sci.: Part A Polym. Chem.*, **44**, 5060 (2006).
- 60) V. O. Gelmboldt, E. V. Ganin, M. S. Fonari, L. V. Koroeva, Y. E. Ivanov and M. M. Botoshansky, *J. Fluorine Chem.*, **130**, 428 (2009).
- 61) G. J. Reiß, *Acta. Cryst.*, **C54**, 1489 (1998).
- 62) A. F. Jalbout, J. Z-Y, A. Ouasri, H. Jeghnou, A. Rhandour, M. C. Dhamelincourt, P. Dhamelincourt, A. Mazzah, *Vibrational Spectroscopy*, **33**, 21 (2003).
- 63) B. D. Conley, B. C. Yearwood, S. Parkin and D. A. Atwood, *J. Fluorine Chem.*,

115, 155 (2002).

64) V. O. Gelmboldt, E. V. Ganin and K. V. Domasevitch, *Acta. Cryst.*, **C63**, O530 (2007).

65) A. F. Jalbout, A. Ouasri, H. Jeghnou and A. Rhandour, *Vib. Spectrosc.*, 44, 94 (2007).

66) C. A. Mattia, O. Ortona, R. Puliti, G. Cascarano and C. J. Giacovazzo, *Molecular Structure*, **350**, 63 (1995).

67) R. Thaimattam, M. Szafran, Z. Dega-Szafran and M. Jaskolski, *Acta. Cryst.*, **B64**, 483 (2008).

CHAPTER 4

Facile Creation of Superoleophobic and Superhydrophilic Surface by Using Perfluoropolyether Dicarboxylic Acid/Silica Nanocomposites

4.1 Introduction

It is well known that fluoroalkanoyl peroxide [$R_F-C(=O)OO(O=)CR_F$; R_F = fluoroalkyl groups] is a useful tool for the synthesis of two fluoroalkyl end-capped oligomers [$R_F-(M)_n-R_F$; M_n = radical polymerizable monomers] via the three bond radical fissions of the peroxide.^{1, 2)} Interestingly, these two fluoroalkyl end-capped oligomers can form nanometer size-controlled self-assembled oligomeric aggregates through the aggregation of end-capped fluoroalkyl groups,^{3 ~ 7)} although the randomly fluoroalkylated polymers are not likely to form such molecular aggregates.^{8 ~ 17)} Fluoroalkyl end-capped oligomeric aggregates can also interact with guest molecules to afford the fluorinated aggregate/guest molecule nanocomposites.^{18 ~ 20)} Not only fluoroalkanoyl peroxide but also perfluoropolyether diacyl peroxide [$-[C(=O)R_FC(=O)OO]_p$; $-R_F-$ = perfluoropolyether units] can be also prepared by the reaction of the corresponding diacid fluoride [$FC(=O)R_FC(=O)F$] with hydrogen peroxide under alkaline conditions.²¹⁾ This peroxide was applied to the direct introduction of perfluoropolyether units into acrylic acid oligomer main chain through the radical process.^{21, 22)} Perfluoropolyether unit-containing acrylic acid oligomers $\{-[R_F-(CH_2CHCO_2H)_q]_p-\}$ are classified according to the structure into AB block-type

fluorinated polysoaps, and these fluorinated oligomers can reduce the surface tension of water effectively, quite different from that of the corresponding non-fluorinated acrylic acid oligomer or randomly fluoroalkylated polysoaps.^{22, 23)} However, ABA triblock-type fluorinated polysoaps such as two fluoroalkyl end-capped acrylic acid oligomers $[\text{R}_\text{F}-(\text{CHCHCOOH})_n-\text{R}_\text{F}]$, which were prepared by using fluoroalkanoyl peroxide $[\text{R}_\text{F}\text{C}(=\text{O})\text{OO}(\text{O}=\text{R}_\text{F})]$, have a superior surface active characteristic to that of the corresponding AB block-type fluorinated acrylic acid oligomers $\{-[\text{R}_\text{F}-(\text{CH}_2\text{CHCO}_2\text{H})_q]_p-\}$.^{3 ~ 6, 18 ~ 20)} This finding is due to the relatively poor surface arrangement ability of perfluoropolyether units $(-\text{R}_\text{F}-)$ above the water surface, compared with that of the end-capped fluoroalkyl groups in ABA triblock-type fluorinated polysoaps.^{3 ~ 6, 22, 23)} Therefore, it is of particular interest to explore novel perfluoropolyether units $(-\text{R}_\text{F}-)$ -containing materials possessing a higher surface-active characteristic than the corresponding perfluoroalkyl groups $(\text{R}_\text{F}-)$ -containing ones with a view to developing new fluorinated functional materials. This chapter shows that perfluoropolyether dicarboxylic acid $[\text{HO}(\text{O}=\text{C})-\text{R}_\text{F}-\text{C}(=\text{O})\text{OH}]$ can be applied to the preparation of the corresponding dicarboxylic acid/silica nanocomposites by using the sol-gel reaction with tetraethoxysilane and silica nanoparticles under alkaline conditions. Interestingly, it

has been found that the modified glass surface treated with these obtained perfluoropolyether dicarboxylic acid/silica nanocomposites can exhibit the superoleophobic and superhydrophilic characteristics, although the perfluoro-oxa-alkanoic acid/ $[R_F-(C=O)OH]$ /silica nanocomposites ²⁴⁾ can afford not superoleophobic but the usual oleophobic characteristic on the modified glass surface. More interestingly, the perfluoropolyether dicarboxylic acid/silica nanocomposites were also applicable to the surface modification of the filter paper and polyester fabrics to exhibit the superoleophobic and superhydrophilic characteristics on the surfaces. These results will be described in this chapter.

4.2 Experimental

4.2.1. Measurements

Thermal analyses were recorded by raising the temperature around 800 °C (the heating rate: 10 °C/min) under atmospheric conditions by the use of Bruker axis TG-DTA2000SA differential thermobalance (Kanagawa, Japan). Size [number - average diameter (average hydrodynamic diameter)] of nanocomposites was measured

by using Otsuka Electronics DLS-7000 HL (Tokyo, Japan). Field emission scanning electron micrographs (FE-SEM) were obtained using JEOL JSM-7000F (Tokyo, Japan). Contact angles were measured using a Kyowa Interface Science Drop Master 300 (Saitama, Japan). Dynamic force microscope (DFM) was measured by using SII NanoTechnology Inc. E-sweep (Chiba Japan).

4.2.2. Materials

Perfluoropolyether dicarboxylic acid

$$[\text{HO}(\text{O}=\text{C})\text{CF}(\text{CF}_3)\{\text{OCF}_2\text{CF}(\text{CF}_3)\}_n\text{O}(\text{CF}_2)_5\text{O}\{\text{CF}(\text{CF}_3)\text{CF}_2\text{O}\}_m-\text{CF}(\text{CF}_3)\text{C}(=\text{O})\text{OH}; n + m = 6 \sim 12]$$
 was used as received HydruS Chemical Inc. (Tokyo, Japan). Silica-nanoparticle methanol solution [30 % (wt.): average particle size: 11 nm (Methanol Silica-sol TR)] was supplied by Nissan Chemical Industrials Ltd. (Tokyo, Japan). Tetraethoxysilane (TEOS), bisphenol A (BPA), and bisphenol AF (BPAF) were purchased from Tokyo Chemical Industry Co., Ltd. (Tokyo, Japan). Aqueous ammonia was purchased from Wako Pure Chemical Industries, Ltd. (Osaka, Japan).

4.2.3. Preparation of perfluoropolyether dicarboxylic acid (PFPE-DACD)/silica

nanocomposites

To a methanol solution (4 ml) of perfluoropolyether dicarboxylic acid [PFPE-DACD: 200 mg] were added tetraethoxysilane (TEOS: 0.05 ml), silica-nanoparticle methanol solution [30 % (wt.): 0.33 g] and 25 % aqueous ammonia solution (0.05 ml). The mixture was stirred with a magnetic stirring bar at room temperature for 3 hrs. After the solvent was evaporated off, to the obtained crude products was added methanol (3 ml). The methanol solution was stirred with magnetic stirring bar at room temperature for 1 day, and then was centrifuged for 30 min. The expected fluorinated nanocomposites were easily separated from the methanol solution, and then was washed with methanol in several times. Fluorinated nanocomposites powders thus obtained were dried in vacuo at 50 ° for 2 days to afford purified particle powders (76 mg).

4.2.4. Preparation of perfluoropolyether dicarboxylic acid (PFPE-DACD)/silica nanocomposites - encapsulated bisphenol A

To a methanol solution (4 ml) of perfluoropolyether dicarboxylic acid

(PFPE-DACD) [200 mg] were added bisphenol A (BPA: 200 mg), tetraethoxysilane (TEOS: 0.05 ml), silica-nanoparticle methanol solution [30 % (wt.): 0.33 g], and 25 % aqueous ammonia solution (0.05 ml). The mixture was stirred with a magnetic stirring bar at room temperature for 5 hrs. After the solvent was evaporated off, to the obtained crude products was added methanol (5 ml). The methanol solution was stirred with magnetic stirring bar at room temperature for 1 day, and then was centrifuged for 30 min. The expected fluorinated nanocomposites-encapsulated BPA was easily separated from the methanol solution, and then was washed with methanol in several times. Fluorinated nanocomposites-encapsulated BPA powders thus obtained were dried in vacuo at 50 °C for 2 days to afford purified particle powders (73 mg). Fluorinated nanocomposites-encapsulated the other low molecular weight aromatic compounds were also prepared under similar conditions.

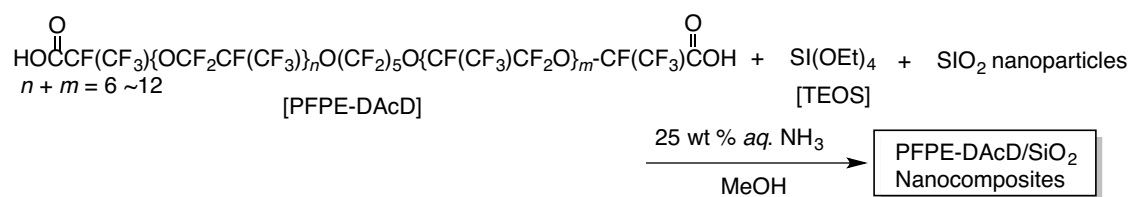
4.2.5. Preparation of modified glass treated with perfluoropolyether dicarboxylic acid acid/silica nanocomposites by dipping method

To a methanol solution (4 ml) containing perfluoropolyether dicarboxylic acid (200 mg) were added tetraethoxysilane (0.05 ml), silica-nanoparticle methanol

solution [30 % (wt.): 0.33 g], and 25 wt% aqueous ammonia solution (0.05 ml). The mixture was stirred with a magnetic stirring bar at room temperature for 5 hrs. The glass plate ($18 \times 18 \text{ mm}^2$ pieces) was dipped into the methanol solution of fluorinated nanocomposites at room temperature and left for 1 min. This was lifted from the solution at constant rate and dried at room temperature for 1 day under vacuum to afford the modified glass.

4.3 Results and discussion

Tetraethoxysilane (TEOS) underwent the sol-gel reaction under alkaline conditions in the presence of perfluoropolyether dicarboxylic acid (PFPE-DACD) and silica nanoparticles to give the PFPE-DACD/SiO₂ composites in 16 ~ 35 % isolated yields as shown in Scheme 4-1. PFPE-DACD/SiO₂ composites thus obtained can exhibit a good dispersibility and stability in not only water but also the traditional organic solvents such as methanol, ethanol, 2-propanol, tetrahydrofuran and 1,2-dichloroethane. Thus, the size of these composites in methanol was studied by the use of dynamic light-scattering (DLS) measurements at 25 °C, and the results were also shown in Scheme 4-1.



Run	PFPE-DACD (mg)	TEOS (ml)	SiO ₂ (mg)	25 wt % aq. NH ₃ (ml)	Yield ^{a)} (%)	Size of the composites ^{b)}	
						Before calcination (nm)	After calcination ^{c)} (nm)
1	100	0.05	100	0.05	24	21.9 ± 2.1	27.8 ± 8.1
2	200	0.05	100	0.05	35	49.6 ± 7.6	55.0 ± 9.7
3	400	0.05	100	0.05	16	28.1 ± 2.8	27.3 ± 3.0

a) Yield based on PFPE-DACD, TEOS and SiO₂

b) Determined by dynamic light scattering (DLS) measurements in methanol

c) Calcination temperature: 800°C

Scheme 4-1 Preparation of PFPE-DACD/SiO₂ nanocomposites

Scheme 4-1 shows that these fluorinated composites are nanometer size-controlled very fine particles from 22 to 50 nm. In order to clarify the formation of fluorinated nanocomposite particles, the field emission scanning electron micrograph (FE-SEM) of well-dispersed methanol solutions of PFPE-DACD/SiO₂ nanocomposites has been measured before and after calcination at 800 °C, and the results are shown in Fig. 4-1.

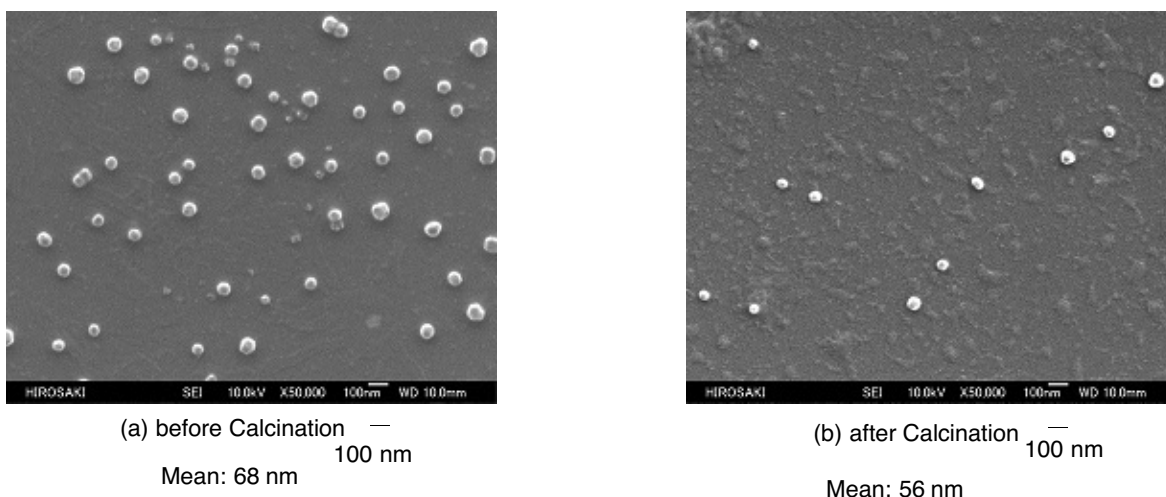


Fig. 4-1 FE-SEM images of well-dispersed methanol solutions of PFPE-DACD/SiO₂ nanocomposites (Run 2 in Scheme 1) before (a) and after (b) calcination at 800 °C

Electron micrographs also showed the formation of fluorinated composite fine particles with a mean diameter of 68 nm (Fig.4-1-a): before calcination), and the similar size value as that (50 nm) of DLS was obtained in FE-SEM measurements. The similar size fine particles (a mean diameter: 56 nm) was observed after calcination at 800 °C (see Fig. 4-1-b)). It was also demonstrated that the appearance of white colored nanocomposite powders did not change at all before and after calcination at 800 °C.

Thermal stability of these fluorinated nanocomposites was studied by the use of thermogravimetric analyses (TGA), in which the weight loss of these nanocomposites was measured by raising the temperature around 800 °C at a 10 °C/min heating rate under air atmospheric conditions, and the results were shown in Fig. 4-2.

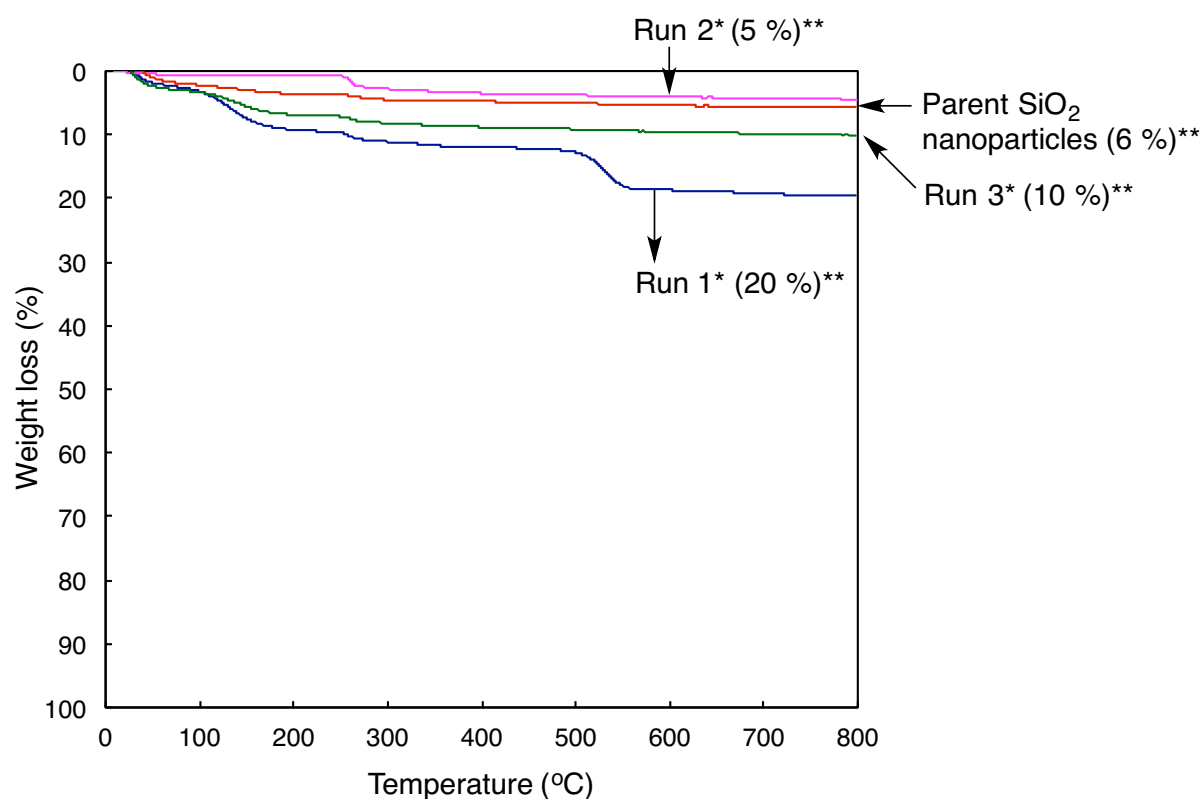


Fig. 4-2 Thermogravimetric analyses (TGA) of PFPE-DACD/SiO₂ nanocomposites

*) Each Run No corresponds to that of Scheme 1

**) Weight loss at 800 °C

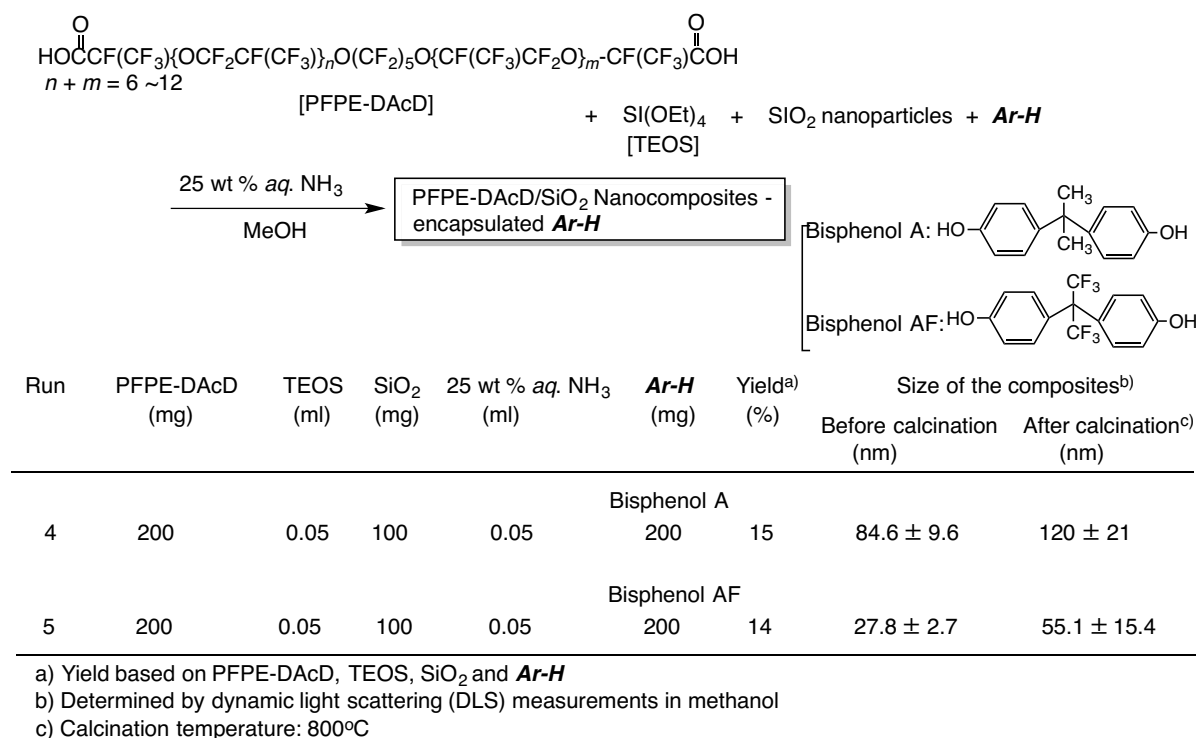
Thermal stability of PFPE-DACD/SiO₂ nanocomposites is in general dependent upon the feed ratios of PFPE-DACD and silica nanoparticles employed, decreasing with the lower feed ratios of PFPE-DACD in PFPE-DACD – silica nanoparticles. It is previously reported that fluoroalkyl end-capped *N*-(1,1-dimethyl-3-oxobutyl)acrylamide oligomer [R_F-(DOBAA)_{*n*}-R_F]/SiO₂ nanocomposites, which were prepared by the sol-gel reaction under alkaline conditions, exhibit no weight loss characteristic even after calcination at 800 °C.²⁵⁾ It is suggested that ammonium hexafluorosilicate is formed through the

dehydrofluorination between the amido protons and fluorines in oligomer during the nanocomposite reactions, and the effective interaction between ammonium hexafluorosilicate and $R_F-(DOBBA)_n-R_F$ oligomer in silica gel matrices should afford a nonflammable characteristic for this fluorinated oligomer.^{26 ~ 28)} Similarly, perfluoro-2-methyl-3-oxahexanoic acid/silica nanocomposites [R_F-CO_2H/SiO_2], which were prepared by the sol-gel reaction of tetraethoxysilane in the presence of silica nanoparticles and the corresponding fluorinated carboxylic acid under alkaline conditions, can exhibit no weight loss in proportion to the contents of fluorinated carboxylic acid in the composites even after calcination at 800 °C.²⁴⁾ This nonflammable characteristic of R_FCO_2H in the silica nanocomposites is due to the dehydrofluorination between fluorines and higher acidic protons in R_F-CO_2H under alkaline conditions (aqueous ammonia) in the presence of silica nanoparticles as a co-catalyst to give tetrafluorosilane, and finally, ammonium hexafluorosilicate.²⁴⁾ In present PFPE-DACD/ SiO_2 nanocomposites, the sol-gel reaction illustrated in Scheme 4-1 is not likely to proceed effectively under the lower feed ratio condition of PFPE-DACD (Run 1 in Scheme 4-1) to give the nonflammable characteristic toward PFPE-DACD in the composites.

The encapsulation of low molecular weight aromatic compounds (*Ar-H*) such as

bisphenol A [BPA] and bisphenol AF [BPAF] into PFPE-DACD/SiO₂ nanocomposite

cores has been studied, and the results are shown in Scheme 4-2.



Scheme 4-2 Preparation of PFPE-DACD/SiO₂/**Ar-H** nanocomposites

As shown in Scheme 4-2, encapsulation of **Ar-H** into PFPE-DACD/SiO₂ nanocomposite cores was found to proceed smoothly to afford the expected PFPE-DACD/SiO₂ composites-encapsulated **Ar-H** in 14 ~ 15 % isolated yields. These fluorinated nanocomposites-encapsulated **Ar-H** afforded good dispersibility and stability in methanol, ethanol, and 2-propanol. Thus, the size of these fluorinated composites in methanol has been measured by the use of DLS measurements at 25 °C.

Fluorinated composites in Scheme 4-2 were nanometer size-controlled very fine nanoparticles from 28 ~ 85 nm.

The thermal stability of PFPE-DACD/SiO₂ nanocomposites-encapsulated *Ar-H* has been studied by the use of thermogravimetric analyses (TGA), in which the weight loss of these nanocomposites was measured by raising the temperature around 800 °C at a 10 °C/min heating rate under air atmospheric conditions, and the results are shown in Figs. 4-3 and 4-4.

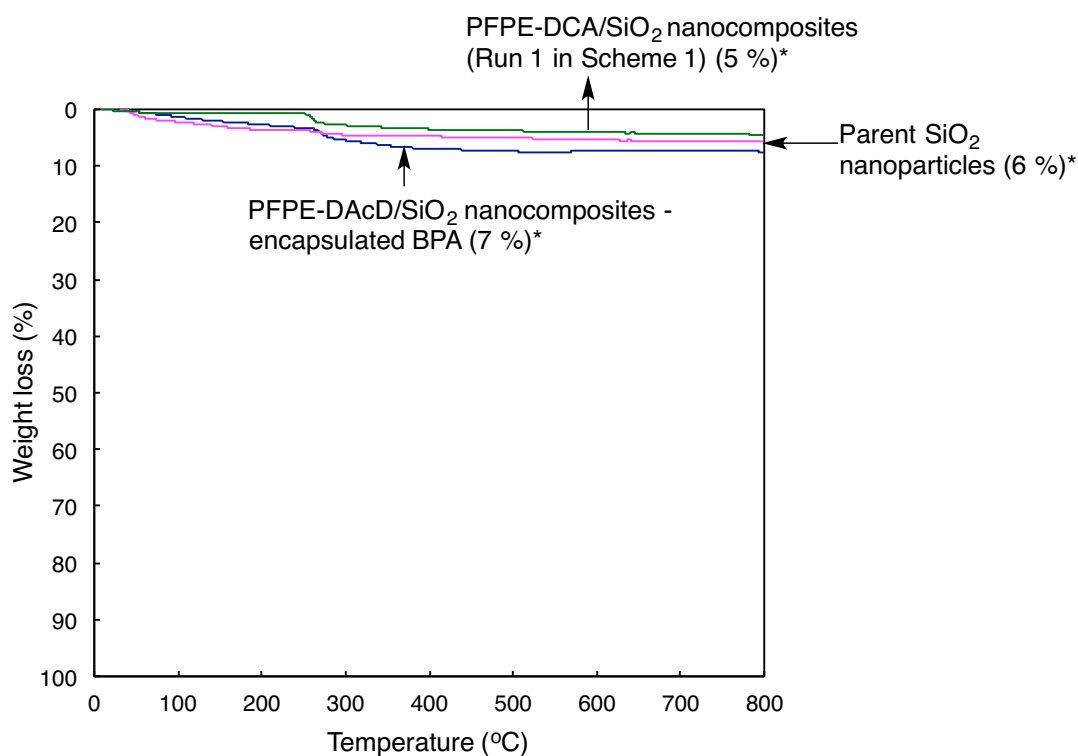


Fig. 4-3 Thermogravimetric analyses (TGA) of PFPE-DACD/SiO₂ nanocomposites - encapsulated BPA
*) Weight loss at 800 °C

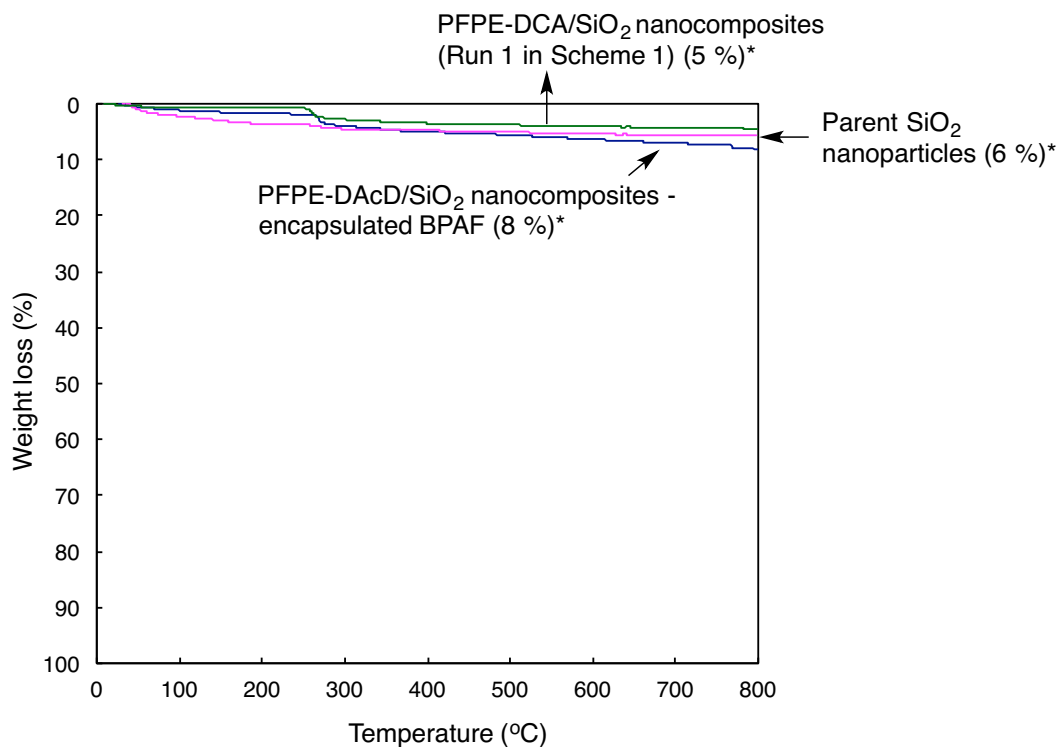


Fig. 4-4 Thermogravimetric analyses (TGA) of PFPE-DACD/SiO₂ nanocomposites - encapsulated BPAF
*) Weight loss at 800 °C

As shown in Figs. 4-3 and 4-4, PFPE-DACD/SiO₂ nanocomposites – encapsulated **Ar-H** were found to exhibit the similar weight loss behavior to that of the PFPE-DACD/SiO₂ nanocomposites or the original silica nanoparticles even after calcination at 800 °C. This finding suggests that encapsulated **Ar-H** should exhibit the nonflammable characteristic in the PFPE-DACD/SiO₂ nanocomposite cores. A similar result has been already reported, and fluoroalkyl end-capped acrylic acid oligomer [R_F-(ACA)_n-R_F]/silica nanocomposites, which were prepared by the sol-gel reaction of the corresponding oligomer with tetraethoxysilane and silica nanoparticles under alkaline conditions, enabled the encapsulated low molecular weight aromatic

compounds such as bisphenol AF to afford a nonflammable characteristic in the composite matrices even after calcination at 800 °C.²⁸⁾ It was also shown that this nonflammable characteristic toward encapsulated guest molecules is due to the formation of ammonium hexafluorosilicate through the smooth dehydrofluorination of phenol-type acidic protons in bisphenol AF with fluorines in oligomers catalyzed by both ammonia and silica nanoparticles.²⁸⁾ Thus, present nonflammable result for the encapsulated *Ar-H* would be due to the similar dehydrofluorination process between the fluorines in the PFPE-DAcD and phenol type-acidic protons in the *Ar-H*.

Perfluoropolyether unit-containing acrylic acid oligomers
 $\{-[R_F-(CH_2CHCO_2H)_q]_p-\};$ $-R_F-$
 $-CF(CF_3)\{OCF_2CF(CF_3)\}_nO(CF_2)_5O\{CF(CF_3)CF_2O\}_m-CF(CF_3)-; n + m = 3\}$ has been already applied to the surface modification of glass to exhibit a good oleophobic characteristic: dodecane contact angle values: 46° ~ 54°. Thus the PFPE-DAcD/SiO₂ nanocomposites and the PFPE-DAcD/SiO₂ nanocomposites – encapsulated *Ar-H* in Schemes 4-1 and 4-2 have been applied to the surface modification of glass, and the contact angles of dodecane and water for these modified glass plates have been measured by depositing a droplet of dodecane or water (2 µl) on these modified glass surfaces. These results are shown in Table 4-1.

Table 4-1 Contact angles of water and dodecane on the modified glass surface treated with PFPE-DACD/SiO₂ nanocomposites and PFPE-DACD/SiO₂ nanocomposites - encapsulated **Ar-H**

Run	Contact angle (degree)							
	dodecane	water						
		time						
		0 m	5 m	10 m	15 m	20 m	25 m	30 m
PFPE-DCA/SiO ₂ nanocomposites								
Run 1 in Scheme 1	63	61	14	0	0	0	0	0
Run 2 in Scheme 1	129	63	19	0	0	0	0	0
Run 3 in Scheme 1	118	43	24	16	0	0	0	0
PFPE-DCA/SiO ₂ nanocomposites - encapsulated BPA								
	83	45	11	0	0	0	0	0
PFPE-DCA/SiO ₂ nanocomposites - encapsulated BPAF								
	102	33	0	0	0	0	0	0

As shown in Table 4-1, the contact angles of dodecane on the modified glass surfaces treated with the PFPE-DACD/SiO₂ nanocomposites showed large values: 63° ~ 129°, of whose values can increase from 63° to 118 or 129° in the case (Run 2 or 3) of the nanocomposites which were prepared under the higher feed ratios of PFPE-DACD: 200 or 400 mg, although the dodecane contact angle on the non-treated glass surface is 0°. On the other hand, the decrease of the dodecane contact angle values has been observed from 129° to 83° or 102° by the encapsulation of bisphenol A or bisphenol AF, indicating that the effective oleophilic - oleophilic interaction between the encapsulated aromatic compounds in the composites and dodecane should become essential on the modified surface. Especially, a higher dodecane contact angle

value (102°) in the PFPE-DACD/SiO₂ nanocomposites – encapsulated bisphenol AF than that (83°) of the bisphenol A would be due to the presence of trifluoromethyl segments in bisphenol AF.

In this way, an extremely higher dodecane contact angle value: 129° was observed, compared with those ($46^\circ \sim 54^\circ$) of previously reported perfluoropolyether unit-containing acrylic acid oligomers $\{-[R_F-(CH_2CHCO_2H)_q]_p-\}$,⁶⁾ or that (73°) of the usual parfluoroalkanoic acid $[C_3F_7OCF(CF_3)C(=O)OH]/SiO_2$ nanocomposites,²⁴⁾ indicating that such extremely higher dodecane contact angle value is due to the effective surface arrangement of PFPE units in present composites on the modified surface. Because, the present PFPE-DACD moieties in the silica nanocomposites should be classified according to the structure into ABA triblock-type fluorinated polysoaps possessing an excellent surface-active property, where A corresponds to the hydrophilic carboxylic groups and B corresponds to the oleo- and hydro-phobic perfluoropolyether (PFPE) units, respectively.

A steep time dependence of water contact angle was observed in each case of the nanocomposites, and the water contact angles decreased smoothly from $63^\circ \sim 33^\circ$ to 0° over 10 min to give a superhydrophilicity on the modified surfaces, although the water contact angle value of the non-treated glass surface is 52° . The PFPE units are

replaced by the hydrophilic carboxylic groups, and it takes about only 5 min to replace the PFPE units by the carboxylic groups when the environment is changed from air to water. In this way, it was verified that present PFPE-DACD/SiO₂ nanocomposites can exhibit the superoleophobic and superhydrophilic characteristics on the modified glass surface as shown in Fig. 4-5.

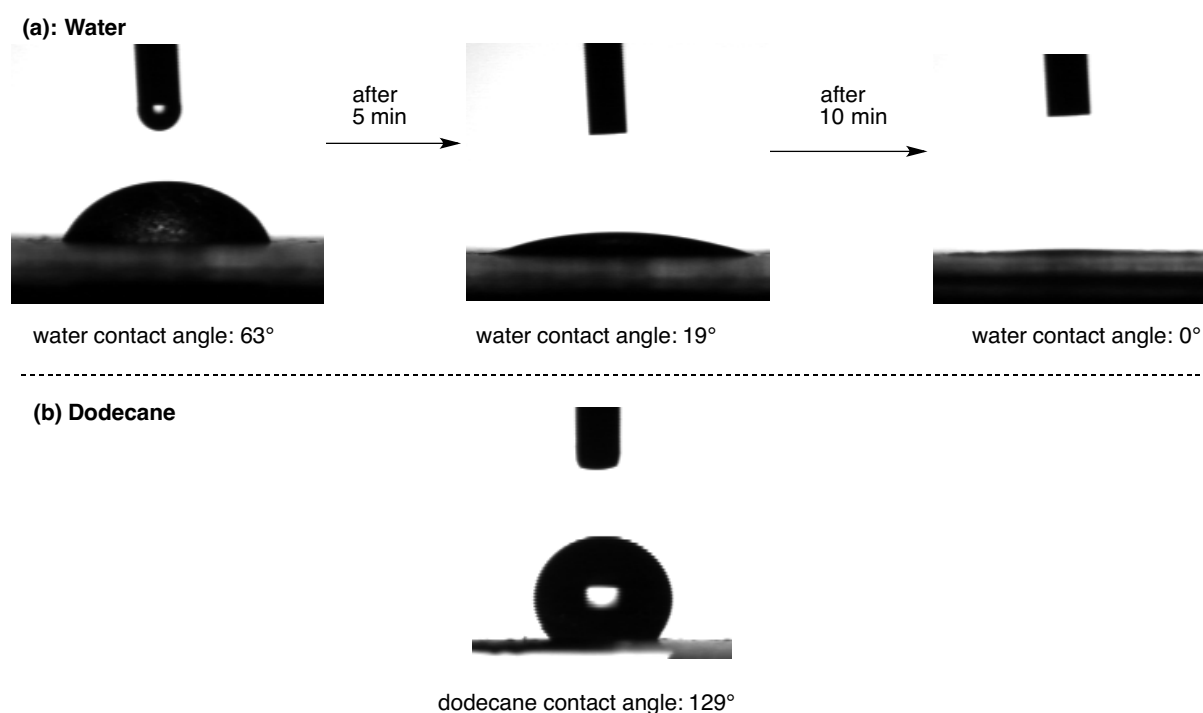


Fig. 4-5 Charge coupled device camera image of the water or dodecane droplet on the modified glass surface treated with PFPE-DACD/SiO₂ nanocomposites (Run 2 in Table 1)

In general, highly oleophobic (superoleophobic) surface are realized by lowering the surface energy and enhancing the surface roughness.^{29 ~ 37)} The fabrication of superoleophobic surface is difficult due to the lower surface tension of

oils than that of water.^{29, 30)} The surface roughness is very important for the wetting properties for liquids. Thus, the surface roughness of the modified glasses treated with the PFPE-DACD/SiO₂ nanocomposites (Runs 2 and 3 in Scheme 4-1) has been studied by DFM (dynamic force microscopy) measurements, and the results were shown in Fig. 4-6.

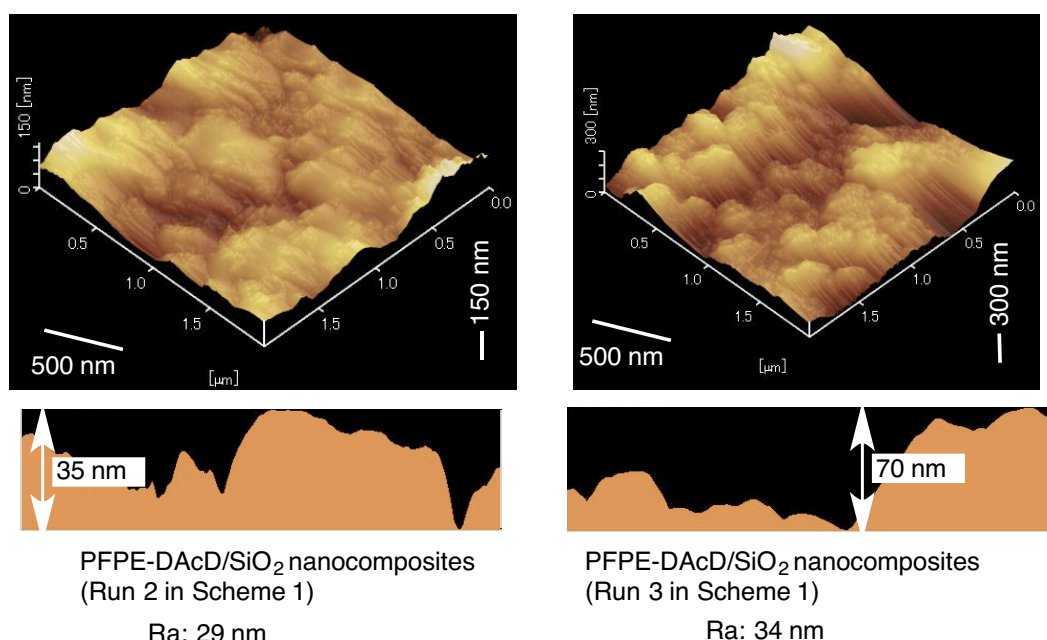


Fig. 4-6 DFM (Dynamic Force Microscopy) topographic images of the modified glass surface treated with PFPE-DACD/SiO₂ nanocomposites (Runs 2 and 3 in Scheme 1)

As shown in Fig. 4-6, DFM measurements show that the topographical image of each surface can exhibit a roughness characteristic, and the roughness average: Ra (29 ~34 nm) of the modified glass surfaces would be derived into the superoleophobic characteristic (dodecane contact angle: 118° ~ 129°; see Table 4-1). In this way, it

was verified that present PFPE-DACD/SiO₂ nanocomposites have the superoleophobic and superhydrophilic characteristics on the modified glass surface.

Hitherto, fluoroalkylated acrylate copolymers have been widely used in the fields of coatings, fabric finish, leather, and packing.^{38, 39)} Among them, textiles are the largest category in which they are used, due to their optimum performance in terms of both hydrophobicity and oleophobicity without impairing the textile's permeability to air and vapor of modifying the handle of the fabrics.^{40, 41)} Especially, much attention has been paid on the superhydrophilic surface due to its potential applications in a wide variety of fields, including the development of anti-fogging films, self-cleaning coatings, microfluiding devices, liquid-liquid separation membranes, and anti-bioadhesion coatings.⁴²⁾ However, traditional superhydrophilic or hydrophilic surfaces are easily fouled by oils, which are difficult to remove the stains.³⁷⁾ From this point of view, the development of the superhydrophilic coatings with superoleophobic characteristic for the polyester fabric is believed to provide an effective way to solve this problem. Thus, it is tried to prepare the modified polyester (PET) fabric swatch and the filter paper by using the present PFPE-DACD/SiO₂ nanocomposites (Run 2 in Scheme 4-1), and the results are shown in Table 4-2.

Table 4-2 Contact angles of dodecane and water on the modified PET fabric swatch and the filter paper treated with PFPE-DACD/SiO₂ nanocomposites (Run 2 in Scheme 1)

		Contact angle (degree)							
		Dodecane	Water						
			Time						
			0 min	5 min	10 min	15 min	20 min	25 min	30 min
Modified PET fabric swatch	105	0	0	0	0	0	0	0	0
Modified filter paper	109	0	0	0	0	0	0	0	0
Parent PET fabric swatch	0	113	0	0	0	0	0	0	0
Parent filter paper	0	0	0	0	0	0	0	0	0

As shown in Table 4-2, the dodecane contact angle value of the parent PET fabric swatch and the filter paper is 0°, respectively. However, the modified PET fabric swatch and the modified filter paper treated the PFPE-DACD/SiO₂ nanocomposites were found to exhibit the dodecane and water contact angle values: 105° ~ 109° and 0°, respectively. This finding suggests that these modified surfaces can exhibit the superoleophobic and superhydrophilic characteristic as well as that of the modified glass surface illustrated in Table 4-1. Thus, the modified PET fabric swatch as has been applied to the liquid-liquid separation membranes in order to separate the mixture of oil (dodecane) and water (water was red-colored with Rhodamine B illustrated in Fig. 4-7), and the result is shown in Fig. 4-8.

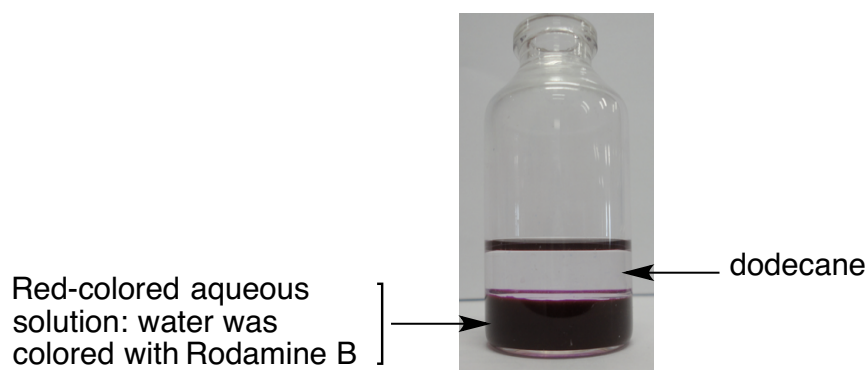
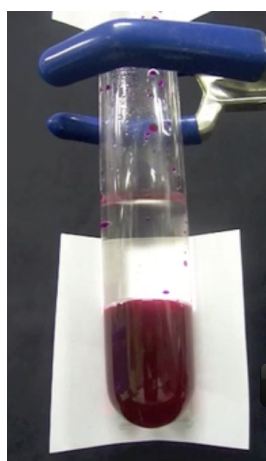
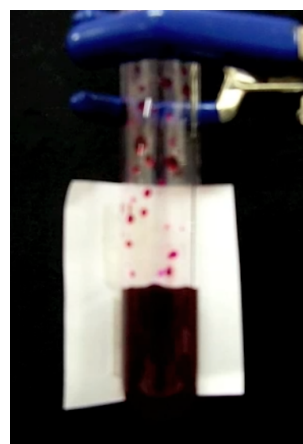


Fig. 4-7 Photograph of the mixture of dodecane and red-colored aqueous solution



(a) the parent PET fabric swatch



(b) the modified PET fabric swatch treated with PFPE-DACD/SiO₂ nanocomposites

Fig. 4-8 Separation of oil (dodecane)/water (red-colored aqueous solution) by using the parent PET fabric swatch (a) and the modified PET fabric swatch treated with PFPE-DACD/SiO₂ nanocomposites (b) under atmospheric conditions

Fig. 4-8 shows that the modified PET fabric swatch can be used for the effective separation of water and oil (dodecane), and only red-colored water has been removed under atmospheric pressure (see Fig. 4-8-b)), although the parent PET fabric swatch cannot be used as the water – dodecane separation membrane under the similar

very fine particles. The PFPE-DACD/SiO₂ nanocomposites were applied to the surface modification of glass to give the superoleophobic and superhydrophilic characteristics. In contrast, AB block-type acrylic acid oligomer containing perfluoropolyether units (-R_F-) in the main chain $\{-[R_F-(CH_2CHCO_2H)_q]_p-\}$ and the usual parfluoroalkanoic acid [C₃F₇OCF(CF₃)C(=O)OH]/SiO₂ nanocomposites can give the usual oleophobic characteristics: dodecane contact angle values: 45° ~ 54° and 73°, respectively. Interestingly, it has been also succeeded in the surface modification of the PET fabric swatch and the filter paper to exhibit superoleophobic and superhydrophilic surfaces. More interestingly, the modified PET fabric material was applied to the excellent oil/water separation membrane. Especially, the superoleophobic and superhydrophilic PET textile should give practical applications such as oil/water separation. Hitherto, there have been some reports on the oil/water separation by using not only superhydrophobic and superoleophilic polyester materials which were prepared by one-step growth of silicone nanofilaments onto the textile via chemical vapor seposition of trichloromethylsilane⁴⁴⁾ but also superhydrophilic and superoleophobic stainless steel mesh prepared by the spray-coating of well-dispersed silica nanoparticles and poly(diallyldimethylammonium) perfluorooctanoate.⁴⁵⁾ However, studies on the facile

creation of the superoleophobic and superhydrophilic surface by the use of the fluorinated polymers/silica nanocomposites including an effective oil/water separation ability have been very limited except for this work. Thus, the present PFPE-DACD/SiO₂ nanocomposites may be a good candidate for the treatment of industrial oil-polluted water and the clean-up of oil spills.

Reference

- 1) H. Sawada, *Chem. Rev.*, **96**, 1779 (1996).
- 2) H. Sawada, *Polym. J.*, **39**, 637 (2007).
- 3) H. Sawada, N. Itoh, T. Kawase, M. Mitani, H. Nakajima, M. Nishida, and Y. Moriya, *Langmuir*, **10**, 994 (1994).
- 4) J. Nakagawa, K. Kamogawa, H. Sakai, T. Kawase, H. Sawada, J. Manosroi, A. Manosroi, and M. Abe, *Langmuir*, **14**, 2055 (1998).
- 5) J. Nakagawa, K. Kamogawa, N. Momozawa, H. Sakai, T. Kawase, H. Sawada, Y. Sano, and M. Abe, *Langmuir*, **14**, 2061 (1998).
- 6) H. Sawada, K. Ikeno, and T. Kawase, *Macromolecules*, **35**, 4306 (2002).
- 7) Z. Shi and S. Holdcroft, *Macromolecules*, **38**, 4193 (2005).

- 8) T. Imae, *Curr. Opin. Colloid Interface Sci.*, **8**, 307 (2003).
- 9) P. Anton, O. Koberle, and A. Laschewsky, *Makromol. Chem.*, **194**, 1 (1993).
- 10) J.-F. Berret, D. Calvet, A. Collet, and M. Viguier, *Curr. Opinion Colloid Interface Sci.*, **8**, 296 (2003).
- 11) B. Ameduri and B. Boutevin, “Well-Architected Fluoropolymers: Synthesis, Properties and Applications”, Elsevier, Amsterdam, 231 (2004).
- 12) D. Cochin, P. Hendlinger, and A. Laschewsky, *Colloid Polym. Sci.*, **273**, 1138 (1995).
- 13) I. J. Park, S.-B. Lee, C. K. Choi, and K.-J. Kim, *J. Colloid Interface Sci.*, **181**, 284 (1996).
- 14) M. Morita, M. Kubo, and M. Matsumoto, *Colloid Surface A*, **109**, 183 (1996).
- 15) I. J. Park, S.-B. Lee, and C. K. Choi, *J. Appl. Polym. Sci.*, **54**, 1449 (1994).
- 16) A.-M. Caminade, C.-O. Turrin, P. Sutra, and J.-P. Majoral, *Curr. Opin. Colloid Interface Sci.*, **8**, 282 (2003).
- 17) A. Zaggia and B. Ameduri, *Curr. Opin. Colloid Interface Sci.*, **17**, 188 (2012).
- 18) H. Sawada, *Prog. Polym. Sci.*, **32**, 509 (2007).
- 19) H. Sawada, *Polym. Chem.*, **3**, 46 (2012).
- 20) H. Sawada, *J. Fluorine Chem.*, **121**, 111 (2003).

- 21) H. Sawada, E. Sumino, M. Oue, M. Mitani, H. Nakajima, M. Nishida, and Y. Moriya, *J. Chem. Soc., Chem. Commun.*, 143 (1994).
- 22) H. Sawada, E. Sumino, M. Oue, M. Baba, M. Mitani, H. Nakajima, M. Nishida, and Y. Moriya, *J. Fluorine Chem.*, **74**, 21 (1995).
- 23) H. Sawada, E. Sumino, Y. Hayakawa, T. Tomita, and M. Baba, *Mater. Technol.*, **15**, 79 (1997).
- 24) E. Sumino, S. Ise, T. Saito, M. Nishida, T. Noguchi, and H. Sawada, *Colloid Polym. Sci.*, **292**, 369 (2014).
- 25) H. Sawada, T. Tashima, and S. Kodama, *Polym. Adv. Technol.*, **19**, 739 (2008).
- 26) H. Sawada, T. Tashima, H. Kakehi, Y. Nishiyama, M. Kikuchi, M. Miura, Y. Sato, and N. Isu, *Polym. J.*, **42**, 167 (2010).
- 27) H. Sawada, T. Tashima, Y. Nishiyama, M. Kikuchi, G. Kostov, Y. Goto, and B. Ameduri, *Macromolecules*, **44**, 1114 (2014).
- 28) H. Sawada, M. Kikuchi, and M. Nishida, *J. Polym. Sci. Part A: Polym. Chem.*, **49**, 1070 (2011).
- 29) X. Yao, Y. Song, and L. Jiang, *Adv. Mater.*, **23**, 719 (2011).
- 30) J. Feng, B. Huang, and M. Zhong, *J. Colloid Interface Sci.*, **336**, 268 (2009).
- 31) R. Taurino, E. Fabbri, M. Messori, F. Pilati, D. Pospiech, and A. Synytska, *J.*

- Colloid Interface Sci.*, **325**, 149 (2008).
- 32) K. Tsujii, T. Yamamoto, T. Onda, and S. Shibuichi, *Angew. Chem. Int. Ed. Eng.*, **36**, 1011 (1997).
- 33) S. Shibuichi, T. Yamamoto, T. Onda, and K. Tsujii, *J. Colloid Interface Sci.*, **208**, 287 (1998).
- 34) S. Srinivasan, S. S. Chhatre, S.; J. M. Mabry, R. E. Cohen, and G. H. McKinley, *Polymer*, **52**, 3209 (2011).
- 35) J. Feng, B. Huang, M. Zhong, *J. Colloid Interface Sci.*, **336**, 268 (2009).
- 36) A. K. Kota, Y. Li, J. M. Mabry, and A. Tuteja, *Adv. Mater.*, **24**, 5838 (2012).
- 37) K. Liu, Y. Tian, and L. Jiang, *Prog. Mater. Sci.*, **58**, 503 (2013).
- 38) Q. An, W. Xu, L. Hao, and L. Huang, *J. Appl. Polym. Sci.*, DOI: 1002/APP.37553 (2013).
- 39) Y. Furukawa and M. Kotera, *J. Appl. Polym. Sci.*, **87**, 1085 (2003).
- 40) A. Ceria and P. J. Hauser, *Sur. Coat. Technol.*, **204**, 1535 (2010).
- 41) H. Ye, Z. Li, G. Chen, and D. Fan, *J. Appl. Polym. Sci.*, DOI: 10.1002/APP. 37632 (2013).
- 42) J. Yang, H. Song, X. Yan, H. Tang, and C. Li, *Cellulose*, **21**, 1851 (2014).
- 43) S. E. Allan, B. W. Smith, and K. A. Anderson, *Environ. Sci. Technol.*, **46**, 2033

(2012).

44) J. Zhang and S. Seeger, *Adv. Funct. Mater.*, **21**, 4699 (2011).

45) J. Yang, Z. Zhang, X. Xu, X. Zhu, X. Men, and X. Zhou, *J. Mater. Chem.*, **22**, 2834 (2012).

Conclusions

The results obtained from this study are summarized as follows:

1. A new polymeric perfluoro-oxa-alkane diacyl peroxide has been prepared by reaction of the corresponding perfluoro-oxa-alkane diacid fluoride and hydrogen peroxide under alkaline conditions. The decomposition behavior of this peroxide was quite similar to those of the fluoroalkanoyl peroxides $[(R_FCOO_2)_2]$; R_F = perfluoroalkyl and perfluoro-oxa-alkyl groups]. This peroxide can decompose homolytically with decarboxylation to afford the $-R_F-$ unit. In addition, this peroxide was also useful for the introduction of the perfluoro-oxa-alkylene ($-R_F-$) unit into acrylic acid homo- and co-oligomer main chains through a radical process. These new acrylic acid oligomers containing the perfluoro-oxa-alkylene unit were soluble in water, methanol, ethanol, and tetrahydrofuran and were not only able to reduce the surface tension of water effectively but also to confer good oil repellency. Furthermore, acrylic acid co-oligomers containing the perfluoro-oxa-alkylene unit were found to be potent and selective inhibitors of human immunodeficiency virus type 1 (HIV-1) in vitro.

2. 2-Acryloxyethyltrimethylammonium chloride and 2-(methacryloxy)ethanesulfonic acid oligomers containing perfluoro-oxa-alkylene groups were prepared by reaction of polymeric perfluoro-oxa-alkane diacyl peroxide and the corresponding monomers under mild conditions. These oligomers were soluble in both water and water-soluble polar organic solvents such as methanol, ethanol, tetrahydrofuran, and *N,N*-dimethylformamide. The oligomer containing either trimethylammonium or sulfo groups can reduce the surface tension of water. Therefore, these oligomers have high potential as new fluorinated polymeric surfactants. The fluorinated oligomers containing sulfo groups can exhibit anti-HIV activity, whereas the oligomers containing trimethylammonium groups have an antibacterial activity against *Staphylococcus aureus*.

3. Perfluoro-2-methyl-3-oxahexanoic acid/silica nanocomposites [$R_F\text{-CO}_2\text{H/SiO}_2$] were prepared by the sol-gel reaction of tetraethoxysilane in the presence of silica nanoparticles and the corresponding fluorinated carboxylic acid under alkaline conditions. $R_F\text{-CO}_2\text{H/SiO}_2$ nanocomposites were found to exhibit no weight loss in proportion to the contents of fluorinated carboxylic acid in the composites even after calcination at 800 °C. The modified glass surface treated with the $R_F\text{-CO}_2\text{H/SiO}_2$

nanocomposites was shown to give a good oleophobicity with superhydrophilicity imparted by fluorinated carboxylic acid in the composites. $R_F\text{-CO}_2\text{H/SiO}_2$ nanocomposites were also applied to the encapsulation of a variety of low molecular weight aromatic and aliphatic compounds such as bisphenol AF [BPAF], bisphenol A [BPA], 4,4'-biphenol [BPOH], octafluoro-4,4'-biphenol [FBPOH], 4,4'-bis(triethoxysilyl)-1,1'-biphenyl [BTSBP], 3-(trihydroxysilyl)propane-1-sulfonic acid [THSP], α -cyclodextrin (α -CD), β -cyclodextrin (β -CD), and γ -cyclodextrin (γ -CD). Encapsulated aromatic compounds possessing acidic hydroxyl groups such as BPAF, BPA, and FBPOH in the $R_F\text{-COOH/SiO}_2$ nanocomposites were found to exhibit no weight loss corresponding to the contents of aromatic compounds in the composites even after calcination at 800 °C. On the other hand, encapsulated aromatic compounds possessing no acidic hydroxyl groups such as BTSBP and aliphatic compounds (THSP, α -, β -, and γ -CD) gave a clear weight loss corresponding to the contents of these compounds in the composites after calcination. In addition, the fluorinated silica nanocomposite-encapsulated these compounds were applied to the surface modification of glass to exhibit a good oleophobicity with superhydrophilicity imparted by fluorinated carboxylic acid on the surface.

4. Perfluoropolyether dicarboxylic acid

$$[\text{HO}(\text{O}=\text{C})\text{CF}(\text{CF}_3)\{\text{OCF}_2\text{CF}(\text{CF}_3)\}_n\text{O}(\text{CF}_2)_5\text{O}\{\text{CF}(\text{CF}_3)\text{CF}_2\text{O}\}_m-\text{CF}(\text{CF}_3)\text{C}(=\text{O})\text{OH}; n + m = 6 \sim 12; \text{PFPE-DACD}]$$
 was applied to the preparation of PFPE-DACD/SiO₂ nanocomposites by the sol-gel reactions of the corresponding diacid with tetraethoxysilane in the presence of silica nanoparticles under alkaline conditions. PFPE-DACD/SiO₂ nanocomposites thus obtained were found to exhibit a good dispersibility and stability in not only water but also the traditional organic solvents such as methanol, ethanol, 2-propanol, tetrahydrofuran and 1,2-dichloroethane. Field emission scanning electron micrograph (FE-SEM) and dynamic light-scattering (DLS) measurements show that these fluorinated composites are nanometer size-controlled very fine particles. Dodecane and water contact angle measurements on the modified glass, filter paper and polyester fabric surfaces treated with these fluorinated nanocomposites were found to exhibit the superoleophobicity and superhydrophilicity. Especially, the modified polyester fabric swatch was applied to the oil/water separation to give the high separation efficiency.

Publications

- 1) H. Sawada, E. Sumino, M. Oue, M. Mitani, H. Nakajima, M. Nishida and Y. Moriya, “Synthesis of a Novel Polymeric Perfluoro-oxa-alkane Diacyl Peroxide. A Convenient Tool for the Introduction of the Perfluoro-oxa-alkylene Unit”, *J. Chem. Soc., Chem. Commun.*, 143 (1994).
- 2) H. Sawada, E. Sumino, M. Oue, M. Baba, T. Kira, S. Shigeta, M. Mitani, H. Nakajima, M. Nishida and Y. Moriya, “Synthesis and surfactant properties of novel acrylic acid oligomers containing perfluoro-oxa-alkylene units: an approach to anti-human immunodeficiency virus type-1 agents”, *J. Fluorine Chem.*, **74**, 21 (1995).
- 3) H. Sawada, E. Sumino, Y. Hayakawa, T. Tomita and M. Baba, “Synthesis and properties of 2-acryloxyethyltrimethylammonium chloride and 2-(methacryloxy)ethanesulfonic acid oligomers containing perfluoro-oxa-alkylene units”, *Zairyo Gijutsu*, **15**, 79 (1997).
- 4) E. Sumino, S. Ise, T. Saito, M. Nishida, T. Noguchi and H. Sawada, “Preparation and properties of fluorinated carboxylic acid/silica nanocomposite encapsulated low molecular

weight compounds”, *Colloid Polym. Sci.*, **292**, 369 (2013).

- 5) E. Sumino, T. Saito, T. Noguchi and H. Sawada, “Facile creation of superoleophobic and superhydrophilic surface by using perfluoropolyether dicarboxylic acid/silica nanocomposites”, *Polym. Adv. Technol.*, **26**, 345 (2015).